Title

Transplantation of olfactory ensheathing cells combined with epidural stimulation and climb training as a long-term treatment for severe spinal cord injury in rodents

Permalink

https://escholarship.org/uc/item/49w4t14w

Author

Dixie, Kaitlin Lee Ingraham

Publication Date

2019

Peer reviewed|Thesis/dissertation

UNIVERSITY OF CALIFORNIA

Los Angeles

Transplantation of olfactory ensheathing cells combined with epidural stimulation and

climb training as a long-term treatment for severe spinal cord injury in rodents

A dissertation submitted in partial satisfaction of the requirements for the degree Doctor

of Philosophy in Molecular, Cellular, and Integrative Physiology

by

Kaitlin Lee Ingraham Dixie

2019

ABSTRACT OF THE DISSERTATION

Transplantation of olfactory ensheathing cells combined with epidural stimulation and

climb training as a long-term treatment for severe spinal cord injury in rodents

by

Kaitlin Lee Ingraham Dixie

Molecular, Cellular, and Integrative Physiology

University of California, Los Angeles, 2019

Professor Patricia Emory Phelps, Chair

Following a severe spinal cord injury (SCI), transplanted olfactory ensheathing cells (OECs) reduce inhibitory factors and promote axonal outgrowth at the lesion site to help reestablish circuit connectivity needed for functional recovery. Another promising therapy, electrical epidural stimulation (EES), also helps to reestablish connectivity but targets the spinal cord caudal to the injury. This study asked if the combination of OEC transplantation and administration of EES during climb training would improve recovery. Two cohorts of inbred Fischer 344 rats received a severe SCI and a two-week delayed transplant of OECs, media, or fibroblasts (FBs). Rats then received EES while performing a climbing task 3 times/week and were perfused at 5.5-6.5 months post-injury. We found that scores on the BBB locomotor test improved for all groups over time, but no consistent changes in climbing ability were detected. When we examined the injury sites, we found surviving GFP-labeled OECs and FBs for the first time at 6 months post-transplant. We

also found that OEC treatment increased the amount of serotonergic and neurofilament (NF)-positive axons in the lesion core compared to media- and FB-treated controls. This was particularly true in areas of the lesion core with OECs where we found greater levels of axon density than in areas without OECs. Further, the percent of NF-positive axons associated with myelin proteins was greater in OEC- compared to media-treated rats. The OECs in the lesion core also interacted with serotonergic axons, myelinating and non-myelinating Schwann cells (SCs), and oligodendrocytes and expressed protein markers typically associated with SC-like myelin. Overall our results provide evidence that OEC transplantation combined with EES may be a beneficial treatment for severe SCI.

The dissertation of Kaitlin Lee Ingraham Dixie is approved.

Victor R. Edgerton

Diane Papazian

Rhonda Voskuhl

Patricia Emory Phelps, Committee Chair

University of California, Los Angeles

2019

DEDICATION

This thesis is dedicated to the many people who have supported me through the years. I would like to thank my mom Susan, dad Howard, sister Amy, grandparents Eileen, Howard, Dotty, Bob, and Natalie, and the rest of my family for believing in me and for their unwavering guidance and enthusiasm- I could always count on them to make me feel better on my toughest days, even from all the way across the country. In particular, I would like to acknowledge my grandfather Bob, and grandmother Dotty who both inspired and fostered my kindness, generosity, passion, and curiosity and who passed away while I was working on this thesis. I would also like to dedicate this to my wife Emma who was always so patient, supportive, and loving and who could always make me smile even when experiments went horribly awry. Thank you also to my many friends and lab mates who have been there for me and helped keep things in perspective. I would like to also wholeheartedly thank my many mentors, especially my thesis advisor Patty Phelps for all their guidance, wisdom, and encouragement. Lastly, I would like to dedicate this thesis to all my students and mentees past, present, and future who helped remind me why all of this was worth it!

TABLE OF CONTENTS

LIST OF TABLES AND FIGURES

ACKNOWLEDGEMENTS

CURRICULUM VITAE
Kaitlin Lee Ingraham Dixie

EDUCATION
University of California Los Angeles, Los Angeles, CA   *Sept 2012 - present*
    Graduate Student, Molecular, Cellular, and Integrative Biology
        Thesis: "*Transplantation of olfactory ensheathing cells combined with epidural stimulation and climb training as a long-term treatment for severe spinal cord injury in rodents.*"

Boston University, Boston, MA   *Sept 2006 - May 2010*
    Bachelor of Arts, Biochemistry and Molecular Biology
        Minor: Psychology
        Graduated Cum Laude, GPA: 3.56
        Participated in the Dresden Science Study Abroad Program Fall 2007

HONORS AND AWARDS
- University Distinguished Teaching Assistant Award   *Spring 2019*
- CIRTL STAR Fellow Certification   *Fall 2019*
- Integrative Biology and Physiology departmental fellowship   *Spring 2018*
- Brain Research Institute's Society for Neuroscience graduate student travel grant   *Fall 2017*
- MCIP Training Grant   *2013-2014*

PUBLICATIONS
University of California Los Angles:
Urban LS, M. Thornton, **Ingraham Dixie KL**, Dale E, Zhong H, Phelps PE, Burdick J, Edgerton VR. (2019) Functional Recovery of Trained Behavior After Paralysis Via Novel Supraspinal-Spinal Network. (In submission)

Thornton MT, Mehta MD, Morad TT, **Ingraham KL**, Khankan RR, Griffis KG, Yeung AK, Zhong H, Roy RR, Edgerton VR, Phelps PE. 2018. Evidence of axon connectivity across a spinal cord transection in rats treated with epidural stimulation and motor training combined with olfactory ensheathing cell transplantation. Experimental Neurology. 309, 119-133. (Article featured on cover)

Boston University:
Varnum MM, Kiyota T, **Ingraham KL**, Ikezu S, and Ikezu T. 2015. The anit-inflammatory glycoprotein, CD200, restores neurogenesis and enhances amyloid phagocytosis in a mouse model of Alzheimer's disease. Neurobiology of Aging. 11, 2995-3007.

Kiyota T, **Ingraham KL**, Swan RJ, Jacobsen MT, Andrews SJ, and Ikezu T. 2011. AAV serotype 2/1-mediated gene delivery of anti-inflammatory interleukin-10 enhances neurogenesis and cognitive function in APP+PS1 mice. Gene Therapy. 19, 724–733.

Kiyota T, **Ingraham KL**, Jacobsen MT, Xiong H, and Ikezu T. 2011. FGF2 gene transfer restores hippocampal functions in mouse models of Alzheimer's disease and has therapeutic implications for neurocognitive disorders. Proceedings of the National Academy of Sciences. 108; 49, E1339–E1348.

DiBenedictis BT, **Ingraham KL**, Baum MJ, Cherry JA. 2011. Disruption of urinary odor preference and lordosis behavior in female mice given lesions of the medial amygdala. Physiology and Behavior. 105, 554–559.

POSTER AND RESEARCH PRESENTATIONS

- **Ingraham Dixie, K.L.** and Kennison, R.L. (2019) Practice makes perfect?: The merits of a restructured course for new graduate student teaching assistants. *CIRTL 2019 Meeting*.
- **Ingraham Dixie, K.L.** (2019) Cells from your nose plus a little electricity: A combined treatment for severe spinal cord injury. *MCIP Program Retreat*. (Voted 2nd best student talk)
- **Ingraham Dixie, K.L.** (2019) Practice makes perfect?: The merits of a restructured course for new graduate student teaching assistants. *CEILS Journal Club.* (Public talk)
- **Ingraham, K.L.** et al., (2018) Olfactory ensheathing cell transplantation combined with electrical epidural stimulation and climb training enhances axonal connectivity across a severe spinal cord injury. Soc. Neurosci. Abst. 477:20. (Poster)
- **Ingraham, K.L.** et al, (2017) Olfactory ensheathing cell transplantation combined with epidural stimulation and climb training as a treatment for severe spinal cord injury. Soc. Neurosci. Abst. 578:24. (Poster)

TEACHING AND MENTORING EXPERIENCE
University of California Los Angeles:
- **Teaching Fellow;** Intro to Undergraduate Evidence-Based Teaching *(1 qtrs)*   Fall 2019
- **Teaching Assistant Consultant;** *Practicum* for teaching assistants *(2 qtrs)* Fall 2017, 2018
- **Graduate Student Mentor; Undergraduate Research Center** *(8 qtrs)*   Fall 2016-2018
- **Teaching Assistant;** Nervous System Development *(2 qtrs)*   Spring 2015, 2017
- **Undergraduate Lab Mentor;** *Student Research Practicum (6 years)*   Fall 2013–present
- **Teaching Assistant***;* Introduction to Cells, Tissues, and Organs *(1 qtr)*   Fall 2013

TEACHING PROFESSIONAL DEVELOPMENT
- Center for the Integration of Research Teaching and Learning (CIRTL):   *2017-present*
- Teaching as Research (TAR) Project   *Fall 2018-2019*
- Preparing Future Faculty Course   *Fall 2018-Spring 2019*
- TA Training Program   *Aug 2017, 2018*
- Mobile Summer Institute at UCLA; *Certified Teaching Fellow*   *July 2017*

RESEARCH EXPERIENCE
University of California Los Angeles, Molecular, Cellular, and Integrative Physiology
    Graduate Student Researcher Laboratory of Dr. Patricia E. Phelps   *Mar 2013-present*
    Project: **"***Transplantation of olfactory ensheathing cells combined with epidural stimulation and climb training as a long-term treatment for severe spinal cord injury in rodents.*"

Boston University School of Medicine, Department of Pharmacology   *May 2010-Jul 2012*
    Research Technician Laboratory of Molecular Neurotherapeutics, Dr. Tsuneya Ikezu

Boston University, Department of Psychology   *Jan 2009 - May 2010*
    Undergraduate Researcher Molecular Neurobiology and Behavior, Dr. James Cherry

LEADERSHIP AND OUTREACH
- *Aspire2Lead Internship*   *Summer 2019*
- *Summer Institute on Scientific Teaching* - Scientific Teaching Mentor   *July 2019*
- *Bsili Leadership for Curricular & Institutional Transformation Retreat*   *June 2019*
- *Bioscience Student Counci*l – Secretary, program representative   *Fall 2016 - Spring 2017*
- *Bioscience Student Council* – MCIP program representative   *Fall 2015 - Fall 2016*
- *City Lab* – Member, laboratory science outreach for high school students   *Spring 2015*

CHAPTER 1. INTRODUCTION AND LITERATURE REVIEW

Spinal cord injury (SCI) results in the variable loss of motor and sensory function depending on the severity of the injury. Over 290,000 people in the United States alone are affected by SCI with over 17,000 new cases occurring every year, yet very few effective treatment options are available that lead to significant recovery, especially for those who are most severely affected (NSCISC, 2019). This is due, in part, to the complex nature of the injury; effective treatments of SCI need to address multiple pathological barriers in order to promote functional recovery. These include spinal cord damage and cyst formation, disrupted axonal connectivity and neuronal circuitry, immune-cell infiltration and increased inflammation, loss of myelin and efficient signal conduction, muscle and neuronal atrophy, increased inhibitory and toxic factors surrounding the injury site, and formation of scar tissue (Venkatesh et al., 2019). While the goal of treatment following SCI is to promote functional motor and sensory recovery, the therapeutic focus to achieve these outcomes can vary widely. Some therapeutic approaches target the spinal cord injury site directly, while others target areas below or above the injury or are more holistic, such as rehabilitation (Silva et al. 2014). The large number of current potential treatments in development is encouraging but perhaps impractical; addressing all the consequences and deficits caused by a SCI will most likely require a combination of treatments targeting different mechanisms and areas in order to provide maximum benefit. This then produces the question: "Which treatment combinations will be most effective?"

Identifying neuropathological targets at the injury site after SCI

The most devastating functional deficits after SCI result from damaged or severed axons that cause the loss of communication between the brain and brain stem and the spinal cord caudal to the injury. Damage to the protective myelin sheaths that surround the axons also exacerbates symptoms. Many therapies, therefore, aim to reestablish neuronal connectivity by stimulating axon growth and increasing myelination to improve functionality. For axonal regeneration to occur, however, treatments must not only overcome the limited growth potential of adult neurons but must also guide regenerating axons across a hostile and inhibitory injury site. Similarly, there are many challenges that must be overcome to improve axon myelination (Silva et al. 2014). It is therefore important to understand the pathological changes that occur after SCI in order to identify mechanisms that can target the promotion of axon outgrowth and myelin recovery. This study will focus mainly on rodent SCI models, but many of the responses to injury are similar to those in humans.

Axonal damage and limited regenerative potential after injury

The severing of axons not only disrupts a signal from reaching its downstream target, but it can also be a threat to the health of the entire neuron. Danger signals triggered by injury can travel back to the soma and potentially initiate apoptosis even in neuronal cell bodies located far from the injury site (Crowe et al., 1997; Liu et al., 1997). In order to seal off the axonal membrane, the cell responds to the drastic calcium influx by triggering acute axon degeneration. This response can initiate the degradation of large distances of the

proximal axon in less than 30 minutes until it eventually forms a dystrophic retraction bulb. The distal half of the axon that was separated from the cell body then undergoes Wallerian degeneration (Kerschensteiner et al., 2005).

The axonal degradation that occurs after injury also results in axons that are far from their initial targets and thus would need to regrow long distances to reestablish connectivity. During early development, the distances between neurons in the embryonic brain and spinal cord are short and axons rely on precise temporal and spatial guidance molecules to reach correct targets (Harel & Strittmatter, 2006). After an adult SCI, however, mature neurons have a limited capacity for axonal growth, axonal targets are much further away, and appropriate guidance molecules may no longer be expressed (Harel & Strittmatter, 2006; Milde et al., 2015; Geoffroy & Hilton, 2016). There are many challenges to guiding axons to their distal spinal cord targets and several therapies that successfully stimulated innate axon growth will be discussed later in this chapter.

Anatomical remodeling contributes to the formation of inhibitory scars

Following SCI, the injury site undergoes a period of significant reorganization; immune cells such as microglia and macrophages infiltrate the lesion area to clear debris, astrocytes and oligodendrocyte progenitor cells (OPCs) become activated and proliferate to create a glial scar, and fibroblasts and other peripheral cells invade the lesion core and form a peripheral fibrotic scar (Alvarez et al. 2013; Burda & Sofroniew 2014; McTigue et al. 2001; Raposo & Schwartz 2014; Whetstone et al. 2003). This reorganization results in persistent and lasting tissue damage including the formation of fluid-filled cysts that can

expand over time and lead to chronic secondary damage to the uninjured spinal cord (Kubasak et al. 2010).

The blood-spinal cord barrier exists to prevent neurotoxic chemicals or peripheral immune cells from attacking irreplaceable neurons. After injury this barrier is disrupted and macrophages, natural killer cells, and other lymphocytes can infiltrate the central nervous system (CNS) and cause extensive cell death, tissue damage, and inflammation (Bethea & Dietrich, 2002; Maikos & Shreiber, 2007; Pineau et al., 2010). Cytokines secreted by these cells increase apoptosis of neurons and oligodendrocytes leading to further disruption of functional circuits and loss of myelin (Pan & Kastin, 1999; Pineau et al., 2010). There are some benefits, however, to the increased phagocytic activity that infiltrating cells provide; several studies reported that increased microglia and macrophage clearance of the inhibitory and toxic debris resulting from damage at the injury site promotes functional improvement in rodent SCI models (Bethea & Dietrich, 2002; Ma et al., 2015). Although the molecular mechanisms of the immune response are complex, they provide important therapeutic targets as they play a crucial role in the anatomical changes that occur around the injury site.

The glial scar is composed of activated astrocytes, OPCs, pericytes, and meningeal fibroblasts and forms within 10-14 days post-injury to help re-establish a barrier to peripheral immune cell infiltration (Burda & Sofroniew 2014; Hackett & Lee 2016; McTigue et al. 2001; Raposo & Schwartz 2014; Whetstone et al. 2003). The formation of the glial scar is vitally important for recovery to occur; studies using methods to ablate the glial scar found increased severity of symptoms and spinal cord damage (Faulkner et al., 2004; Burda & Sofroniew, 2014; Anderson et al., 2016). While the glial

scar is necessary for protection of the intact spinal cord tissue, it also can be inhibitory to axon growth and therefore can act as a double-edged sword (Okada et al., 2006; Pineau et al., 2010). Activated astrocytes not only change their morphology and re-orient their processes to form a physical barrier, but they can also express inhibitory molecules (Povysheva et al. 2018; Tan et al. 2005). After injury, astrocytes and OPCs upregulate chondroitin sulfate proteoglycans (CSPGs), that, like neurocan and neural/glial antigen-2 (NG2), are potent growth inhibitors leading to axonal growth cone collapse (Dou & Levine 1994; Hackett & Lee 2016; Jones et al. 2002; Mckeon et al. 1999; McTigue et al. 2001). Therapies targeting the glial scar, therefore, often aim to reduce CSPGs or alter astrocyte morphology to allow axons to cross through the scar and into the lesion cavity (Chen et al. 2016; Faulkner et al. 2004; Rodriguez et al. 2014).

The fibrotic scar in the lesion core provides yet another, even more inhibitory barrier to axon regeneration. Peripheral cells such as fibroblasts and immune cells expand in the injury core and create a hostile environment for CNS neurons (Barnabé-Heider et al., 2010; Soderblom et al., 2013). Proteins secreted from these cells create a fibrous, stiff, and inhibitory extracellular matrix that differs substantially from the softer, more permissive extracellular matrix of the uninjured spinal cord (Dityatev et al. 2010; Keung et al. 2012). For a severe injury, this peripheral fibrotic scar area acts as a "no-man's land" and is detrimental to axon regeneration (Klapka et al., 2005) . Indeed, many studies that use implanted scaffolds or matrices to provide growth-permissive bridges across the injury core show increased axon growth and functional recovery (Jain et al., 2006; Prang et al., 2006; Joosten, 2012; Thompson et al., 2018; Zaviskova et al., 2018).

Together, the glial and fibrotic scars that form after injury are both important therapeutic targets to increase axon growth and limit tissue damage.

Changes in myelin contribute to axonal dysfunction following SCI

As important as axon regeneration is to recovery, it is only the first of many steps to ensure that the reformed and surviving axonal connections are functional. Many functional deficits are likely due to the loss of myelin leading to less efficient signal conduction rather than a loss of synaptic connections (Goldman & Osorio 2014; Hesp et al. 2015; Mekhail et al. 2012). Therefore, the changes in myelin after injury are additional factors to consider when designing SCI treatments.

Myelin provides insulation to increase the speed and efficiency of neuronal communication by allowing the action potential to be transmitted through saltatory conduction. Oligodendrocytes, the myelinating cells in the CNS, are in close contact with axons to provide nutrients to and allow for communication with neurons (Poliak & Peles, 2003; Baumann & Pham-dinh, 2019). Myelin also provides a layer of protection from any insult or excitotoxicity that can occur after immune cell infiltration (Taniike et al., 2002; Lopez et al., 2012). The widespread death of oligodendrocytes after an injury, therefore, leads to not only loss of myelin and reduction in signal propagation, but also leaves axons vulnerable to further damage (Almad et al. 2011; Black et al. 1991; Goldman & Osorio 2014; Mekhail et al. 2012; Totoiu & Keirstead 2005). Symptoms of diseases like multiple sclerosis, where extensive immune-cell-mediated oligodendrocyte death occurs,

demonstrate the importance of myelin and the detrimental effects on sensory and motor function that can arise following myelin loss (Mahad et al. 2015).

Increasing the number of mature oligodendrocytes is one of the ways researchers have tried to improve myelination after injury (Cao et al. 2010; Erceg et al. 2010; Keirstead et al. 2005; Sun et al. 2013). Interestingly, OPCs proliferate extensively in response to injury, however, many of them fail to differentiate into mature oligodendrocytes to replace those that have died (Almad et al. 2011; Assinck et al. 2017; Goldman & Osorio 2014; Hesp et al. 2015; Segovia et al. 2008). The increased numbers of OPCs can negatively affect axon outgrowth due to their high expression levels of inhibitory CSPGs (Dou & Levine 1994; Jones et al. 2002; McTigue et al. 2001). The lack of factors needed for OPC differentiation, such as glial-derived neurotropic factor (GDNF) and neurotrophin-3 (NT3), is thought to contribute to reduced maturation, and therapies delivering these factors have improved oligodendrocyte differentiation and myelin production (Cao et al. 2005; Sun et al. 2014; Wilkins et al. 2003; Xu et al. 2019).

An interesting dichotomy exists for oligodendrocytes and their progenitors: myelin is beneficial for axon health and function yet is also inhibitory towards axonal regeneration; myelin debris that occurs after oligodendrocyte death both increases inflammation and is strongly inhibitory to axon growth (Chen et al. 2015; McKerracher et al. 1994; Meves et al. 2018). Myelin proteins, such as Nogo and myelin-associated glycoprotein (MAG), can inhibit cytoskeletal reorganization and growth cone extension and studies show that blocking receptors for Nogo on axons can lead to significant increases in axon growth (Merkler et al., 2001; Fournier et al., 2002; Kucher et al., 2018).

Together, these studies suggest that successful targeting of oligodendrocytes and their progenitors may depend on the timing and location of the treatment, thereby adding another layer of complexity to the challenges in treating SCI. Perhaps OPC proliferation and differentiation at the injury site may be detrimental early after injury but would be beneficial either further from the scar border or at later timepoints after axon regeneration has occurred (Almad et al. 2011).

Local Schwann cells aid in the response to SCI

Unlike CNS axons, PNS axons have a high potential for regrowth and recovery after nerve damage, part of which is attributed to the injury response mediated by Schwann cells (SCs; Vargas and Barres 2007). While oligodendrocytes often initiate apoptosis after axonal injury, SCs are capable of de-differentiating and downregulating their expression of myelin proteins after an axon is injured (Guertin et al., 2005; Jessen & Mirsky, 2005). This process of de-differentiation results in a switch from a "myelinating" to a "non-myelinating" phenotype (Griffin & Thompson, 2008). The highly motile non-myelinating SCs are then able to proliferate, phagocytose debris, and secrete growth factors and cytokines that can aid in recovery by removing inhibitory factors and stimulating axon elongation (Fontana et al. 2012; Frostick et al. 1998; Gaudet et al. 2011; Gomez-Sanchez et al. 2017; Jang et al. 2016; Sanchez et al. 2015; Stoll et al. 1989). The non-myelinating SCs then form tube-like structures that provide a conduit by which axon regeneration can occur (Gomez-Sanchez et al. 2017; Thomas & King 1974). After a peripheral axon has

8

recovered, the SCs are able to differentiate into myelinating SCs which re-myelinate the newly generated part of the axon (Barton et al., 2017).

While this response is specific to peripheral nerve injury, local SCs mount a similar response to a CNS injury. The damage caused after SCI can trigger the de-differentiation of nearby SCs which migrate into and fill the injury site (Guest et al., 2005; Nagoshi et al., 2011). Reportedly, SCs contribute to axonal outgrowth into the lesion core by providing a permissive surface for guidance through the hostile lesion core environment (Lu et al., 2007). Additional evidence suggested that SCs can even infiltrate the spinal cord in order to temporarily myelinate surviving CNS axons until oligodendrocytes can differentiate and take over (Jasmin et al., 2000; Jasmin & OHara, 2002; Guest et al., 2005; Totoiu & Keirstead, 2005). Further, there is evidence that OPCs are capable of differentiating into SCs that can also help aid in recovery (Assinck et al., 2017). Studies that use exogenous SC transplants as a method to induce recovery after injury will be discussed later in this chapter.

Assessing anatomical recovery after injury

After identifying pathological therapeutic targets, the ability to evaluate changes and improvement is essential to assess whether a treatment will be successful. The complexity of a SCI presents distinct challenges for designing appropriate assessments. There are, however, a few well-defined methods used in rodent models of SCI to help determine if any anatomical changes at the injury site could be indicative of improvement that would translate to functional recovery.

Distinguishing axon regeneration versus axon sparing

As alluded to above, human SCIs are highly variable and therefore a treatment that may work for one type of injury may not work for another. In response, several different rodent and simian models of SCI that vary in severity, location, and type were developed to test treatments for different conditions. When studying the effects of different treatments, the injury type can be essential to inform what kind of analyses are possible. Mild injury models such as a contusion or dorsal crush are more physiologically similar to human injuries and result in significant tissue and axon sparing. Axon regeneration, therefore, is extremely difficult to evaluate (Steward & Willenberg, 2017). Even slightly more severe injuries, such as hemi-sections, can still leave doubt on whether axon bundles have regenerated or were spared. Models in which axons are completely severed, i.e., a complete spinal cord transection, are therefore considered the most rigorous model to determine if a treatment stimulates axon regeneration (Chen et al. 2015; Steward et al. 2003; Tuszynski & Steward 2012). The downside to transection models, however, is that functional recovery is rare and often subtle, even if axon outgrowth is established. Further, because very few patients present with complete transections, the transection model is not as clinically relevant as other models, and therefore may not be the best option to test functional improvements.

Regardless of the SCI model employed, there are multiple established criteria to convincingly distinguish regenerated from spared axons. Steward et al. (2003) described seven characteristics of regenerating axons that differentiate them from spared axons. Regenerated axons should: 1) extend from the CNS into the peripheral scar tissue, 2) infiltrate and associate with grafts, implants, or transplanted cells, 3) originate from an

area near the injury, 4) form pathways that are indirect or abnormal, 5) grow realistic distances according to the established regeneration rates, 6) contain growth cones at axon tips, and 7) have atypical morphology such as branching. While most regenerating axons will not display all seven criteria, having several of these traits is often sufficient to establish that regeneration has occurred. Other standard, but less accurate, methods include quantifying the area of axons in the fibrotic lesion core but distinguishing between the growth of PNS and CNS axons adds additional complexity with this method (Steward et al. 2003; Thornton et al. 2018; Tuszynski & Steward 2012).

Another issue with assessing axon regeneration includes the difficulty of determining which type of axon may be regenerating. It is possible that the regenerated axons are not connected to circuits that are relevant for functional recovery. Indeed, formation of incorrect connections could lead to chronic pain or even worsen symptoms (Burchiel & Hsu, 2001; Sangari et al., 2019). There are, however, a few markers that can be used to identify specific descending motor associated pathways, such as serotonin (5HT)-positive raphespinal axons. Because there are very few serotonergic interneurons in the rat spinal cord, evidence of 5HT-labeled axons directly caudal to a severe injury site suggests that motor-specific pathways have regenerated (Ghosh & Pearse 2015; Kubasak et al. 2010; Takeoka et al. 2010, 2012).

Neuronal tracers are used to assess axonal origins and connectivity

Molecular tracing techniques are commonly used to assess axonal connectivity and specificity after SCI. There are many types of neuronal tracers and each has its own

benefits and caveats. Retrograde tracers are taken up by axons and transported to the neuron cell body of origin and therefore the presence of the tracer rostral to the injury suggests evidence of regeneration (Card & Enquist, 1999). Unlike anterograde tracers that are often used to identify specific descending motor tracts, retrograde tracers can help distinguish if axons are establishing connections with long-range targets through multiple pathways. Further, because most connectivity following SCI is likely re-established by the reorganization of a relay of interneurons, multi-synaptic retrograde tracers such as rabies viruses are considered the most effective to detect spinal interneurons involved in recovery (Rotto-Percelay et al., 1992; Card & Enquist, 1999; Bareyre et al., 2004).

Pseudo-rabies (PRV) is a unique retrograde tracer that is transported through multiple synapses in adult rats (Rotto-Percelay et al., 1992; Card & Enquist, 1999). PRV that is injected into a muscle such as the tibialis anterior (TA) will be retrogradely transported to somatic motor neurons in the spinal cord and subsequently transported to any cells that are synaptically connected to the labeled motor neurons. This multi-synaptic viral tracer can help elucidate the reorganization of circuits between a muscle and the brain and determine if propriospinal interneurons are involved (Rotto-Percelay et al., 1992; Flynn et al., 2011; Han et al., 2015; Thornton et al., 2018). Obviously, there is no perfect tracer and PRV tracing has one drawback: PRV is also taken up by sympathetic neurons that innervate blood vessels in the muscle and is transported to the thoracic spinal cord via the sympathetic trunk and thus circumvents the injury site altogether (Rotto-Percelay et al., 1992; Kerman et al., 2003; Deuchars & Lall, 2015; Ueno et al., 2018). This caveat can be addressed in several ways. The most definitive option, which

is not feasible in complete SCI models, is to perform a sympathectomy before PRV injection to sever connections between the sympathetic chain and the spinal cord (Daniels, Miselis, & Flanagan-Cato, 2001; Kerman et al., 2003). Alternately, using markers for sympathetic-associated neurons compared to those for somatic motor-associated propriospinal interneurons in a previous study we were able to distinguish whether PRV was likely transported directly across the injury site or not (Thornton et al., 2018).

Challenges for assessing remyelination

Another common therapeutic target to evaluate the efficiency of treatments for spinal cord injury is axon myelination. As with axon regeneration, determining whether myelin sparing or remyelination has occurred can be challenging. There are a few distinguishing characteristics of remyelinated axons, however, that can be assessed with specific techniques: 1) new myelin tends to be thinner than spared myelin (Ludwin & Maitland, 1984; Powers et al., 2012, 2013), 2) the internodal distances (i.e., the length between nodes of Ranvier) in newly remyelinated areas are much shorter than spared myelin (Blakemore, 1974), and 3) the presence of peripheral myelin (i.e., myelin generated by SCs) is indicative of SC infiltration that would not normally occur in the spinal cord (Guest et al. 2005; Jasmin et al. 2000; Jasmin & OHara 2002).

When evaluating myelinated axons, the gold standard has long been electron microscopy to clearly visualize the morphology of a myelin sheath wrapping around an axon (Stoeckenius, 1959). This method, however, can be impractical as the fixation and

processing parameters for quality electron microscopy cannot be easily combined with immunohistochemical methods (Karnovsky, 1965). Therefore, antibodies are more commonly used to distinguish and identify myelin markers. For example, immunohistochemistry for peripheral myelin protein zero (p0) can distinguish peripheral myelin from CNS myelin (often marked by myelin oligodendrocyte glycoprotein, MOG; D'Urso et al. 2018; Gardinier et al. 1992).

When conducting an analysis of axons associated with myelin in the injury core, antibodies can be used to identify myelin associated glycoprotein (MAG; Sternberger et al., 1979). In addition, the number of mature oligodendrocytes and SCs can also be determined with specific markers and may indicate cell survival, migration, or differentiation near the site of interest (Guest et al. 2005; Jasmin et al. 2000; Powers et al. 2012, 2013; Stidworthy et al. 2003). A combination of these techniques can help distinguish whether axons found near the injury are likely myelinated or not. The overall presence of myelin and myelinating cells can be used to assess myelination status, but this fails to distinguish between the prevention of myelin loss versus the promotion of remyelination.

Assessing treatment effects on functional recovery

While increases in axon outgrowth and myelination at the injury site is encouraging, the ultimate goal of any therapy is to improve motor and sensory function. For injured humans, the use of their upper limbs to feed themselves, the ability to stand and take a few steps, or the restoration of bladder and sexual function can make a huge difference

in their quality of life. When it comes to pre-clinical treatment of rodent SCI models, the recovery of functional activity is measured by established methods to help elucidate the level of treatment efficacy.

Observation-based behavioral tests for motor function

Evaluating recovery of motor function in rodent models of SCI can be challenging for several reasons: 1) even if using the same methods, no injury is identical thus can produce variable behavioral results, 2) local spinal circuitry and reflexes respond to stimuli without requiring cortical input or re-connectivity, and 3) much of the motor behavior is dependent on motivation, which is difficult to simulate with rodent models (Steward & Willenberg, 2017). Unlike people, who follow verbal directions, having a rat perform a specified task requires ingenuity and some level of conditioning or training.

The most commonly used method to analyze rodent motor recovery was developed by Basso, Beattie, and Bresnahan (1995), and is known as the BBB open-field locomotor test. The test examines rat hindlimb movement, overall coordination, and body posture during free exploratory behavior. Rats are scored on a 21-point scale by two independent observers. The lower third of the scoring matrix evaluates the range of movement in the hindlimb joints, which is often the maximum recovery seen in severe injuries such as complete transections. The middle third of the scale determines the ability of a rat to support its weight or take steps, while the highest scores focus on coordination and balance. This scoring system works well for mild injuries, but it is not as useful for detecting improvements in severe injury models. Furthermore, the BBB is often criticized

as it lacks a motivated task which negates the need for top-down cortical input to elicit specific behaviors (Eloy et al. 2008).

The main cause of paralysis after injury is the loss of information coming from brain and brainstem structures such as the motor cortex and raphe nucleus. Regeneration of connections to these specific circuits is thought to be important for recovery, and therefore several motivated tasks were developed to encourage animals to perform behaviors that recruit circuits requiring input from the brain. For example, in the ladder task, rodents are trained to climb across a suspended ladder and are scored based on the number of mistakes or misses that occur as they perform the task. This test is often used to assess moderate thoracic or lumbar injuries (Metz & Whishaw, 2009; Onifer et al., 2011). Unfortunately, many of these tasks cannot be performed with rodents that have severe injuries.

After a complete transection in rats at thoracic levels T7-8, all descending motor pathways are severed thereby causing complete hindlimb paralysis. For complete transections, supported hindlimb treadmill stepping is frequently used to assess motor recovery (Cha et al. 2007; de Leon et al. 2011; Takeoka et al. 2011; Ziegler et al. 2011). The limitations of this task, however, are that local central pattern generator (CPG) circuits in the lumbar spinal cord are activated by the sensory feedback from paw placement on the treadmill surface and this activation leads to movement that may be independent of cortical input (Cha et al. 2007; Ichiyama et al. 2008; Lavrov et al. 2006). Climbing on an inclined grid, alternatively, is used to measure recovery of hindlimb function that requires cortical input and will be discussed further in the materials and methods section (Ramon-Cueto et al., 2000; Ziegler et al., 2011; Thornton et al., 2018).

Analyses using electrophysiology after severe SCI

Electrophysiological techniques can assess motor recovery using electrodes embedded in hindlimb muscles to record muscle activity while an animal is performing a behavioral task or receiving cortical stimulation (Steward & Willenberg, 2017). Motor evoked potentials (MEPs), for example, can be obtained from muscle recordings following electrical stimulation directly to the motor cortex. In the context of a SCI, eliciting a response in a hindlimb muscle below a complete transection could indicate an existing or regenerated connection between the lumbar spinal cord and motor cortex i.e., axon regeneration may have occurred (Iyer et al., 2010; Takeoka et al., 2011). The latency between the stimulus and the response is often longer after recovery from injury and can provide further evidence of regeneration through propriospinal circuit relays as signals would pass through multiple synaptic connections (Courtine et al. 2008; Filli & Schwab 2015). Takeoka et al. (2011) recorded MEP responses to transcranial stimulation in the tibialis anterior and medial gastrocnemius 1, 4, and 7-months after injury in lightly anesthetized rats that received olfactory ensheathing cell (OEC) transplants and treadmill stepping therapy. This provided evidence that some physiological connectivity across the injury site was established and was further supported by the loss of this activity following re-transection of the spinal cord at the end of the study.

MEPs rely heavily on artificial stimulation parameters that may not replicate actual physiological relevance. Therefore, understanding the electrophysiological responses in animals while they are awake and performing tasks is important to test if the connections will make a functional difference. While performing a treadmill stepping task, for example, the interactions and coordination between antagonistic flexor and extensor muscles in

both hindlimbs may help distinguish whether a movement is likely reflexive or more controlled and refined. Gerasimenko et al. (2007) found that electrical epidural stimulation (EES) paired with serotonergic agonists improved hindlimb muscle coordination and recovery of EMG amplitude and duration by recording bilaterally from three different muscles involved in stepping.

Unfortunately, there are some drawbacks to using electrophysiological recordings. In long-term studies electrode placement can shift over time thereby resulting in recordings with high background or that are originating from incorrect muscles (Wenger et al., 2016). Regardless, the use of electrophysiology can provide powerful evidence of functional connectivity and rewiring that can be paired with anatomical findings obtained after a study has concluded.

Therapeutic interventions: treatments that target anatomical changes associated with the lesion core

There are several promising SCI therapies that directly target the pathological changes at the injury site, and they involve a wide variety of mechanisms. Some aim to reduce inhibitory factors and increase axon growth, while others decrease tissue damage and increase remyelination. Many approaches include the injection of specific molecules, matrices, cells, or a combination into or around the injury site.

Individual therapies target axon growth and myelination

As mentioned above, there are several challenges to overcome to promote axon regeneration. These include the limited growth potential of adult neurons and the inhibitory CSPGs and myelin debris at the injury site associated with the glial and fibrotic scars. Approaches to overcoming these challenges can vary drastically even if targeting the same molecular mechanism. A genetic deletion of PTEN, a protein that inhibits mTOR signaling leading to reduced axonal growth, was shown to dramatically increase axon regeneration and improve functional recovery in moderate SCI rodent models (Liu et al., 2010). Subsequent studies have employed several different methods to inhibit PTEN function to enhance axonal outgrowth. Experimental designs included the study of conditional genetic knockout mice, injection of PTEN-specific miRNAs into the spinal cord, administration of pharmacological inhibitors, and delivery of RNAs using exosomes (Song et al., 2010; Liu et al., 2012; Walker & Xu, 2014; Du et al., 2015; Goncalves et al., 2015; Zhu et al., 2017). This provides an example by which a single mechanism for recovery that directly targets axons can be differentially manipulated.

Other successful methods of improving axon growth in SCI models have involved 1) removing inhibitory factors in the injury site, such as through delivery of chondroitinase-ABC (Ch-ABC) to degrade CSPGs (Bradbury et al., 2002), 2) increasing growth factor expression, such as using viral delivery of growth factors (Alto et al., 2009), 3) providing more growth-permissive environments, such as injecting fibrin or alginate matrices into the lesion core (Prang et al., 2006; King et al., 2010), 4) increasing clearance of debris, such as increasing microglia phagocytic ability through drug administration, and 5)

promoting vascularization and reducing inflammation, such as through the delivery and uptake of miR-126 into cells at the injury site (Guerrero et al., 2014; Hu et al., 2015).

Other therapies have used similar methods to promote remyelination by administering factors to drive oligodendrocyte differentiation and maturation such as Neurotrophin-3 and Sonic hedgehog (Thomas et al. 2014). As myelin is inhibitory to oligodendrocyte differentiation and to axon growth, inhibitors to certain proteins in myelin can assist with oligodendrocyte maturation. For example, inhibitors for LINGO1 or TROY, proteins that respond to inhibitory Nogo associated with myelin debris, have resulted in significant increases in remyelination (Merkler et al. 2001; Mi et al. 2005; Sun et al. 2014).

A caveat to these molecular approaches, however, is that they can only target a small number of the many mechanisms capable of promoting axonal outgrowth or myelination. Furthermore, many of them would require multiple manipulations or viral infections that would likely be impractical for human use.

Cell transplantation therapies can target multiple mechanisms at once

Transplanted cells, on the other hand, last longer in the injury site and can harness the benefits of several treatments in a single package. Not only can they target multiple mechanisms at once, but they can do so through a variety of methods. Cells can secrete growth factors, cytokines, miRNA-containing exosomes, extracellular matrix-modifying enzymes, and even phagocytose debris. As each cell type has its own combination of effects on the injury site, the type of transplanted cells can be chosen to provide specific functions. Common transplanted cell therapies include neural progenitors (NPCs),

mesenchymal stem cells, OPCs, SCs, OECs, and others (Harrop et al. 2012; Rosner et al. 2012; Silva et al. 2014).

Some cell types, such as NPCs and OPCs, are chosen in order to replace neurons and oligodendrocytes, respectively, that were lost after injury. Studies found that transplanted NPCs differentiated into neurons that have greater axonal growth potential than mature spinal cord neurons and led to extensive growth and increased connectivity of functional circuitry (Lu et al., 2012, 2014; Medalha et al., 2014; Kumamaru et al., 2018). Studies that transplanted OPCs into the spinal cord have had some success, especially in moderate injury models where intact but denuded axons are present (Cao et al. 2005, 2010; Erceg et al. 2010; Keirstead et al. 2005; Sun et al. 2014; Sun et al. 2013). Currently, OPCs derived from human induced pluripotent stem cells (iPSCs) are being optimized to provide a potential allogenic transplantation system for human trials (Wang et al., 2013; Myers et al., 2016). The safety of such transplants will be a concern, however, as NPCs and OPCs have high tumorigenic potentials (Casarosa et al. 2014; Thomas & Moon 2011).

Rather than replacing neurons and oligodendrocytes lost to injury, alternative transplant approaches use non-native cells that have unique properties that are beneficial for SCI recovery. SCs, for example, are used for transplantation due to their ability to promote axon growth, myelinate axons, and modify the injury site (Hill et al., 2006; Woodhoo et al., 2007; Zhang et al., 2013). Several studies have found functional improvements when SCs were transplanted into the lesion core of contused or transected rats (Barakat et al. 2005; Deng et al. 2015; Honmou et al. 1996; Mousavi et al. 2019).

OECs are also often used for transplantation for similar reasons and will be discussed further in the next section.

OEC transplantation as a treatment for SCI

OECs (also known as olfactory ensheathing glia, OEGs) are unique SC-like glial cells that originate from neural crest cells in the olfactory placode (Forni et al., 2011). OECs are capable of performing multiple functions including 1) secreting growth factors such as BDNF to stimulate axon growth, 2) ensheathing and protecting growing axons, 3) providing a permissive substrate and extracellular matrix for axon growth to occur, 4) reducing inflammation, and 5) phagocytosing debris (Chuah et al. 2011; Kocsis et al. 2009; Roet et al. 2011; Runyan & Phelps 2009; Wang et al. 2011; Yang et al. 2013). For these reasons, among others, OECs are a promising treatment for SCI.

OECs are found in two different locations in the olfactory system and there is some debate over the type of OECs that should be used for transplantation (Ekberg & St John 2015; Guérout et al. 2010; Novikova et al. 2011). CNS olfactory bulb-derived OECs are often chosen for their ability to interact with astrocytes and integrate well into the spinal cord, however, isolation of these OECs requires invasive surgeries to remove the olfactory bulb (Chuah, Hale, & West 2011; Higginson & Barnett 2011; Khankan et al. 2015; Ramón-Cueto and Nieto-Sampedro 1992; Ramon-Cueto & Avila 1998; Roet et al. 2011). Conversely, PNS mucosal lamina propria-derived OECs are more easily accessible but are often transplanted without purification and tend to produce less robust effects on recovery (Au & Roskams, 2003; Lu et al., 2006; Centenaro et al., 2011, 2013;

Dlouhy et al., 2014; Stepanova et al., 2018). Our lab has always used olfactory bulb-derived OECs due to their important ability to interact with astrocytes, and therefore we will focus on studies that have used these OECs for SCI treatment.

Functional recovery following OEC transplantation has been achieved in multiple models of SCI including after complete transections. As mentioned above, OEC transplantations combined with step training were able to re-establish functional connections in long-term transection models (Takeoka et al., 2011; Ziegler et al., 2011). Further studies found that OEC transplantation has improved performance on grid climbing, the BBB test, sensory tests, and other behavioral tasks (Keyvan-Fouladi et al., 2003; Kubasak et al. 2010; Pearse et al. 2007; Ramon-Cueto et al. 2000; Takeoka et al. 2012; Ziegler et al. 2011). Autologous olfactory bulb-derived OECs have even resulted in successful functional recovery in a single human patient (Tabakow et al., 2014).

OECs can influence the injury site after SCI

Recovery resulting from OEC transplantation is likely due to multiple mechanisms related to the promotion of axonal outgrowth and tissue sparing. In the Phelps and Edgerton labs alone, *in vitro* and *in vivo* studies showed that OECs increase axon outgrowth through secretion of BDNF and their association with astrocytes, 5-HT axonal outgrowth into the injury core, and removal of myelin debris, and decrease CSPGs in the injury site and immune cell infiltration into the spinal stumps (Khankan et al. 2016; Khankan et al. 2015; Runyan & Phelps 2009).

OECs also affect myelination after transplantation, although their role in the process is not well understood. While OECs do not produce myelin in their native environment, several studies suggest that under certain conditions they produce SC-like myelin and can express peripheral myelin proteins *in vitro* (Babiarz et al., 2011; Plant et al., 2018) and after transplantation (Akiyama et al., 2004; Sasaki et al., 2006, 2011, 2013). The effects of OECs on endogenous myelinating cells also are not well known; OECs and OEC-conditioned media can increase OPC differentiation *in vitro* and are proposed to work synergistically with endogenous, infiltrating SCs (Au et al., 2007; Lamond & Barnett, 2013; Carvalho et al., 2014). OEC interactions with oligodendrocytes and OPC post-transplantation and their direct effects on endogenous infiltrating SCs, however, remain uncertain.

OEC transplant survival

There are only a few studies in the OEC field that have determined OEC transplant survival after injury, with some reporting massive cell death within a few weeks and others reporting survival up to 4 months (Lu et al., 2006; Roet, Eggers, & Verhaagen, 2012; Barbour et al., 2013a). In our previous studies, we could not determine OEC survival as there are no unique markers for OECs to distinguish them from other glial cells. In a short-term experiment, Khankan et al. (2016) transplanted GFP-expressing OECs or fibroblasts (FBs) control cells following complete transection in outbred Sprague-Dawley rats in order to clearly determine if the cells could survive for at least 2 months. This study found that GFP-OECs survived for 4 weeks but died by 8 weeks post-injury. Cell survival, however,

was extended to 8 weeks with the administration of the immune suppression drug cyclosporine. Differences in injury site morphology, axon sparing, and injury site permissiveness between OEC- and FB-transplanted spinal rats that did not receive cyclosporine were most significant between 1-4 weeks post-injury. Similarly, in our most recent study that combined EES and climb training with OEC or FB transplantation in Sprague-Dawley spinal rats, no surviving cells were detected and no significant differences in functional recovery were found between the groups at 7 months post-injury (Thornton et al., 2018). These findings suggest that long-term survival of the transplanted cells is critical in order to maximize the effects of OECs. A few studies reported long-term OEC or neural stem cells transplant survival using different surgical techniques in an inbred rat model (Fischer 344), which inspired changes to the methods used in the current study in order to augment transplant survival (Plant et al., 2003; Lu et al., 2006, 2012).

OEC versus SC transplantation

OECs most closely resemble non-myelinating SCs in how they 1) wrap around axons, 2) have similar gene expression profiles, and 3) are derived from neural crest lineages (Thompson et al., 2000; Wewetzer et al., 2002; Omar et al., 2013; Ulrich et al., 2014). Even their effects on axon growth and functional recovery after SCI are comparable. Many SCI studies have directly compared OEC and SC transplantation with mixed results regarding which therapy is preferable; some concluded that SCs may be better, others favor OECs, and yet others suggest that a mix of the two are best for SCI recovery (Akiyama et al., 2004; Lu et al., 2006; Andrews & Stelzner, 2007; Sorensen et al., 2008;

Techangamsuwan et al., 2009; S. Zhang et al., 2011; Lamond & Barnett, 2013; Barton et al., 2017; Carwardine et al., 2017).

Importantly, the preparation of OECs in these studies varied. When examined carefully, most comparisons between peripheral nerve SCs and OECs from the nasal lamina propria find there is not much difference. Olfactory bulb-derived OECs , however often produce more significant recovery and axon growth (Novikova et al., 2011; Ekberg & St John, 2015). This is believed to be, in part, due to the ability of olfactory bulb-derived OECs to migrate within the spinal cord tissue and better integrate with astrocytes and due to the differential expression of growth-promoting factors (Franssen et al. 2008; Kocsis et al. 2009; Lakatos et al. 2000, 2003; Lamond & Barnett 2013; Lankford et al. 2008; Omar et al. 2013).

Combining injury site-specific treatments

Many recent studies have used a combination of injury site-directed treatments. For example: 1) Lu et al. (2012) transplanted embryonic NPCs in a fibrin matrix containing multiple growth factors and saw a large increase in cell survival, differentiation, and connectivity with moderate functional improvement, 2) Wilkins et al. (2003) and Cao et al. (2005, 2010) studied OPCs that were genetically modified to overexpress glial-derived neurotrophic factor (GDNF), NT3 and other growth factors resulted in increased axon myelination, and 3) Carwardine et al. (2017) transplanted OECs overexpressing Ch-ABC and showed decreased CSPG levels and increased axon sprouting when transplanted in

a canine SCI model. In addition, combinations of cells, such as OECs and SCs, have been transplanted together (Zhang et al., 2017).

Because of the complexity of the injury site it is perhaps not surprising that these combinatorial approaches are able to further improve effects on recovery. Unfortunately, such combinatorial treatments may not alter the injury site enough to produce the larger goals of functional recovery. In addition to these therapies, targeting other areas affected by SCI at the same time may further increase these benefits.

Therapeutic interventions: treatments that do not target the injury site directly

Many of the injury-site targeting treatments require highly invasive surgical procedures especially in comparison to safer therapies such as rehabilitation training or functional electrical stimulation. Therefore, it is important to consider alternative treatments that may result in functional recovery that have moderate or indirect effects on the injury site.

The importance of rehabilitation and training

Rehabilitative training and motor tasks are common following a human SCI, and include activities that target stepping, balance, trunk stability, grasping, or reaching. In rodents, some of the tasks that are used to assess functional recovery are similar, such as treadmill stepping, standing, or climbing (Fouad & Tetzlaff, 2012; Burns et al., 2017). Studies have reported that something as simple as intermittent stretching in rats with SCI can result in marked improvement in behavioral outcomes (Caudle et al., 2015).

Interestingly, other studies found that rehabilitative training can have an influence not only in circuit reorganization and strengthening but can also modify the anatomy of the injury site (Cote & Gossard 2004; Leblond et al. 2008). Additionally, training and exercise is able to increase the expression of growth factors such as BDNF and increase inhibitors of PTEN, thereby leading to increased axon growth and sprouting (Al-majed et al. 2000a; Liu et al. 2012; Vaynman & Gomez-Pinilla 2005).

Electrical stimulation therapies

New advances in electrical stimulation therapy have provided a minimally invasive therapeutic option that can be added to rehabilitative training to enhance functional improvement. Because several studies reported that electrical activity in developing neurons helps increase neuronal survival, axon outgrowth, synaptogenesis, and axon myelination, it follows that electrical stimulation may be useful for the recovery of damaged neurons (Mennerick & Zorumski, 2000; Grumbles et al., 2013; Fields, 2015). In studies using direct electrical stimulation of severed peripheral nerves, for example, the injured motor neurons had increased levels of growth factors like BDNF. Such electrical stimulation-induced increases in growth factors were shown to lead to recovery of cell survival and axon outgrowth and myelination. This is believed to occur partly due to BDNF-mediated activation of the cyclic-AMP pathway (Al-majed et al. 2000a; Al-majed et al. 2000b).

A common target of electrical stimulation for SCI is the spinal cord itself. Electrical epidural stimulation (EES) is one of the most promising treatment methods to enhance

functional recovery both in human and rodent SCI after injury. Extensive studies conducted by the Edgerton lab at UCLA found that EES of the lumbosacral spinal cord can induce coordinated muscle activity and recovery of stepping and/or standing ability following severe SCI in humans and rodents; this effect was greatly enhanced when locomotor training was performed together with EES (Edgerton et al. 2015; Gad et al. 2013; Gerasimenko et al. 2007; Ichiyama et al. 2005, 2008; Lavrov et al. 2006, 2008; Shah et al. 2016). Pharmacological agents such as 5-HT agonists were also found to enhance stepping performance and EMG activity when paired with EES (Courtine et al. 2009; Gerasimenko et al. 2007; Ghosh & Pearse 2015; Lavrov et al. 2008). Evidence showed that such improvements likely occur through activation and reorganization of the lumbosacral central pattern generator circuits, potentially through sensory propriospinal input refinement (Courtine et al. 2008, 2009; Lavrov et al. 2006; Lavrov et al. 2008; Shah et al. 2016; Tillakaratne et al. 2014). Although EES can induce plasticity of neuronal circuitry, the cellular and molecular mechanisms of this circuit reorganization and its effects on the injury site remain unclear.

Combining stimulation and other therapeutic approaches

The steps towards combinatorial approaches also include rehabilitative training and electrical stimulation with other injury-site directed treatments. For example, treadmill training was used successfully with the delivery of Ch-ABC into the injury site, and functional recovery was seen when OEC transplantation was combined with regular step training in rodent SCI models (Lakatos et al. 2003). Administration of neuromodulating

drugs such as serotonergic agonists in conjunction with EES and treadmill training improved motor outcomes in rodent SCI (Gerasimenko et al., 2007; Alam et al., 2017). These studies together provide a foundation for continuing the exploration of combinatorial treatments targeting different aspects of SCI.

The current study proposes to combine the transplantation of olfactory ensheathing cells within a fibrin matrix with long-term, consistent electrical epidural stimulation and climb training as a treatment for severe spinal cord injury in rats.

RESEARCH PROJECT AIMS

Aim 1: Compare the behavioral effects of long-term treatment with electrical epidural stimulation (EES) and climb training combined with olfactory ensheathing cell (OEC) versus control transplants following severe spinal cord injury.

    Hypothesis 1.1: OEC-transplanted spinal rats will perform better on non-biased, score-based behavioral tests including the BBB open-field locomotor test and an adapted climbing BBB, than media or fibroblast (FB) controls 5-6 months after injury.

    Hypothesis 1.2: OEC-transplanted rats will show more incidences of push-offs and increased coordination of EMG activity in the tibialis and soleus hindlimb muscles while climbing than control rats.

Aim 2: Determine OEC and FB long-term cell survival and whether OEC transplantation combined with EES and climb training improved injury site parameters related to axon regeneration compared to controls.

    Hypothesis 2.1: The use of inbred rats and delayed transplantation techniques will facilitate OEC and FB cell survival throughout the 5-6-month experiments and surviving OECs will create bridges across the injury site and associate with axons in both the injury site and spinal stumps.

    Hypothesis 2.2: The injury sites from OEC-transplanted rats will have a higher volume of spared tissue and neuron survival near the injury site than controls.

Hypothesis 2.3: OEC-transplanted rats will have more serotonergic axons near or crossing the injury, axons on glial bridges, and evidence of pseudorabies virus (PRV) labeled neurons immediately rostral to the injury site than control rats.

Aim 3: Determine the long-term effects of EES and climb training combined with OECs or controls on myelin found in and around the injury site.

Hypothesis 3.1: Spinal rats that received OEC transplants will have a higher percentage of myelin-associated axons in and around the injury site compared to controls.

Hypothesis 3.2: OEC-treated rats will have greater numbers of oligodendrocytes and Schwann cells (SCs) in the lesion core and spinal stumps than controls.

Hypothesis 3.3: Surviving OECs will closely interact with SCs and oligodendrocytes and subsets of OECs will express SC- and OEC-specific markers.

CHAPTER 2. MATERIALS AND METHODS

Animals

All experiments were approved by the Chancellor's Animal Research Committee at UCLA. Wild type (Charles River, SAS-FISCH) and transgenic green fluorescent protein (GFP)-expressing (RRRC P40OD011062, University of Missouri) Fischer 344 rats were housed in pairs or in isolation with access to food and water *ad libitum* under standard housing conditions. Forty wild-type Fischer 344 rats (9-11 weeks old) received four surgeries: 1) electrode implantation, 2) a complete transection at the mid-thoracic level, 3) cell or media transplantation, and 4) injection of PRV in two hindlimbs. After transection, their bladders were expressed 3x/day for two weeks and then at least twice/day until the end of the study. The rats were perfused 5.5-6.5 months after injury with periodate-lysine-4% paraformaldehyde (4% PLP). Olfactory bulb-derived OEC and dermal fibroblast (FB) cultures were isolated from GFP-expressing Fischer 344 rats (8-10 weeks old).

Primary Cultures

Olfactory bulb-derived OECs were isolated and cultured from 8-10 week old GFP-expressing Fischer 344 rats and then immunopurified as described in Khankan et al. (2016) and Ramon-Cueto et al. (2000). Two rats for each primary culture received a lethal dose of ketamine and xylazine followed by removal of the olfactory bulbs. The meninges, white matter, and blood vessels were removed from the bulbs and the first two layers were isolated. The tissue was then dissociated with 0.1% trypsin (Life Technologies #1509046) and 0.01% DNase (Sigma #10-104-159-001). Cells were then plated on a

flask containing 25 μg/mL poly-L-lysine (Sigma #P9155) and cultured for 5-7 days. Cells were then immunopurified with an antibody against p75-nerve growth factor receptor (p75, 1:5, mouse, Hybridoma line 192) and cultured for 5-7 more days in the presence of 2 μM bovine pituitary extract (Gibco #13028) and 20 μg/ml forskolin (Sigma #F6886) before transplantation.

Skin dermal FBs were isolated from rats used for OEC cultures and used as the cellular control group (cohort F2). Skin biopsies were obtained after shaving the abdomen of a euthanized rat and the dermal layers were isolated and dissociated (Takashima, 1998; Khankan et al., 2016). Cells were passaged 1-2 times over the course of 12-14 days *in vitro* before transplantation.

Implantation of head-plug, epidural stimulation electrodes, and EMG electrodes

All surgeries were conducted under sterile conditions with rats under heavy anesthesia (1-2.5% isoflurane gas). The methods for implantation of the head-plug and the stimulating and recording electrodes are identical to those described in Thornton et al. (2018). Briefly, the skull was exposed by a midline incision and two stainless steel screws were embedded into the skull to contact the dura mater. A head-plug (Amphenol) connected to Teflon-coated wire electrodes (Cooner Wire #AS632) was then secured with dental cement and the wire electrodes were passed under the skin. Rats received partial laminectomies at spinal levels L2 and S1 and stimulating electrodes connected to the head-plug were secured along the epidural surface of the spinal cord (Ichiyama et al., 2005; Iyer et al., 2010). For EMG electrode placement, the soleus and tibialis anterior

(TA) muscles were exposed bilaterally. Two electrodes were embedded into each muscle and proper placement was verified by eliciting contraction following stimulation (Gad et al., 2013). Finally, a ground wire was placed subcutaneously, and the skin was sutured followed by disinfection with betadine. Rats were administered fluids and pain medication before recovering in an incubator. Rats received pain medication and antibiotics for 5 additional days under close supervision.

Complete transection

Three weeks after electrode implants, the rats received a transection surgery. The method of transection differed for the two cohorts in this study: for cohort F1, we used a microaspiration method and for cohort F2, a microscissor cut method.

Microaspiration method: Rats from cohort F1 received a transection performed similar to the method used in Lu et al. (2012). Briefly, a partial laminectomy was performed at spinal level T7-T9 and a small incision was made in the dorsal dura, leaving the rest of the dura mater intact. Scissors were inserted through the hole and the spinal cord was cut at two sites spaced 1 mm apart. Afterwards, a sterile glass pipette tip connected to a surgical vacuum hose was inserted through the incision in the dura and a 1 mm section of spinal cord tissue was removed. The surgeon carefully scraped with a probe to sever any remaining axons. The dura was then closed with a suture and Gelfilm (Pfizer Injectables #9-0283-01).

Microscissor cut method: The method used for cohort F2 was identical to that used in Takeoka et al. (2011), Khankan et al. (2016), and Thornton et al. (2018). A partial

laminectomy was performed at spinal level T7-T9 and the dura was cut longitudinally and laterally to expose a large section of the dorsal spinal cord. Micro-scissors were then used to completely cut the spinal cord at a single site while leaving most of the ventral, but not dorsal, dura intact. The surgeon separated and lifted the rostral and caudal stumps and scraped the surface of the dura with a probe to sever any remaining axons. The dura was then sutured and gelfilm was placed between the dura and overlying tissue.

Following both transection methods, a stainless-steel bar was attached to the spinous processes at levels T7 and T13 as in Takeoka et al. (2011). The skin was then sutured and sterilized with betadine. Rats were administered fluids and pain medications and recovered in an incubator. Spinal rats had their bladders expressed 2-3 times/day for the remainder of the study (5.5-6.5 months). Once a week, rats were weighed, and their urine was tested using Multistix 10 SG reagent strips (Siemens) to monitor for bladder infection or kidney dysfunction.

Cell Transplantation

Two weeks after spinal cord transection, the same T7-T9 spinal cord levels were exposed and new incisions were made in the dura. Purified OECs or FBs were dissociated from the culture flasks and re-suspended at a concentration of 100,000 cells/µl in serum-free Dulbecco's Modified Eagle Media (DMEM, Life Technologies #11995-065) containing calpain inhibitor (MDL28170, 50 mM, Sigma #M6690) for spinal stump injections. For lesion core injections, cells (50,000 cells/µl) were suspended separately in fibrinogen (25 mg/ml, Sigma # F6755) and thrombin (25 U/ml, Sigma #T5772) containing calpain

inhibitor (Lu et al., 2012). Fibrinogen and thrombin containing ~200,000 total cells were injected into the center of the lesion core. Approximately 300,000 total cells suspended in DMEM were injected 1 mm rostral and caudal to the injury site at 4 depths as described in Ramon-Cueto et al. (2000). Media controls received injections of DMEM in fibrinogen and thrombin with calpain inhibitor into the lesion core and DMEM containing calpain inhibitor into the stumps.

Climb training and stimulation

Prior to surgeries, rats were trained to climb an inclined 1-inch grid at 60- and 90-degree angles onto a covered plexiglass platform (A. Ramón-Cueto et al., 2000; Ziegler et al., 2011; Thornton et al., 2018). Rats were trained and tested on the apparatus during our light-cycle. Starting 1-month post-transection, rats were further trained at a 60-degree incline for 20 mins, 3 times/week, for 4-5 months, while receiving 40 Hz EES. Stimulation was administered at a voltage rate that was sub-threshold, i.e. 95% of palpable muscle response (Thornton et al., 2018). EES was paired with climb training, rather than treadmill stepping as used in previous studies, for three reasons: 1) EES effects on treadmill stepping is believed to be a result of local spinal circuit activation and reorganization based on proprioceptive feedback rather than connectivity with cortical circuits (Cote & Gossard, 2004), 2) climb training is used as a motivated task that encourages the recruitment of cortical motor circuits (Ramón-Cueto et al., 2000), and 3) we found that climb training combined with OEC-transplantation had beneficial effects on recovery in a

previous study (Ziegler et al., 2011). Rats received food rewards when they climbed onto the top of the platform. They also were trained in pairs for additional social motivation.

Behavioral tests

BBB open-field locomotor test: The Basso, Beattie, and Bresnahan (BBB) open-field locomotor test is widely used to assess functional recovery after rodent SCI (Basso et al., 1995). For our study, BBB tests were administered beginning at 1-month post-injury and were conducted either monthly or bi-monthly for 4-5 months. Briefly, rats were allowed to explore a large enclosed area for 4 minutes. During exploratory behavior, two independent observers scored hindlimb movements, body posture, stepping ability, and coordination according to the 21-point scale.

Grid climbing tests: Rats were tested pre-injury on the climbing apparatus at 60- and 90-degree inclines. Starting at 1-month post-injury, rats were tested either monthly or bi-monthly on both 60- and 90-degree inclines, either with or without EES. Rats were given three trials for each of the 4 test conditions. Trials began with placement on the grid by the handler and ended when the rat's body was positioned fully on the platform. The amount of time spent on the grid varied between trials. Video and hindlimb EMG activity were recorded during each test and synchronized for analyses (Thornton et al., 2018).

Traditional climbing analyses

Videos obtained during climbing tests were reviewed by two separate observers to assess hindlimb function while performing the task. Observers counted the number of "pushoffs"

that occurred when a rat placed its hindpaw on a grid rung and then "pushed off" of the rung with clear ankle extension, as described (Ziegler et al., 2011). The rat did not have to complete the step for a pushoff to be counted, however a pushoff was discounted if it appeared uncontrolled or spastic. Each pushoff was confirmed by a third observer. Pushoff numbers were averaged between groups (OEC, Media, or FB) and were compared across three time-points (0, 2, and 5 or 6 months) either with or without EES for both angles (60- or 90-degrees).

Videos were synchronized with EMG recordings and the EMG activity corresponding to the video frames for each pushoff was analyzed. Peak, mean, and integral amplitudes of the soleus and TA muscles of both ipsi- and contralateral hindlimbs were normalized to pre-injury levels and were compared between each condition.

Climbing-adapted BBB development

We developed a novel analysis for the climbing test to provide a more in-depth quantification of rodent climbing ability. Because climbing requires complex movements and coordination beyond the ability to push off a grid, we adapted features from the BBB and horizontal ladder task, and added other climbing-specific features to assess five different categories of climbing ability (Basso et al., 1995; Metz & Whishaw, 2009). This climbing-adapted BBB scoring system (cBBB) went through several iterations to establish reliable criteria to assess 1) rodent hindlimb movement, 2) paw placement on grid rungs, 3) weight-bearing ability, 4) pushoffs and step completion, and 5) body coordination and posture, primarily of the trunk and tail. Rats were scored by 2-3 independent observers

on a 33-point scale. The scoring sheet for the cBBB is shown in the results section and the evaluation guide is in the appendix.

PRV Injections and perfusion

After the completion of the behavioral tests (at 5.5- or 6.5-months post-injury), GFP- and RFP-expressing pseudorabies virus (PRV) was used to trace hindlimb connectivity across the injury site in the experimental rats. PRV surgeries were conducted in a BSL-2 biosafety cabinet as described in Thornton et al. (2018). Briefly, rats were deeply anesthetized with isoflurane and an incision was made to expose the muscles of one hindlimb. RFP-expressing PRV was injected into the soleus (4 injections of 2.5 µL of Bartha-614, 9.05 X 10^8 pfu/mL) using a 30-gauge stainless steel needle. The needle was left in place for 2 minutes to prevent backflow, and then the muscle and skin were sutured. The process was repeated on the other hindlimb, however, the contralateral TA received injections of GFP-expressing PRV (8 injections of 2.5 µL of Bartha-152, 1.21 X 10^9 pfu/mL). The sides of injections varied for each rat. Rats were perfused in the biosafety cabinet 4 days post-PRV injection.

Tissue preparation

Rats were deeply anesthetized with intraperitoneal injections of ketamine (90 mg/kg) and xylazine (10 mg/kg) and perfused intracardially with 4% PLP. Tissue was post-fixed in 4% PLP for 3 hours. Dissected spinal cords were cryoprotected in a 30% sucrose solution for

2-3 days. Spinal cords were blocked and embedded in OCT (Fisher #4585) and stored at -80°C. Spinal cord injury sites were sectioned sagittally (25 μm thick) on the cryostat and slide-mounted in series. Each slide contained 5-6 sections 400 μm apart for a total of 16 slides. This provided comparable samples between rats for analyses.

Immunohistochemical procedures

To evaluate the injury site, slides containing every 16th section were labeled using immunohistochemistry for 3-4 antigens per slide. Briefly, slides were washed in buffer (0.1% Tris-buffer with 1.4% sodium chloride and 0.1% bovine serum albumin, TBS-BSA, pH 7.4) and permeabilized with a 0.1 - 0.5% Triton-X in TBS-BSA solution for 10-15 mins. Slides were incubated in blocking solution (0.05 – 0.1% Triton-X in TBS-BSA) with 5% normal donkey serum (NDS, Jackson ImmunoResearch Laboratories, #017-000-121) for 1-1.5 hrs and then incubated with primary antibody diluted in blocking solution for 16-24 hours (unless noted). Primary antibodies, their sources, concentrations, and variable incubation times are listed in Table 1. Sections were then washed in buffer and incubated in blocking solution containing species-specific fluorescent secondary antibodies (Table 2). For some analyses, sections were counterstained to identify the nuclei with Hoechst dye (Bis-benzimide, 1:500 Sigma-Aldrich #B2261). Sections were washed briefly with 70% ethanol and incubated in 1X TrueBlack (Biotium, #23007) in 70% ethanol for 45-85 seconds, rinsed in TBS-BSA, and then coverslipped in either Fluorogel (Electron Microscopy Sciences #17985-10) or EverBrite (Biotium #23001) mounting media.

Injury site analyses

After immunolabeling, slides were imaged on an Olympus AX70 microscope with an AxioCam HRcRv.2 or on a Zeiss LSM 780 confocal microscope system using ZEN software (Zeiss). Images were analyzed using Neurolucida and Neurolucida Explorer (v10, MicrobrightField) and were pseudocolored, organized, and edited in Adobe Photoshop.

Spared tissue volume and transplant survival: Tissue analysis was performed on spinal cord sections of the injury site labeled for the astrocytic scar border (glial fibrillary acidic protein, GFAP, and aquaporin-4), the fibrotic lesion core, (fibronectin, FN), and GFP-positive transplanted cells (OECs or FBs). Images of 5-6 sections on one slide per rat were arranged in Adobe Photoshop. Total spinal cord tissue area was traced using the Neurolucida contours tool between 5000 μm rostral and 5000 μm caudal to the lesion epicenter. Lesion core and cyst areas were also traced. Tracings were aligned to create a 3-D reconstruction in order to estimate volume measurements as described in Thornton et al. (2018). The lesion and cyst volumes were subtracted from the total cord volume and are reported as a percent of the total cord volume.

Neuron cell counting: Spinal cord sections of the injury site were immunolabeled to identify neurons using an antibody for Fox-3 (NeuN, a label for most neurons), the glial scar border (GFAP), transplanted OECs or FBs (GFP), and PRV-positive cells. The area of the spinal stumps was determined by tracing the GFAP area 1000 μm rostral and caudal to the injury core (excluding cyst area). The number of NeuN-positive cells were counted within this area and are reported as a ratio of the number of cells to the area

measured (Khankan et al., 2016). The distance of the closest neurons to the rostral and caudal scar borders and to the lesion epicenter were also measured for each rat.

Axons and myelin: Serotonergic axons were immunolabeled for serotonin (5HT), transplanted cells were labeled for GFP, and the lesion core was outlined using GFAP to delineate the scar border. The area of 5HT-positive axons in the lesion core was normalized by the number of sections analyzed for each rat (Khankan et al., 2016). On a separate slide, antibodies for axonal neurofilament (NF200, NF), myelin associated glycoprotein (MAG), GFP, and GFAP were used to identify axons, myelin, transplanted OECs and FBs, and the glial scar border, respectively. To determine the amount of axonal overlap with myelin and transplanted cells, the area of NF-positive axons in the lesion core was traced and grouped into four categories: 1) NF-positive only, 2) NF- and MAG-positive, 3) NF- and GFP-positive, and 4) NF-, MAG-, and GFP-positive areas. Areas of NF-labeled axons that clearly originated from dorsal or ventral roots were excluded. The lesion core and transplanted cell areas also were measured, and the data is represented as either a percent of the total lesion core area, cell transplant area, or total NF-positive area.

SCs and OECs in the lesion core: Non-myelinating and myelinating SCs were identified with p75 or peripheral myelin protein zero (p0), respectively. The lesion core was outlined using GFAP and the area of GFP-positive cells in the lesion core was determined. The p75- and p0-positive areas were traced in the lesion core, as well as the p75 and p0 overlap with GFP-positive cells. The data is represented as a percent of the total lesion core area or GFP-positive cell area.

OPC and oligodendrocyte counting: The GFAP-positive spinal cord area within 500 μm of the injury epicenter and the GFAP-negative lesion core area was determined. Slides were also immunolabeled with an antibody for adenomatous polyposis coli (APC i.e. the CC-1 antigen) to identify oligodendrocytes and glutathione-S-transferase-pi (GSTpi) to identify oligodendrocyte progenitor cells (OPCs) and counterstained with Hoescht. Three categories of Hoescht-positive cells were counted within the spinal cord and lesion core areas: 1) CC1-positive mature oligodendrocytes, 2) CC1- and GSTpi-double positive immature oligodendrocytes, and 3) nuclear GSTpi-positive OPCs. Cell counts were normalized to spared spinal cord tissue.

Statistics for Behavioral Analyses

BBB, cBBB, and pushoff behavioral analyses were compared separately for the two cohorts of rats used in this study. For each, comparisons were made across 3-5 timepoints (1-5 months, 1, 2, 4, and 6 months, or 0, 2, and 5 or 6 months post-injury) and 2 groups (OECs and media or FBs), and for the climbing tests, they were also compared across 2 stimulation conditions (with and without epidural stimulation) and 2 grid angle climbing conditions (60- and 90-degree inclines). The means of each condition were compared using a parametric repeated measure (mixed) model to account for the multiple data points for each rat. A Shapiro-Wilks test and normal quantile plots were determined to confirm that errors followed a normal distribution as described in Thornton et al. (2018).

Statistics for Anatomical Analyses

For injury site analyses, both cohorts had small sample sizes thereby requiring the use of re-sampling techniques to conduct statistical comparisons. Using a non-parametric bootstrap estimation program in R (3.2.2; R Cor Team 2015), the null hypothesis was simulated 10,000 times to reduce assumptions regarding data distribution. The group means and effect sizes were compared to the bootstrapped confidence intervals to generate *p*-values as in Thornton et al. (2018).

Table 1: List of primary antibodies

Antigen	Species	Company	Catalog #	Dilution
Green fluorescent protein (GFP)	Chicken	Aves Lab	GFP-1020	1000
Glial fibrillary acidic protein (GFAP)	Mouse Rabbit Goat	BD Biosciences Dako Sigma-Aldrich	556327 Z0334 SAB2500462	1000 10000 1000
Fibronectin (FN)	Mouse	BD Biosciences	5338748	200
NeuN (neuron cell bodies; Fox-3)	Mouse	Millipore	MAB377	1000
Myelin-associated glycoprotein (MAG)	Mouse	Millipore	MAB1567	1000
Nerve growth factor receptor (p75)	Mouse		Clone 192	20
APC (oligodendrocytes; CC1)	Mouse	Calbiochem	OP80	250 (3 days)
Aquaporin-4 (Aqp-4)	Rabbit	Sigma-Aldrich	A5971	1000
Neurofilament-200 (NF)	Rabbit	Millipore	AB1989	1000
Peripheral myelin marker zero (p0)	Rabbit	Millipore	ABN363	1000
Glutathione transferase-pi (GST-pi)	Rabbit	Enzo	ADI-MSA-102E	1000
Serotonin (5HT)	Goat	Immunostar	20079	5000

Table 2: List of Secondary Antibodies

Antigen	Conjugate	Species	Company	Catalog #	Dilution
Chicken	488	Donkey	Jackson ImmunoResearch Laboratories	703-545-155	500
Goat	405	Donkey	Jackson ImmunoResearch Laboratories	705-475-003	250
Goat	488	Donkey	Jackson ImmunoResearch Laboratories	705-545-003	500
Goat	Cy3	Donkey	Jackson ImmunoResearch Laboratories	705-165-003	500
Goat	647	Donkey	Jackson ImmunoResearch Laboratories	705-605-147	200
Mouse	405	Donkey	Jackson ImmunoResearch Laboratories	715-475-151	250
Mouse	555	Donkey	Life Technologies	A31570	500
Mouse	647	Donkey	Jackson ImmunoResearch Laboratories	715-605-150	200
Rabbit	555	Donkey	Life Technologies	A31572	500
Rabbit	647	Donkey	Jackson ImmunoResearch Laboratories	711-605-152	200

CHAPTER 3. RESULTS

Experimental timeline and design

The experimental design and timeline are outlined in Fig. 1A-B. To address the aims of this study, Fischer 344 rats were first trained to climb an inclined grid before undergoing four separate surgeries which are detailed in the methods section. The initial surgery implanted EES electrodes between lumbosacral levels L2 and S1, EMG recording electrodes bilaterally into the TA and soleus muscles, a transcranial stimulator, and a headplug. Three weeks later, pre-injury behavioral tests were conducted to obtain baseline recordings. Rats then received a transection injury at thoracic level T8/T9. Two weeks later, spinal rats received transplant injections of OECs, media, or FBs with a calpain inhibitor into the spinal stumps and into the lesion core within a fibrin matrix. Following two weeks of recovery, rats began climb training while receiving sub-threshold (95%) EES for 20 min/day, 3x/week. Behavioral tests were performed monthly or bimonthly. At ~5.5-6.5 months post-injury, spinal rats received injections of RFP-expressing pseudorabies virus (PRV) into one tibialis anterior (TA) and GFP-expressing PRV into the contralateral soleus. Rats were perfused 4 days after the PRV injections.

This study includes the analyses of two slightly different cohorts of Fischer 344 rats referred to as Fischer cohort 1 (F1), and Fischer cohort 2 (F2). The experimental design and timeline are parallel for both cohorts, except for the variables listed below (Fig. 1B):

1) *Method of transection*: For the F1 cohort, we used a microaspiration injury method to reduce damage to the dura mater and therefore increase the likelihood of cell transplant survival (Lu et al., 2012). This method resulted in several rats with incomplete injuries. To

ensure more complete transections for the F2 cohort we returned to a microscissor cut transection method used previously by our lab (Takeoka et al., 2011; Khankan et al., 2016; Thornton et al., 2018).

2) *Control transplants*: Experimental spinal rats for both cohorts received OEC transplant and media injections were used as the control for the F1 cohort. FB transplants as a cellular control for the F2 cohort.

3) *Timing of behavioral tests and final endpoint*: Due to the incomplete injuries in the F1 cohort of spinal rats these rats were perfused at 5.5 months post-injury and behavioral tests were conducted monthly to better assess their functional recovery over time. The completely transected F2 spinal rats were perfused at the intended 6.5 months post-injury time point and bimonthly behavioral tests were conducted to reduce stress.

All other methods and treatments were identical for both cohorts. Due to the small number of rats that completed the entire study (F1, n = 9; F2, n = 10), we reported individual data first and then combined the two cohorts if appropriate.

All groups improved on the BBB open-field locomotor test

We used the BBB open-field locomotor test to assess general recovery of hindlimb movement during simple exploratory behavior. The scale ranges from 0 (no movement of the hindlimbs) to 21 (full recovery of complete and coordinated stepping). Scores were obtained by two independent observers and averaged as described (Basso et al., 1995).

For cohort F1, rats were tested monthly for 5-months post-injury. Each leg was scored individually and averaged (Fig. 2A). At 1-month post-injury, OEC- and media-treated rats had an average score of 2.2 +/- 3 and 1.7 +/- 1.6, respectively (Fig. 2A, green diamonds and blue circles). These scores indicate a slight range of movement in only 1-2 hindlimb joints. Between months 1 and 2, OEC-treated rats improved to an average score of 4.3 +/- 2.2 ($*p$ = 0.017) corresponding to extensive movement of several hindlimb joints, whereas media-treated rats did not improve significantly (3.1 +/- 1.7, p = 0.075). At month 3, however, both groups had improved from month 1 (OEC, 5.7 +/- 1.4, $***p$ = 0.0001; Media, 4.4 +/- 2.8, $***p$ = 0.0008). This improvement was maintained during month 4 (OEC, 5.4 +/- 1.5, $***p$ = 0.0004; Media, 4.33 +/- 3.1, $**p$ = 0.0011) and month 5 (OEC 5.7 +/- 1.9, $***p$ = 0.0001; Media 6.2 +/- 2, $***p$ < 0.0001). The only significant improvement was detected when the scores at month 1 were compared to other months. Final scores at month 5 correspond to extensive movement of multiple hindlimb joints.

At month 1, rats from cohort F2 also had average BBB scores that corresponded to mostly slight movement of the hindlimb joints (Fig. 2B, OEC, 3.2 +/- 1.8, green diamonds; FB, 2.1 +/- 2.2, red circles). Most of the OEC-treated rats in this cohort did not improve between months 1 and 2 (4.1 +/- 1.8, p = 0.203). FB-treated rats, on the other hand, had a significant increase to an average score of 4.1 +/- 1.7 ($**p$ = 0.0075). Compared to month 1, the average scores increased for both groups at months 4 (OEC 5.4 +/- 1.8, $**p$ = 0.0019; FB 3.9 +/- 2, $*p$ = 0.021) and 6 (OEC 5.5 +/- 2.4, $**p$ = 0.0011; FB 4.6 +/- 2, $**p$ = 0.0013). These scores corresponded to extensive movements of several joints. As with rats in the F1 cohort, no significant change was detected compared to any other month except for month 1.

The number of pushoffs during climbing did not change for OEC-treated rats

Because the BBB is not task oriented, it has been criticized as a reliable measure for recovery of functional connectivity with rostral circuits (Pessoa de Barros Filho et al., 2008). Therefore, we also analyzed changes in hindlimb movement on a motivated grid-climbing task. Rats were tested on the same grid apparatus used for climb training and EES treatment at inclines of both 60- and 90-degrees both with (+ EES) and without stimulation. Both video and EMG recordings were obtained during these tests.

One measure of recovery we assessed on the grid climbing task was the number of pushoffs, i.e., the number of times a rat planted its hindpaw and pushed off a rung of the grid, as described previously (Ramon-Cueto et al., 2000; Thornton et al., 2018; Ziegler et al., 2011). For OEC-treated rats in the F1 cohort, no change in pushoff numbers was detected between 2- and 5-months post-injury with (Fig. 3A-B, dark green bars) or without (Fig. 3A-B, light green bars) EES at either 60- or 90-degree inclines. There was, however, a decrease in the number of pushoffs for media-treated rats at a 60-degree incline while receiving EES between months 2 (3.3 +/- 3) and 5 (0.3 +/- 0.6, **p = 0.0016, Fig. 3A, dark blue bars). There were no other changes for media-treated rats (Fig. 3A-B, light and dark blue bars).

The number of pushoffs for OEC-treated rats in cohort F2 also did not change over time for any condition (Fig. 3C-D, light and dark green bars). For FB-treated rats at month 6 while climbing at 60-degrees, there was a slight effect of EES administration (1.3 +/- 0.5, Fig. 3C, dark red bars) that increased the number of pushoffs compared to conditions without stimulation (0.3 +/- 0.5, *p = 0.02, Fig. 3C, light red bars). The same trend

occurred at a 90-degree incline but only at month 2 instead of 5 (Fig. 3D); the average

number of pushoffs with EES was 2 +/- 2.5 (Fig. 3D dark red bars) compared to 0.5 +/-

0.6 without EES (*p = 0.012 Fig. 3D, light red bars). Overall these results suggest that the

OEC and EES treatments did have consistent effects on the average number of grid

pushoffs during climb training.

A climbing-adapted BBB scoring system was developed to assess climbing ability

While a rat attempts to climb a grid, there are many more features to their movements

that occur in addition to grid pushoffs. Indeed, the video recordings of the climbing tests

contain rich information on rat hindlimb and body movements. To quantify and analyze

the climbing more thoroughly, we created a novel 33-point scoring system adapted from

the BBB and ladder task and named it the climbing-adapted BBB, or cBBB (Basso, et al.,

1995; Onifer et al., 2011). The cBBB assesses multiple features of climbing behavior in

five categories:1) joint movement, 2) paw placement, 3) weight bearing, 4) pushoffs and

steps, and 5) body control (primarily of the trunk and tail movements). Development of

the cBBB underwent multiple revisions to determine which features were most important

for climbing and what point allotments should be given to each feature. Examples of

different climbing features that were evaluated on the cBBB and the final cBBB score

sheet and scoring guide are shown in Fig. 4 and the assessment guide used for scoring

is included in the Appendix, Item 1.

Scores on the cBBB assessment scale varied slightly between time points and groups

Videos of the climbing tests were rated using the cBBB scoring system by two independent observers who were not involved in cBBB development. Spinal rats in cohort F1 had no significant changes from month 2 to 5. Only when OEC-treated rats were climbing at a 90-degree incline at month 5 did EES administration improve scores (18.6 +/- 5.1, Fig. 5B, dark green bar) compared to conditions without EES (14.6 +/- 3.5, *p = 0.012, Fig. 5B, light green bar). Rats in the F2 cohort, however, did have a few more changes. Scores for OEC-treated rats climbing at a 60-degree incline with EES (Fig. 5C, dark green bars) decreased from month 2 (14.9 +/- 2.0) to month 6 (11.5 +/- 5.0, *p = 0.011). The scores for FB-treated rats climbing at a 60-degree incline also decreased, but only in conditions without EES, specifically between months 2 (14.3 +/- 1.3, Fig. 5C, light red bars) and 6 (7.7 +/- 1.9, ***p = 0.0001). In addition, the cBBB scores for FB-treated rats climbing at a 60-degree incline at month 2 combined with EES (11.3 +/- 1.4, Fig. 5C, dark red bar) decreased compared to scores without EES (14.3 +/- 1.3, *p = 0.024, Fig. 5C, light red bar). When climbing at 90-degrees under the same conditions at month 2, however, FB-treated rat scores increased with EES administration (16 +/- 1.3, Fig. 5D, dark red bar) compared to conditions without EES (12.6 +/- 3.2, *p = 0.0275, Fig. 5D, light red bar). These results indicate that EES may have had inconsistent effects on climbing abilities, however more evidence would be needed to make further conclusions.

EMG recordings of hindlimb muscles did not produce reliable or consistent results

Muscle activity of the soleus and TA, antagonistic muscles important for stepping, was recorded for both hindlimbs during climbing tests to assess changes in muscle activation patterns (Gad et al., 2013; Thornton et al., 2018). To analyze these changes, we looked specifically at EMG patterns during steps or pushoffs. Because the activation patterns of the soleus and TA during stepping are well characterized and distinct in intact rats, instances of steps and pushoffs can be compared to pre-injury patterns. Typical pre-injury stepping patterns consist of long bouts of soleus activation followed by shorter bursts of TA activation, and the ipsilateral soleus and TA are rarely active concurrently (Fig. 6A-B, top images marked month 0). In addition to steps and grid pushoffs, we also looked at activation patterns during "breach periods" when the rat was climbing over the top of the platform. A breach period began when the rat placed her forepaws on the platform surface and ended when the entire body was on the platform. We chose to assess the breach periods because these periods require voluntary recruitment of hindlimb muscles rather than forelimb use which is difficult due to the slippery surface of the platform. Also, each rat had at least 3 breaches per trial, as opposed to the variable and infrequent periods of steps or pushoffs post-injury.

The step, pushoff, and breach periods were identified using video footage and the corresponding EMG patterns were isolated and assessed for the peak, mean, and integral amplitudes. For rats in cohort F1 we compared changes in rectified traces normalized to values at month 0 and analyzed them by group (OEC vs media), timepoint (2- or 5-months post-injury), stimulation conditions (with or without EES), and climbing angles (60- or 90-degrees). We also assessed the values without normalization, or with normalization to

resting periods (results not shown). These analyses provided highly variable results, and thus no conclusions could be drawn about treatment effects on the recovery of muscle activation patterns (data not shown).

Despite inconsistent group data, we were able to identify several trends. After injury, soleus and TA activation patterns were less coordinated, more erratic, and contained shorter bursts compared to pre-injury patterns (Fig. 6A-B, months 0 vs. 2 and 5). Additionally, there were more frequent instances of concurrent activation between the soleus and ipsilateral TA for both hindlimbs (Fig. 6 A-B, co-activation plots on the right of each panel, months 0 vs. 2 and 5). Otherwise, surprisingly few differences were seen between trials without and with EES (Fig. 6 A-B, +EES). At month 5, and occasionally at month 2, many traces showed evidence of broken wires; in many traces we detected either the complete absence of activity despite limb movement on the corresponding frames of video, or extremely high and consistent EMG activity despite the absence of limb movement. Rats in cohort F2 showed the same trends and lack of consistency (data not shown). Unfortunately, we were unable to draw conclusions about treatment effects from these analyses.

Transplanted OECs and FBs survived 5-6 months post-transplantation

After completing the behavioral tests and PRV surgeries, the spinal rats were perfused to analyze the spinal cord. Several of these analyses focused on changes that occurred primarily at and around the injury site. First, we assessed transplanted-cell survival. Because previous methods in our lab using outbred Sprague-Dawley rats and an acute

transplant method resulted in transplant death before 8-weeks post-injection (Khankan et al., 2016), a goal of the current study was to increase the survival of transplanted cells by switching to an inbred Fischer 344 rat model and a delayed transplant technique. To evaluate transplanted cell survival, we examined spinal cord sections of the injury site that were immunolabeled for the astrocytic glial scar (Fig. 7, GFAP, light blue) and GFP-positive OECs or FBs (Fig. 7, green). Surviving GFP-positive cells were found in all OEC-transplanted rats in both cohorts F1 (4/4, Fig. 7A-C) and F2 (4/4) and in 3/6 FB-transplanted rats in the F2 cohort (Fig. 7D-F). Most FBs were found in large clumps in the spinal stumps (Fig. 7D-F, yellow arrowheads) and were rarely located within the GFAP-negative lesion core (Fig. 7D, asterisk). OECs, conversely, were often present in clusters or integrated into chain-like patterns in both the lesion core and the spinal stumps. We also detected evidence of clear OEC "bridges" between the two spinal stumps in at least two rats, as illustrated by the example shown in Fig. 7A-C (yellow arrowheads). This suggests that the changes in the rat model and transplant procedures drastically improved cell survival and that OECs can survive in the toxic lesion core for long periods of time. As both cohorts had surviving cells, it also suggests that the method of transection did not seem to alter the viability of the transplanted cells.

Spared tissue volume did not differ between OEC-, media-, or FB-treated rats in either cohort

The spinal cord undergoes acute and chronic tissue damage after a severe injury that leads to the formation of a glial scar made of astrocytes and OPCs, a fibrotic scar

composed of inhibitory peripheral cells (i.e., the lesion core), and fluid filled cysts (Kubasak et al., 2008; Takeoka et al., 2011). To assess whether cell treatment affected tissue sparing at the injury site, we identified the glial scar border with GFAP and Aquaporin-4 (Fig. 8A, C-F, light blue), transplanted cells with GFP (Fig. 8A, C-F, green), and the lesion core with FN (not shown, asterisks) in multiple spinal cord sections. Estimated volumes of the glial scar, lesion core, cysts, transplanted cells, and total spinal cord within 5000 μm rostral and caudal to the lesion core epicenter were calculated by creating a 3-D reconstruction. The average percent spared tissue was determined as described previously (Thornton et al., 2018). Fig. 8A shows an example of a series of sagittal sections compiled across the width of one spinal cord from one spinal rat that were traced and combined into a 3-D rendering (Fig. 8B). No differences were found when the percent spared tissue was compared between groups in either the F1 or F2 cohorts (Fig. 8G, H). The presence of surviving cells, regardless of whether they were OECs or FBs also did not appear to affect tissue sparing (Fig. 8I, right panel), nor did the type of injury. The cyst and lesion volumes also did not differ between any of the groups (data not shown).

Further analysis of the spinal sections revealed interesting trends in lesion site morphology in the different cohorts. In the F1 cohort, the injury site morphology varied greatly between each spinal rat. Some rats had extremely large caudal and/or rostral cysts (Fig. 8D, Fig. 9B), whereas others had well-preserved tissue with smaller cysts in both stumps (Fig. 8A-C, Fig. 9A). We also noted that 2/4 OEC- and 4/5 media-treated rats in the F1 cohort had distinct areas of GFAP-positive tissue that were continuous between the rostral and caudal sides of the injury (Fig. 9A-B, marked by yellow

arrowheads). These connections indicate that the initial injury was likely incomplete, but nevertheless resulted in severe SCIs. To prevent such variability in the injury sites for cohort F2, we switched to the complete transection method we used in previously (Takeoka et al., 2011; Khankan et al., 2016; Thornton et al., 2018). The injury sites for cohort F2 were more consistent; 8/10 rats contained a large rostral cyst and a more preserved caudal stump (Fig. 8E-F). Only 1/10 rats had evidence of an incomplete injury (Fig. 9C). Despite the lack of differences in spared tissue measures, these data show that there may be traits in injury site morphology that differ between the two cohorts.

The average density of NeuN-positive cells near the injury site did not differ between OEC-, media-, or FB-treated spinal rats

Following a SCI there is widespread death of neurons near the lesion site that are not easily replaced. In theory, however, the greater the number of neurons close to the injury site, the more likely these neurons can re-establish connections (Takeoka et al., 2011; Khankan et al., 2016). To measure neuron survival near the injury, NeuN-positive neurons (Fig. 10A-F, red) were counted within 1000 μm rostral and caudal to the injury epicenter in every 16th section/rat. Cell counts were normalized to the area of GFAP-positive tissue (Fig. 10A, C, and D; light blue) and is reported as a density measurement. When the NeuN density was compared between groups, no differences were determined for either cohort or when the cohorts were combined (Fig. 10G-I). Interestingly, each group appeared to have a single outlier with significantly more NeuN-positive cells than the others. The distances between the two closest neurons from each stump and of the

neurons closest to the scar border and lesion epicenter (Fig. 10A-F, yellow arrowheads) also did not differ between groups in either cohort or when combined (data not shown).

5-HT-positive axon area in the lesion core was larger in OEC- compared to either media- or FB-treated rats

Increasing axonal outgrowth at the injury site is an important target for many SCI treatments. Serotonergic (5-HT-positive) axons relay signals from the raphe nucleus to produce locomotion, and due to the small number of local sources of 5-HT in the spinal cord, they also provide a useful measure to assess the recovery of motor circuit-specific axons (Ghosh & Pearse, 2015; Kubasak et al., 2010; Takeoka et al., 2010). Studies suggested that OECs have potent effects on 5-HT-axonal outgrowth (Kubasak et al., 2008; Khankan et al., 2016; Thornton et al., 2018), and therefore we assessed 5-HT-positive axons that extended into the lesion core in rats at 5.5- and 6.5-months post-injury (Fig. 11A-D, arrows). When comparing the normalized areas of 5-HT in the lesion core for the rats in cohort F1, we found that OEC-treated rats (83,011 +/- 29,939 μm^2) had significantly more 5-HT than media-treated rats (38,038 +/- 20,861 μm^2, *p = 0.03, Fig. 11I). The area of 5-HT in the lesion core in cohort F2 was also significantly greater in OEC-treated rats (50,118 +/- 35,826 μm^2) than in FB-treated controls (6,893 +/- 3,666 μm^2, *p = 0.025, Fig. 11J). When the two cohorts were combined (Fig. 11K), the 5-HT area was greater in OEC- (66565 +/- 35258 μm^2) compared to FB- (**p = 0.0013) but not media-treated rats (p = 0.151). These results suggest that OECs increased 5-HT-positve axonal outgrowth into the lesion core, especially when compared to transplanted FBs.

OECs but not FBs are associated with 5-HT-positive axons that project past the rostral scar border

When the injury site sections were examined further, 5-HT axons were found caudal to the lesion in several rats in cohort F1. An image from one of the OEC-treated rats shows that 5-HT-positive axons were detected in GFAP-negative areas on the caudal side of the lesion core but only in areas where OECs were present (Fig. 11E-H, white arrowheads). Although the 5-HT axons do not cross the lesion core in this image (Fig. 11), most likely the axons originated from the rostral border and crossed the injury site in other sections. Unlike in cohort F1, no 5-HT axons were found in the caudal stump in the F2 cohort, although OECs in the rostral stumps and scar border often associated with 5-HT fibers. We never detected 5-HT axons that associated with transplanted GFP-positive FBs either rostral to the injury site or in the lesion core. The different associations between the two transplanted cell types and axons provide further evidence that surviving OECs, unlike transplanted FBs, likely contribute to 5-HT axonal outgrowth.

Both 5-HT- and NF-positive axons crossed the lesion core on OEC bridges in a completely transected rat

One OEC-treated rat in the F1 cohort had an area where OECs filled the lesion core and created multiple bridges between the spinal stumps. We asked if axons used these bridges to cross the lesion core. In spinal sections of this rat, we found several 5-HT-positive axons associated with OECs that crossed the lesion core and penetrated into the caudal stump (Fig. 12A-F, red, arrowheads). In a section 100 µm lateral to the section in

Fig. 12A-F, many neurofilament (NF)-positive axons (Fig. 12G-L, red) also appeared to project across the lesion core along OEC bridges (Fig. 12G-L, arrowheads). These two examples suggest that the surviving OECs may have played a direct role in protecting and promoting outgrowth of 5-HT- and NF-positive axons across the GFAP-negative lesion core.

OEC-treated rats had a greater density of NF-positive axons in the lesion core than either media- or FB-treated rats

To further assess general axonal outgrowth, we measured the area of NF-positive axons in the lesion core and normalized it to the total area of the lesion core in each rat to provide an area density measurement (Fig. 13A-E, NF-positive axons in white). Consistent with our previous findings (Thornton et al., 2018), OEC-treated rats had a greater amount of NF in the lesion core in both cohorts compared to controls and when combined (Fig. 13F-H). For cohort F1, OEC-treated rats had a greater overall density of NF (32.5 +/- 4.5%, Fig. 13F) than media-treated rats (18.8 +/- 6.0%, $*p = 0.011$). For cohort F2, the density of NF was also greater in OEC- (27.9 +/- 4.1%, Fig. 13G) than in FB-treated rats (15.2 +/- 8.0%, $*p = 0.023$). When combined, the same trend remained where the density of NF was greater in OEC-treated rats (30.2 +/- 4.7%, Fig. 13H) compared to either media ($*p = 0.025$) or FB controls ($**p = 0.002$). These results further emphasize the potent effects that OEC transplantation has on axonal outgrowth.

NF-positive axons in the lesion core were more frequently associated with the myelin protein MAG in OEC- compared to media- and FB-treated rats

Axon myelination is another important target for SCI repair. Sparing or regeneration of myelin is important for axon health and function (Taniike et al., 2002; Lopez et al., 2012; Goldman & Osorio, 2014). As a potential indicator of axon myelination, we assessed whether or not axons in the injury site associated with myelin-associated glycoprotein protein (MAG). As we did not conduct electron microscopy, the gold standard to confirm that myelination has occurred, we cannot definitively conclude that these axons are myelinated based solely on their association with MAG. This association, however, is suggestive that myelin is present. We calculated the percentage of the area of NF-positive axons in the lesion core (Fig. 13A-E, white) that overlapped with MAG-positive immunoreactivity (Fig. 13A-E, MAG shown in red, arrows). The percent of MAG- and NF-positive area in OEC-treated rats (86.6+/- 4.3%, Fig. 13I) in cohort F1 was greater than in media-treated rats (73.4 +/- 6.3%, $*p$ = 0.013). In cohort F2, MAG/NF overlap did not differ between OEC- (79.3 +/- 4.8%) and FB-treated rats (71.7 +/- 6.2%, p = 0.13, Fig. 13J). When the cohorts were combined, OEC treatment (82.9 +/- 5.8%) increased MAG/NF overlap compared to media- and FB-treatment ($*p$ = 0.027, $**p$ = 0.0064, Fig. 13K). The increased association between axons and MAG in OEC-treated rats, therefore, suggests that OECs may influence the presence of myelin in the core of the injury site.

Areas of the lesion core containing transplanted OECs, but not FBs, had a greater percent density of NF-positive axons than areas without cells

When analyzing the amount of NF and MAG in the GFAP-negative lesion core, we noticed that areas with OECs typically contained a high density of axons compared to areas without OECs. This contrast of NF density with and without OECs in the lesion core is shown in Fig. 13B-D (areas with NF and OECs are indicated by yellow arrowhead) and even more convincingly in Fig. 14A-F (areas with NF and OECs are indicated by arrowheads, whereas NF in areas without OECs are marked by arrows). Conversely, we found that areas with transplanted FBs rarely had NF immunoreactivity, as shown in Fig. 14G-L. Although this image shows FBs that are near, rather than directly in, the lesion core, the difference in the pattern of NF immunoreactivity in areas with GFP-positive FBs (Fig. 14G-L) is in stark contrast to the pattern associated with OECs (Fig 14A-F). Surprisingly, MAG immunoreactivity remained high in areas with FBs despite the lack of axons. Accumulated growth-inhibitory MAG-positive myelin debris near the transplanted FBs may have contributed to the low levels of axon growth into areas with FBs (McKerracher et al., 1994).

When we compared NF density in areas of the lesion core that contained OECs (76.5 +/- 2.6%, Fig. 14M, green dots) to areas where OECs were absent (25.1 +/- 4.5%, dark grey dots) in cohort F1, we found that there was a distinct and significant increase in the density of NF-positive axons (***p = 0.0006). Although the total density of NF-positive axons was greater in OEC- than in media-treated rats (reported in Fig. 13), the areas without OECs in the OEC-treated rats (25.1 +/- 4.5%) had similar NF densities as the media-treated lesion cores (18.8 +/- 6.0%, Fig. 14M, grey dots). This suggests that

the differences seen between these two groups are due to the direct presence of the OECs in the lesion core.

For cohort F2 we also assessed the NF density in areas with transplanted FBs in addition to areas with OECs (Fig. 14N). As in cohort F1, the density of NF in areas with OECs (64.7 +/- 5.3%, Fig. 14N, green dots) was significantly greater than areas without them (26.2 +/- 2.9%, **p = 0.005, dark grey dots). The density of NF in OEC areas was also greater than the NF density in lesion core areas where transplanted FBs were present (26.2 +/- 3%, *p = 0.016, Fig. 14N, red dots). Unlike areas with OECs, areas with and without FBs did not differ in the density of NF detected (Fig. 14N, red and dark grey dots), however FBs were only detected in the injury sites of 2 of the 6 rats. As reported in Fig. 13, the overall density of NF was greater in OEC- than in FB-treated rats, and unlike in cohort F1, this was also true even in areas without OECs (26.2 +/- 2.9) compared to areas without FBs (*p = 0.014, Fig. 14N, dark grey dots).

Finally, when the OEC-treated rats from both cohorts were combined, the same trends were seen. The average percent area of NF in the entire lesion core was greater in OEC- than in either media- or FB-treated rats. Areas with OECs (70.6 +/- 25.7%) had a greater density of NF than areas without them (25.7 +/- 3.6%, ***p = 0.0001, Fig. 14O) in the same lesion core. Together we found that NF-labeled axons associated with OECs significantly more than with FBs in the injury core (32.4 +/- 13.6, **p = 0.0025, Fig. 14O).

Areas with transplanted OECs have higher expression of peripheral, Schwann cell-like myelin than areas without OECs

After finding that OEC-transplantation increased the amount of NF that associated with MAG in the lesion core, and therefore possibly myelinated axons, we next sought to determine the cellular origin of the myelin. SCI can cause de-differentiation of local Schwann Cells (SCs) that then migrate into the injury site. These SCs either provide trophic support for axon growth (non-myelinating SCs), or re-differentiate to myelinate axons in the injury site and reportedly even in the spinal stumps (myelinating SCs; Guest et al., 2005; Lu et al., 2007; Nagoshi et al., 2011). We thus assayed the average area of p0 immunoreactivity, a peripheral myelin marker of myelinating SCs, in the lesion core of the spinal rats (Fig. 15A-I, red). Fig. 15 shows examples of p0 expression 300 μm lateral from the same OEC- and FB-spinal cord sections shown in Fig. 14. The large group of OECs on the caudal side of the injury had high levels of p0 expression (Fig. 15A-E, yellow arrow), whereas areas with FBs usually had lower levels of p0 immunoreactivity (Fig. 15F-I, yellow arrow). In certain conditions, OECs can produce p0-positive myelin and therefore p0 expression may not be limited solely to SCs (Franklin et al., 1996; 2003; Sasaki et al., 2006).

In cohort F1 we found that OEC-treated rats had a similar percent area of p0 in the entire lesion core (28.6 +/- 3.7%, Fig. 15J, light grey dots) compared to media-treated rats (24.7 +/- 8.1%, Fig. 15J, light grey dots). In areas where OECs were present, however, there was an increase in the density of p0 immunoreactivity (48.5 +/- 7.5%, Fig. 13J, green dots) compared to areas without them (26.0 +/- 3.1%, **p = 0.0027, Fig. 13J, dark grey dots). Because of the close association of OECs and SCs in these areas, it is difficult

to distinguish which cell type expresses p0 at this magnification. Possibly, therefore, this increase may be due to the presence of myelinating SCs and/or myelin-producing OECs.

Areas with transplanted OECs contain high levels of p75 immunoreactivity compared to areas without OECs or with FBs

Non-myelinating SC infiltration into the lesion core and spinal stumps can be beneficial to recovery due to their abilities to promote axonal outgrowth, clear debris, and differentiate into myelinating SCs (Frostick et al., 1998; Griffin & Thompson, 2008; Sanchez et al., 2015). To analyze the level of SC infiltration into the injury core, we quantified the area of p75 expression, a marker of both non-myelinating SCs and OECs, in the lesion core (Fig. 15A-I, dark blue). Importantly, OECs commonly express p75 and can closely integrate with SCs. Therefore, it was difficult to distinguish infiltrating SCs from the transplanted OECs (Fig. 15A-E, yellow arrowhead) at low magnification. Areas in the caudal stumps with FBs had low levels of p75 immunoreactivity (Fig. 15F-I, yellow arrowhead) compared to surrounding regions (Fig. 15F-I, thin white arrowhead), a result suggesting that there are low levels of non-myelinating SC infiltration into the transplanted FB grafts.

In cohort F1 we found that OEC-treated rats had similar levels of p75 in the total lesion core (48.53 +/- 6.51%) compared to media-treated rats (43.3 +/- 12.5%, Fig. 15K, light grey dots). In areas without OECs, this was also true (37.2 +/- 6.3%, Fig. 15K, dark grey dots), however in areas where OECs were present, there was a large increase in p75 immunoreactivity (87.6 +/- 8.0%, ***p = 0.0006, Fig. 15M, green dots). Because of

the close association of the GFP-positive OECs and GFP-negative SCs in these areas, it is difficult to distinguish which cell type is expressing p75 in this analysis.

Transplanted OECs vary in their expression of p75 and p0

Because we initially transplanted p75-positive OECs, we asked if they continued to express p75 or if some surviving cells instead expressed p0 at 5-6 months post-transplantation. To address these questions, we examined confocal images of OECs in the lesion core. Fig. 16A-E shows an example of GFP-positive OECs (green) that also expressed p0 (Fig. 16 A-E, red and green overlap, yellow arrows) or p75 (blue and green overlap, yellow arrowheads), or did not express either marker (green only, small white arrows). We did not detect any cells that expressed both p0 and p75, however. In this area, p0-positive myelinating SCs (red) and p75-positive non-myelinating SCs (blue) are also present and interact with the different types of OECs. Many of the OECs in the spinal stumps also appeared to express p75 or p0 (not shown). This suggests the originally p75-positive OECs were able to modulate their expression levels of different markers, possibly indicating the presence of at least 3 subtypes of OECs associated with the injury sites.

The density of oligodendrocytes and OPCs at the glial scar border did not differ between OEC- and media-treated rats

After SCI, there is widespread cell death of oligodendrocytes in addition to neurons. This results in demyelination of axons around the injury (Almad et al., 2011; Black et al., 1991;

Totoiu & Keirstead, 2005). After injury, OPCs proliferate and contribute to the glial scar but often fail to efficiently differentiate into mature oligodendrocytes to promote recovery of myelination (Goldman & Osorio, 2014; Hesp et al., 2015). Oligodendrocytes and their progenitors vary in their expression levels of GSTpi and CC1 (Bhat et al., 1996; Tamura et al., 2007). OPCs can be identified by the expression of nuclear GSTpi and the lack of expression of the CC1 antigen (Fig. 17, green, yellow arrowheads), whereas oligodendrocytes typically express the CC1 antigen, and varying levels of GSTpi, in the cytoplasm (Fig. 17B-E, yellow arrows). To determine if OEC treatment had any effect on the density of oligodendrocytes or OPCs in the spinal stumps close to the injury core, we counted the number of CC1-positive oligodendrocytes (Fig. 17A-E, red, yellow arrows) and nuclear GSTpi-positive, CC1-negative OPCs (Fig. 17A-J, green and grey overlap, yellow arrowheads) within 500 µm to the injury site epicenter. Cell counts were normalized to tissue area to get an approximate density measurement. When compared, we found no differences in the density of CC1-positive oligodendrocytes (Fig. 17K) or nuclear GSTpi-positive OPCs (Fig. 17L) between OEC- and media-treated rats in cohort F1.

Oligodendrocytes and OPCs are in the lesion cores of some OEC-treated rats

While p0-positive SCs and OECs may account for the presence of myelin in the injury site, another alternative is that the CNS-derived oligodendrocytes could provide a source of myelin for axons in the lesion core. Oligodendrocytes and OPCs are typically only found in the GFAP-positive spinal cord tissue. In our study, however, we detected a small number of OPCs and oligodendrocytes in the lesion core of some of the spinal rats.

Confocal images shown in Fig. 17F-J depicts an area of the GFAP-negative lesion core with CC1-positive oligodendrocytes (red and green overlap, yellow arrows) and nuclear GSTpi-positive, CC1-negative OPCs (green and grey overlap, yellow arrowhead) in an OEC-treated rat. The presence of CC1- and GSTpi-double positive oligodendrocytes (red and green overlap, yellow arrows) is particularly interesting; as oligodendrocytes mature, GSTpi expression moves to the cytoplasm until it eventually gets downregulated in fully mature oligodendrocytes (Bhat et al., 1996; Tamura et al., 2007). This finding suggests that OECs may have enhanced the differentiation and survival of new oligodendrocytes in the injury site. While these sections were not labeled for OECs, adjacent sections confirmed that OECs were present in this area and associate with oligodendrocytes and OPCs in the lesion core and spinal stumps (data not shown).

Axons may be partially myelinated by newly differentiated oligodendrocytes in areas of spared ventral white matter in incomplete spinal cord injuries

As mentioned earlier, several rats in cohort F1 contained regions of ventral white matter that were likely spared during the initial injury. An example of an incomplete injury in an OEC-treated rat is shown in two nearby sections in Fig. 18A and F. The presence of straight, continuous NF-positive axons (Fig. 18A-E, white, arrows) in the ventral GFAP-positive tissue (Fig. 18A-E, light blue) is consistent with an incomplete injury (Steward et al., 2003). Many of the axons in this region are closely associated with MAG (Fig. 18A-E, red, yellow arrow), and therefore are likely myelinated.

When we examined oligodendrocyte and OPC markers in a spinal section 125 μm lateral to the one seen in Fig. 18A, we found several CC1-positive oligodendrocytes (Fig. 18G-J, red, yellow arrow and arrowhead) in organized columns in the intact ventral white matter. This suggests that the MAG seen in Fig. 18A-E may be derived from local oligodendrocytes. We also found several CC1- and GSTpi-double positive immature oligodendrocytes (Fig. 18G-J, red and green overlap, yellow arrowhead) that may indicate that oligodendrocyte differentiation occurred at 5.5 months post-injury. Many GSTpi-positive, CC1-negative OPCs were detected around the dorsal scar borders (Fig. 18G-J, green, small white arrows) and in the GFAP-negative lesion core (Fig. 18G-J, thin white arrowhead). These may provide continual sources of new oligodendrocytes or may contribute to the inhibitory glial scar. Media-treated rats with incomplete injuries also appeared to contain mature and immature oligodendrocytes along the intact spinal cord with many OPCs in similar locations (data not shown).

Transplanted OECs closely associate with myelinating cells in the lesion core

OEC interactions with myelinating cells after transplantation are generally not well documented. Several papers reported OEC and SC interactions and co-transplanted both cell populations together (Au et al., 2007; Zhang et al., 2017), however only a few studies have considered OEC effects on oligodendrocytes and OPCs (Lamond & Barnett, 2013; Carvalho et al., 2014). In our study we found evidence of transplanted OECs interacting with axons co-localized with the myelin protein MAG, myelinating SCs, and

oligodendrocytes in the lesion core. Confocal images of such interactions in the lesion core are illustrated in Fig. 19.

In Fig. 19A-F, GFP-positive OECs (green) interact with and wrap around NF-positive axons (white) in the lesion core. In addition, many of these axons are also associated with MAG (red) as numerous OECs are seen intertwined with the MAG-positive cells (yellow arrowheads). Images from the lesion core of an OEC-treated rat (Fig. 19G-K) depict GFP-positive OECs in close association with myelinating, p0-positive cells (red, yellow arrows) and non-myelinating, p75-positive cells (blue, small white arrows). Both p75-positive and p75-negative OECs (green, yellow arrowheads) were entwined with the GFP-negative SCs. In Fig. 19L-P, OECs (green, yellow arrowhead) are closely associated with immature oligodendrocytes (CC1- and GSTpi-labeled, red and blue, yellow arrows) and OPCs (GSTpi only, blue, small white arrow) in the lesion core. Together, these results suggest that OECs associate with axons and with myelinating cells and their progenitors within the normally hostile lesion core and suggest that OECs facilitate the association between axons and myelin proteins in addition to axonal outgrowth.

CHAPTER 3.2. FIGURES AND LEGENDS

Figure 1:
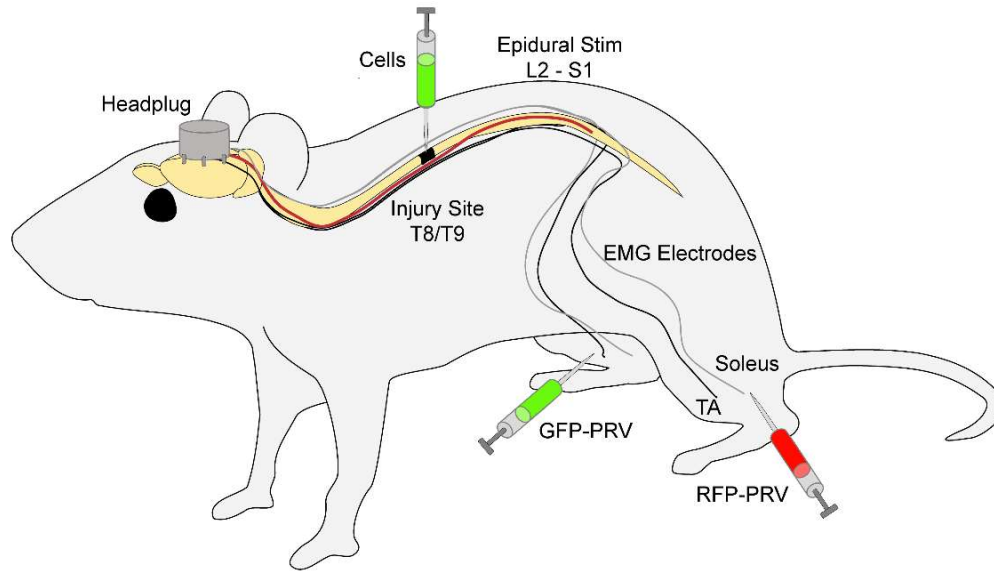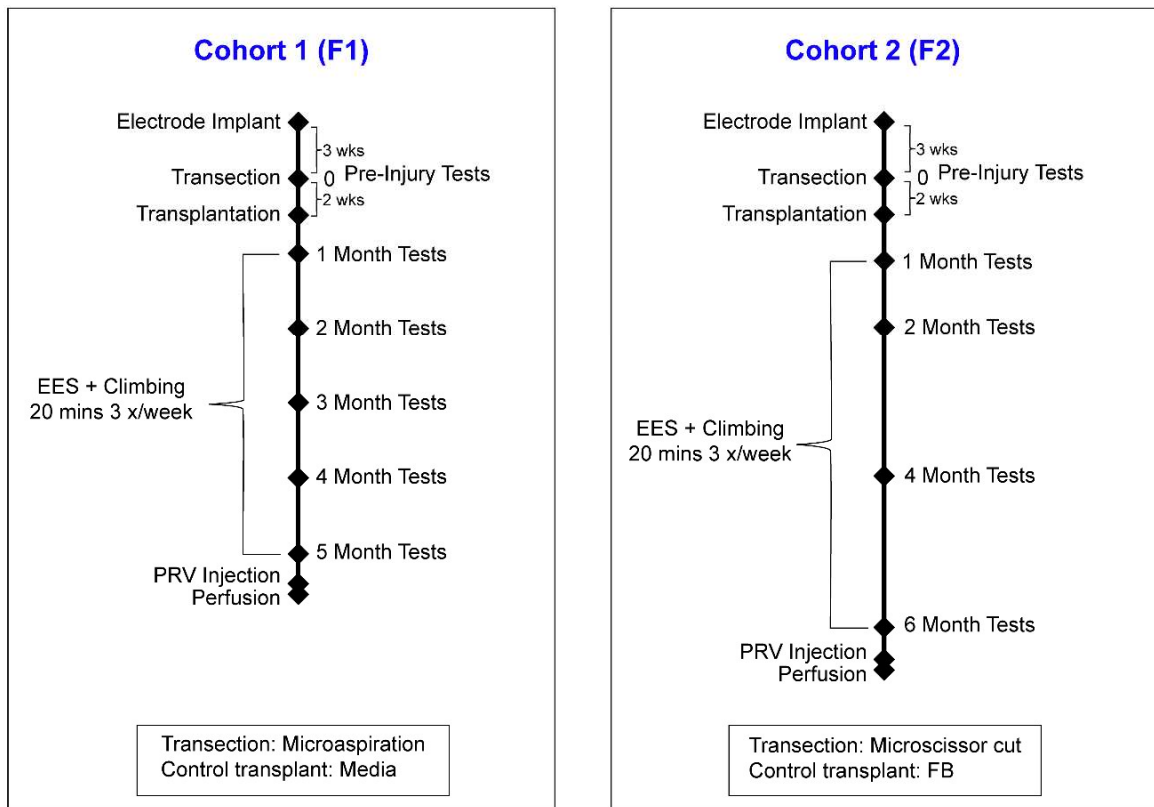
Figure 1 Legend: Experimental design with Fischer 344 rats.

A: The diagram shows a rat with a headplug (grey cylinder) affixed to the skull. The headplug is attached to EMG electrodes that were implanted bilaterally into the soleus and tibialis anterior (TA, grey and black wires) and an epidural stimulation wire was implanted at spinal level L2-S1 (red wire). Rats also received a transection at spinal level T8/T9 (black mark on the spinal cord) followed by a delayed cell transplantation of GFP-expressing OECs, media, or FBs (cells, green syringe). At the end of the study, GFP- and RFP-expressing PRV was injected into the TA and contralateral soleus muscles, respectively (green and red syringes). **B**: Study timelines for cohorts F1 and F2 of the surgeries, electrical epidural stimulation (EES) and climb training therapy, and behavioral tests. Note the differences in the transection methods, control transplants, frequency of behavioral testing, and study endpoints between the two cohorts.

Figure 2:
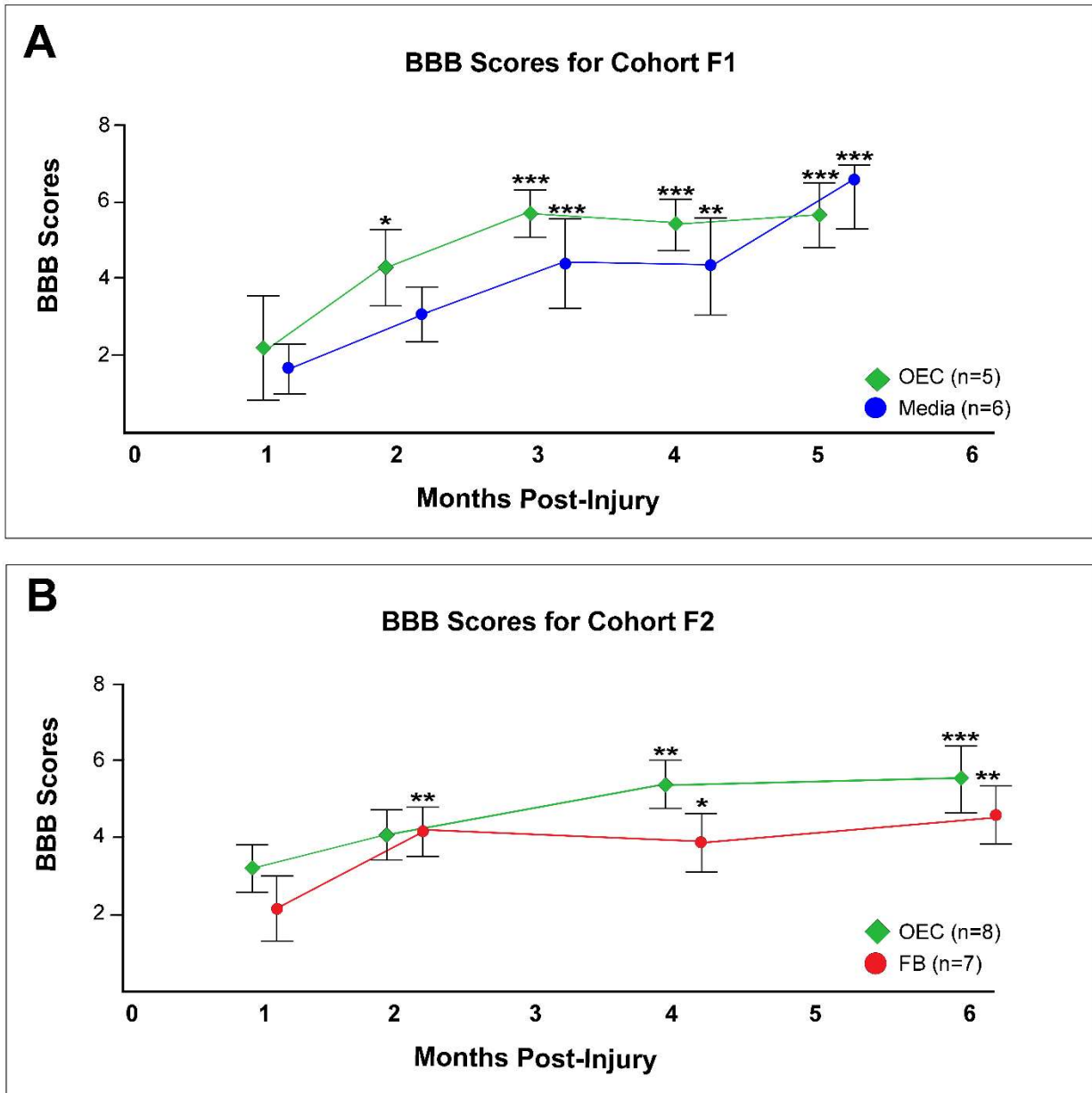
Figure 2 Legend: **BBB scores showed improvement over time for all groups in both cohorts.**

A: In the F1 cohort, OEC-treated rats (green diamonds) showed a significant increase in BBB performance between months 1 and 2. Scores at months 3, 4, and 5 were also greater than scores at month 1 but did not differ from month 2 scores. The media-treated rats (blue circles) did not change from months 1 to 2 but showed improvements at month 3 that continued through month 5. OEC- and media-treated rats did not differ at any timepoint. **B:** BBB scores for the F2 cohort showed improvements between month 4 compared to month 1 for OEC-treated rats (green diamond) that persisted to month 6. FB-treated rats (red circle) improved between months 1 to 2 and the improvement remained through month 6. The F2 transplant groups also did not differ. Data represents group means +/- standard error measurements (SEM) in this and subsequent figures. Statistical significance is compared to month 1 scores (* $p < 0.05$, ** $p < 0.01$, *** $p < 0.001$).

Figure 3:

Number of Pushoffs for Cohort F1

Number of Pushoffs for Cohort F2
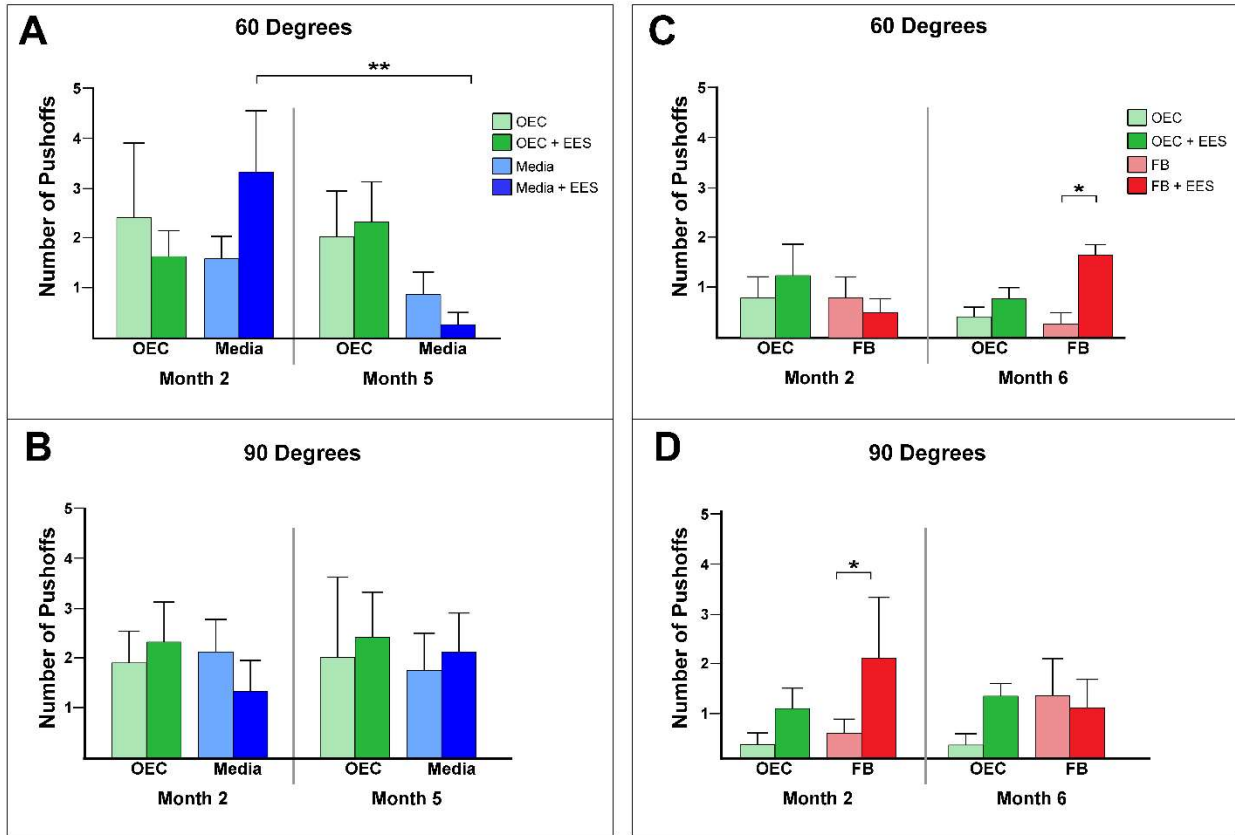
Figure 3 Legend: Few differences in the number of grid pushoffs were found between groups while climbing at 60- or 90-degree inclines.

A-B: When climbing at a 60- or 90-degree incline (A and B, respectively), the average number of pushoffs did not change for OEC-treated rats (green bars, n=5) in cohort F1 either over time or with electrical epidural stimulation (EES, dark green bars). The average number of pushoffs in media-treated rats (blue bars, n= 6) decreased from month 2 to 5 when climbing a 60-degree grid but only when combined with EES (dark blue bars).

C-D: The average number of pushoffs for OEC-treated rats in the F2 group (green bars, n= 8) also did not change over time. EES appeared to increase pushoff numbers in FB-treated rats at month 6 at 60-degrees (C, light and dark red bars, n= 7) and at month 2 at 90-degrees (D). Note the overall low number of pushoffs for both cohorts. (* $p < 0.05$, ** $p < 0.01$).

Figure 4:

A

A1 A2 A3 A4 A5

A6 A7 A8 A9 A10

B

					Right Subscore:				Left Subscore				Body:		Total Score:		
					1	2	3	4	1	2	3	4					

1) Limb Movement								2) Paw Placement								3) Weight Bearing								4) Steps						5) Body					
Hip		Knee		Ankle		Sweep		Dorsal		Back		Mid-Front		Freq		Back		Mid-Front		Curled		Freq		Pushoffs		Misses		Completions		Trunk		Tail		Abdomen	
R	L	R	L	R	L	R	L	R	L	R	L	R	L	R	L	R	L	R	L	R	L	R	L	R	L	R	L	R	L	R	L	R	L	R	L
Ø	Ø	Ø	Ø	Ø	Ø	Y	Y	Y	Y	Y	Y	Y	Y	O	O	Y	Y	Y	Y	Y	Y	O	O	O	O	O	O	O	O	Leaning		Leaning		Drag	
S	S	S	S	S	S	N	N	N	N	N	N	N	N	F	F	N	N	N	N	N	N	F	F	F	F	F	F	F	F	Wobbly		Wobbly		Parallel	
E	E	E	E	E	E									C	C							C	C			C	C			Stable		Stable		High	

C

1. Joint Movement: (from BBB, Total 8 pts)
- 0. No observable HL movement
- 1. Slight of one or two joints
- 2. Extensive of one with or without slight of one other
- 3. Slight movement of all three joints
- 4. Slight of 2 joints, extensive of the third
- 5. Extensive movement of 2 joints (none of the third)
- 6. Extensive movement of 2 joints, slight of the third
- 7. Extensive movement of all 3 joints
- 8. Sweep: Coordinated movement of all 3 joints
- Averaged for both legs. SUCCESSIVE NOT ADDITIVE.

2. Paw Placement: (Total 6 pts)
- +0 No placement
- +1 Placement of dorsal surface of foot on rung
- +2 Placement of back of foot on rung
- +3 Placement of mid-front of foot on rung
- +1 Occasional placement (more than once!)
- +2 Frequent placement
- +3 Consistent placement
- Averaged for both legs. ADDITIVE.

3. Weight Bearing: (Total 6 pts)
- +0 No WB
- +1 WB on back or dorsal surface of foot
- +2 WB on middle or toes without curling
- +3 WB with toes curled around the rung
- +1 Occasional WB (more than once!)
- +2 Frequent WB
- +3 Consistent WB
- Averaged for both legs. ADDITIVE.

4. Steps: (Total 7 pts)
- 0. No pushoffs or step attempts
- 1. Pushoff / lift occasionally attempted
- 2. Pushoff / lift frequently attempted
- 3. Step attempt that failed occasionally
- 4. Pushoff / step attempt that failed frequently
- 5. Step attempt that failed consistently
- 6. Step attempts successful occasionally (once or more)
- 7. Step attempts successful frequently
- Averaged for both legs. SUCCESSIVE.

5. Control: (Total 6 pts)
Trunk:
- +0 Leaning
- +1 Wobbly
- +2 Stable

Tail:
- +0 Leaning
- +1 Wobbly
- +2 Controlled

Abdomen:
- +0 Dragging
- +1 Parallel
- +2 High
- Scored for entire body. ADDITIVE.

TOTAL POINTS POSSIBLE: 33

Figure 4 Legend: Videos of grid climbing were used to develop a scoring sheet and point distribution guide for the climbing-adapted BBB (cBBB).

A: A series of 10 sequential video still frames viewed from below an intact rat climbing a grid at a 60-degree angle during a pre-injury test. Five different colored arrowheads indicate specific features that were analyzed. An example of the full range of motion of the knee and hip joints are indicated in frames A1-A5 by the cyan arrowheads (top right). The red arrowheads (frames A1-A5, bottom right) mark the movement of the left foot and ankle as the rat steps to a higher rung. The yellow arrowheads (frames A4-A8, bottom left) point to the hindpaw grasping the bar with curled toes (A4), followed by the coordinated and extensive movement of all three hindlimb joints in a full step. Note that the weight shifts to the left hindpaw between frames A5 and A6 (magenta arrowhead). The magenta arrowheads show the rat in a "weight-bearing" posture (frames A6-A8) followed by a "pushoff" of the grid (frames A8-A9). The green arrowheads (frames A7-A10) mark the tail that remains stable and centered as the rat steps onto the platform. **B-C:** An example of the cBBB scoring sheet (B) and point distribution (C) used to assess changes in climbing features after injury. Scoring is divided into five categories based on climbing features: 1) joint movement, 2) paw placement, 3) weight bearing, 4) pushoffs and steps, and 5) body control. The top of the scoring sheet has an area to record trial information and tally scores. Detailed descriptions of the scoring system are described in Appendix Item 1. Sub-scores for categories 1-4 are averaged between both legs and added to the sub-score of category 5. Final scores are reported out of a total of 33 points.
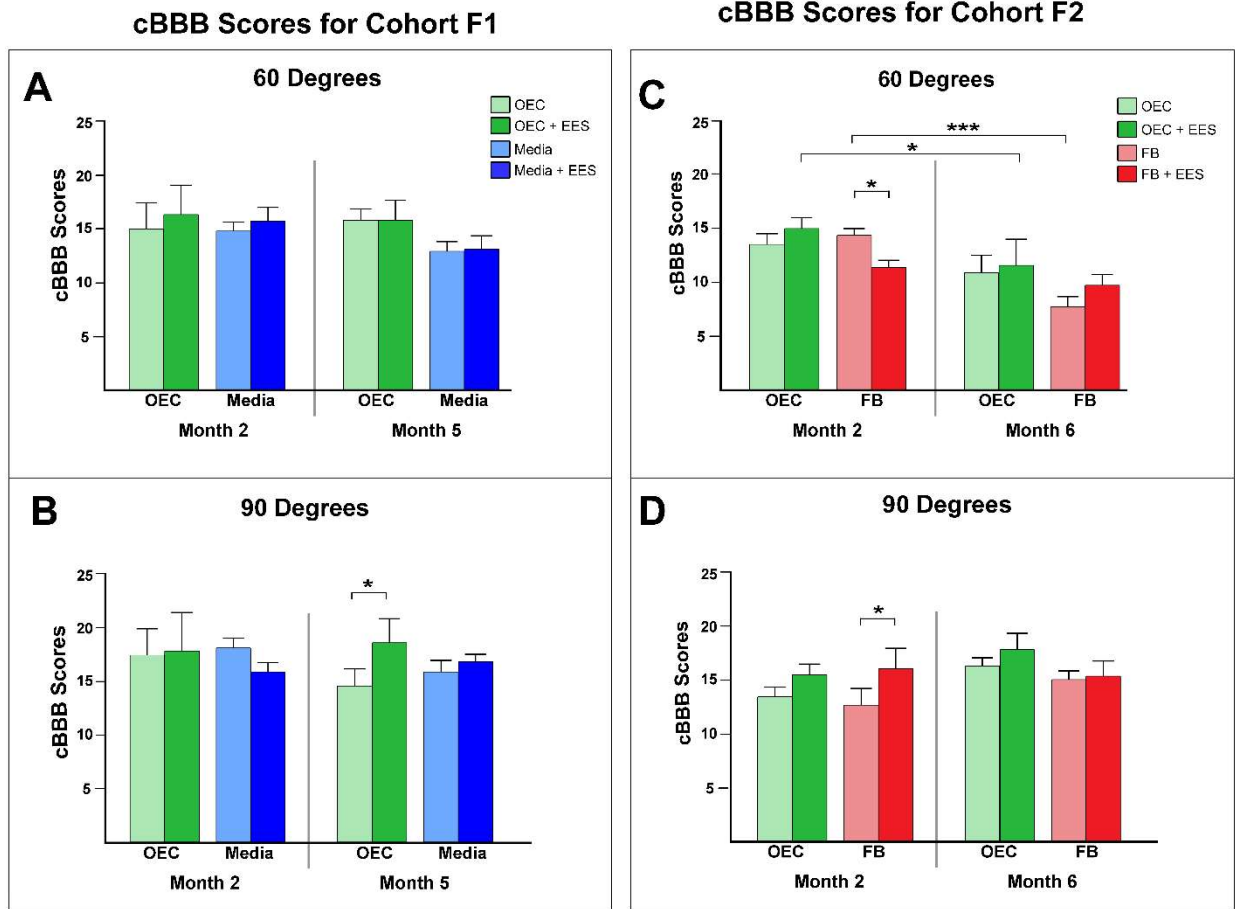
Figure 5:

cBBB Scores for Cohort F1

A. 60 Degrees

B. 90 Degrees

cBBB Scores for Cohort F2

C. 60 Degrees

D. 90 Degrees

Figure 5 Legend: **cBBB scores showed few differences between groups or stimulation conditions at months 2 and 5 or 6.**

A-B: When climbing at a 60-degree incline (A), the average cBBB scores did not change for OEC- or media-treated rats in cohort F1 either over time or with EES. When climbing at a 90-degree incline (B), the cBBB scores increased with EES in OEC-treated rats compared to scores without EES at the same timepoint. **C-D:** The cBBB scores decreased slightly for OEC-treated rats in cohort F2 between months 2 and 6 at a 60-degree incline when EES was administered (C). EES appeared to decrease average cBBB scores in FB-treated rats at month 2 at 60-degrees compared to those without EES. Scores for FB-treated rats without EES decreased from months 2 to 6. At a 90-degree incline (D), scores increased with EES in FB-treated rats at 2 months post-injury. This differed from what was seen at 60 degrees. (* $p < 0.05$, *** $p < 0.001$).
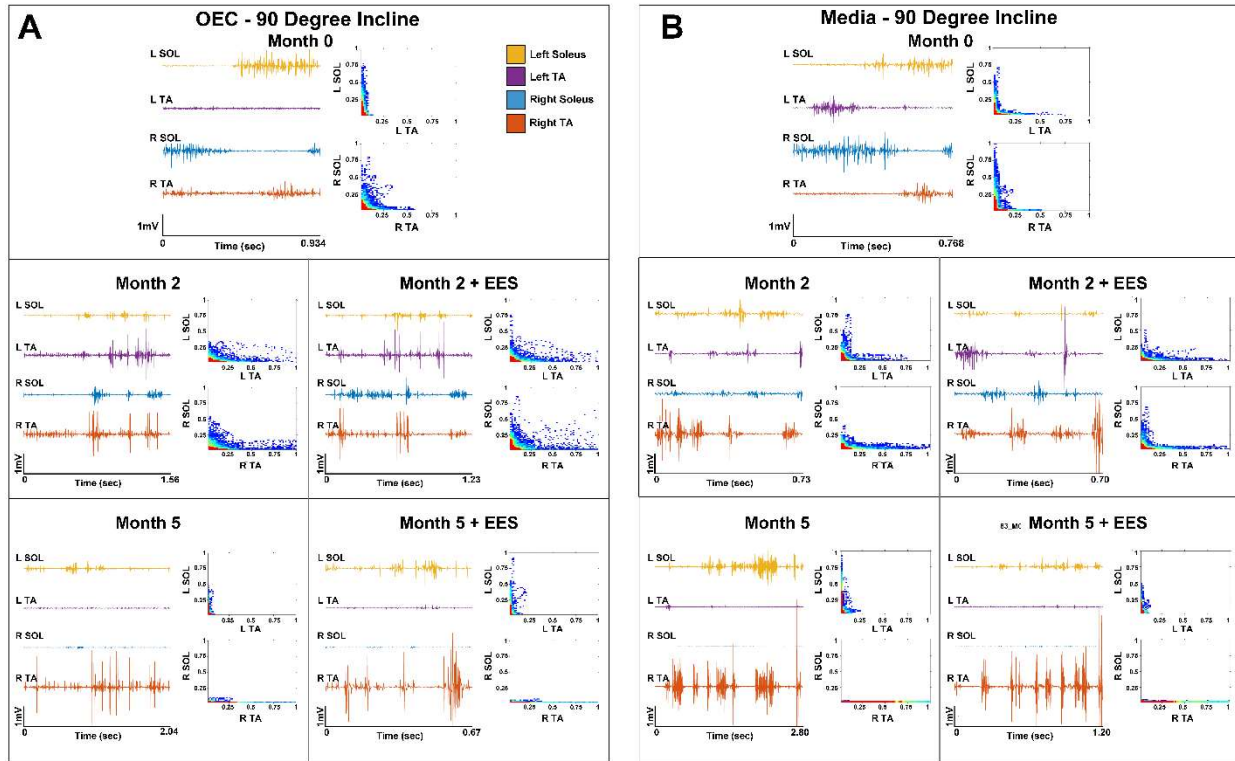
Figure 6:

Figure 6 Legend: Example traces of EMG patterns of the right and left soleus and TA of OEC- and media-treated rats indicated few changes with EES and inconsistent recordings over time.

A, B: Traces of muscle EMG patterns during a step or "pushoff" at 0-, 2-, and 5-months post-injury of OEC- (A) and media- (B) treated rats climbing at a 90-degree incline. Traces from the left soleus (L SOL) are illustrated in yellow, left tibialis anterior (L TA) in purple, right soleus (R SOL) in blue, and right TA (R TA) in orange. Co-activation plots of the L SOL and L TA and R SOL and R TA are shown to the right of each graph and indicate the frequency that the two muscles are activated concurrently. On co-activation plots, data points mapped in red indicate high frequency and dark blue indicate lower frequency of occurrence. Traces at month 0 show a typical pattern of activation during stepping. At 2 months post-injury, either with or without EES the activation patterns for both rats were more erratic with shorter burst periods. More co-activation also occurred after injury between the ipsilateral TA and SOL of both hindlimbs compared to the month 0 recordings. At month 5, bursts of activation are higher in amplitude and longer than at month 2 and show improved coordination with contralateral muscles. Two muscles for each rat appear relatively inactive at month 5, likely due to electrode malfunction. These patterns do not change with EES administration. Note the y-axis scale is the same for each image, but the x-axis varies depending on the amount of time the rat took to complete the step or pushoff.
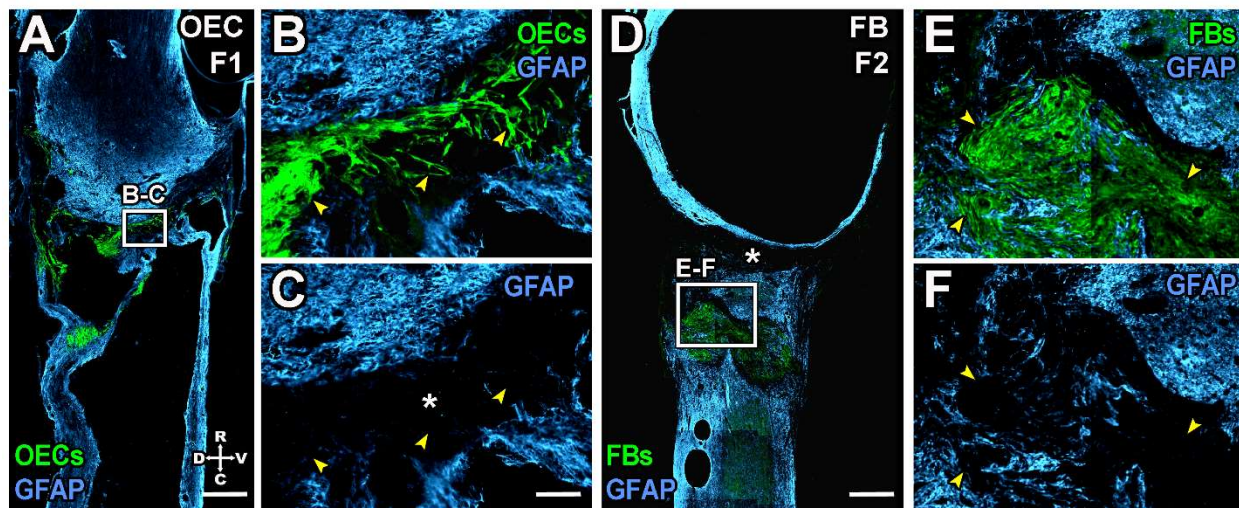
Figure 7:

Figure 7: GFP-positive OECs and FBs survived 5-6 months post-transplantation.

A: An example of GFP-expressing OECs (green) that survived in both the injury core and in the astroglial scar border (GFAP, light blue) in a transplanted spinal rat for 5 months. The same color-scheme for the glial scar (light blue) and GFP-positive cells (green) is used in this and subsequent figures unless otherwise noted. **B-C:** Enlargement of the box in A shows that OECs (B) created "bridges", marked by yellow arrowheads, that connected the rostral and caudal stumps. The two stumps are otherwise fully separated as seen when the OECs are removed digitally (C, asterisk). **D:** An example of GFP-expressing FBs (FBs, green) that survived for 6 months. FBs were generally found in large clumps within the spinal cord stumps rather than in the lesion core (asterisk). **E-F**: Boxed area in D is enlarged in E and shows a dense clump of GFP-FBs (E, green) in the caudal stump. When FBs are removed from the image (F), little GFAP immunoreactivity is associated with FBs in the spinal cord stump. No FBs were found in the lesion core. Rostral (R) is toward the top and dorsal (D) to the left in this and subsequent spinal cord images unless otherwise stated (see directional in A, bottom right; ventral, V, caudal, C). The top right of each panel indicates the transplantation group and cohort. Scale bars: A, D = 500 μm, B-C = 50 μm, E-F: 100 μm.
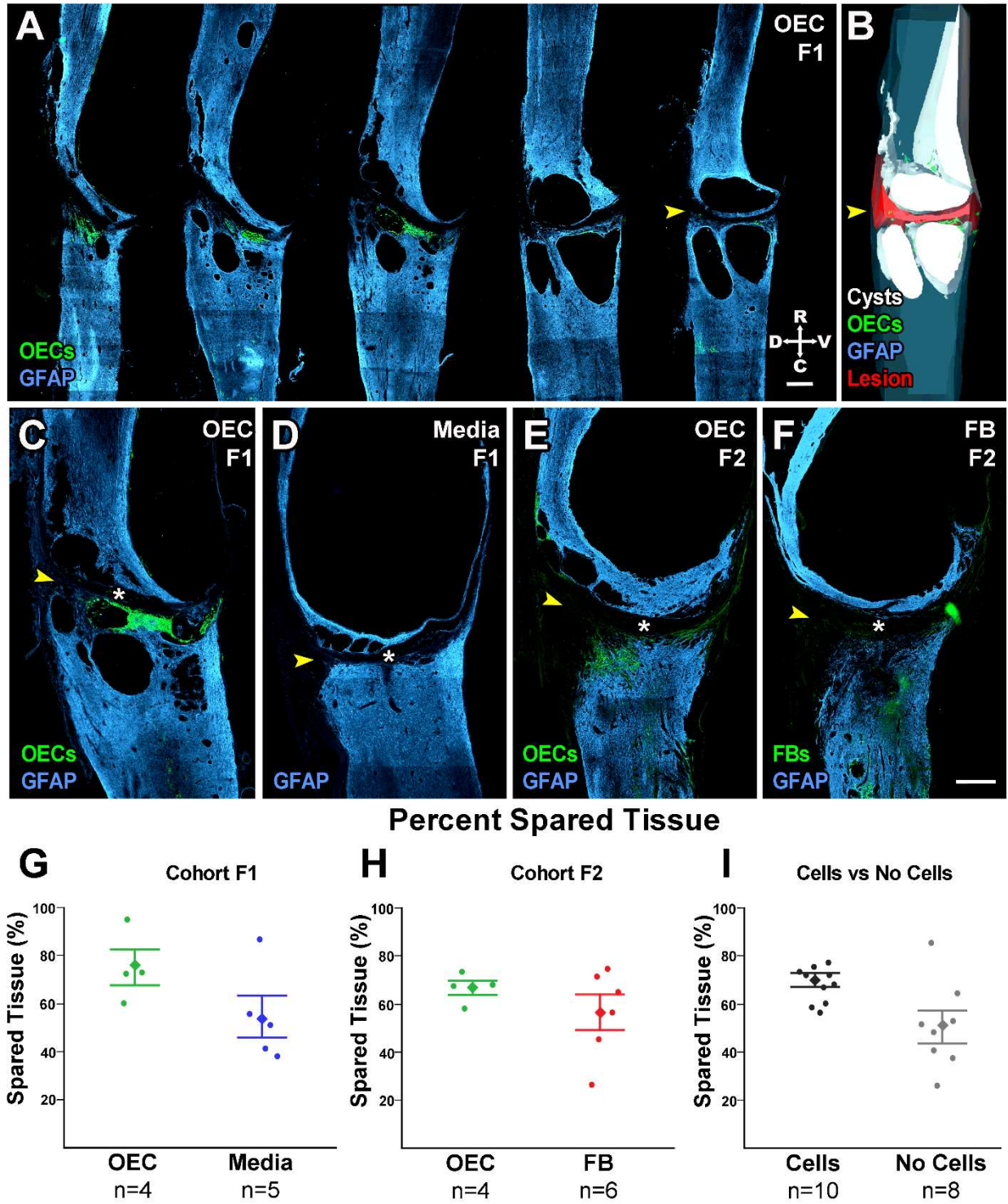
Figure 8:

Figure 8 Legend: 3-D reconstructions of rat injury sites were used to determine that the percent spared tissue did not differ between groups.

A: Five 25 μm sagittal spinal cord sections spaced 400 μm apart (arranged left to right) from an OEC-treated rat in cohort F1 at 5.5-months post-injury. The GFAP-positive astroglial scar (light blue) shows spared spinal cord tissue with fluid filled cysts (holes) and the lesion core. Yellow arrowhead indicates the dorsal part of the lesion core. Surviving OECs (green) were present near the injury site. **B**: The 3-D reconstruction (B) is shown at the same orientation as the last section in the sequence in A. Traces of the spared tissue (light blue), cysts (white), lesion core (red), and transplanted cells (green) within 5 mm rostral and caudal to the injury epicenter were compiled to create a 3-D reconstruction of the spinal cord spared tissue. **C-F**: Representative injury sites from OEC-, and media-treated rats from cohort F1 (C and D respectively) and OEC- and FB-treated rats from F2 (E and F, respectively) at 5.5-6.5 months post-injury. The GFAP-positive astroglial scar (blue) shows the spared spinal cord tissue and the borders of fluid filled cysts and the lesion core (asterisks and yellow arrowheads). Some surviving transplanted cells (GFP, green) are shown in all images except D. **G-I**: Estimates of the spared tissue volume were calculated using the 3-D reconstructions. Spared tissue was defined as the GFAP-positive tissue volume minus the cyst and lesion volumes divided by the total tissue volume. No differences were seen in OEC-treated rats compared to controls in either cohort F1 (G) or F2 (H). The presence or absence of surviving cells (OECs or FBs) also did not affect spared tissue volume (I). Small dots represent data points from individual rats and diamonds represent group means +/- SEM in this and subsequent images. Scale bars: A-F = 500 μm.
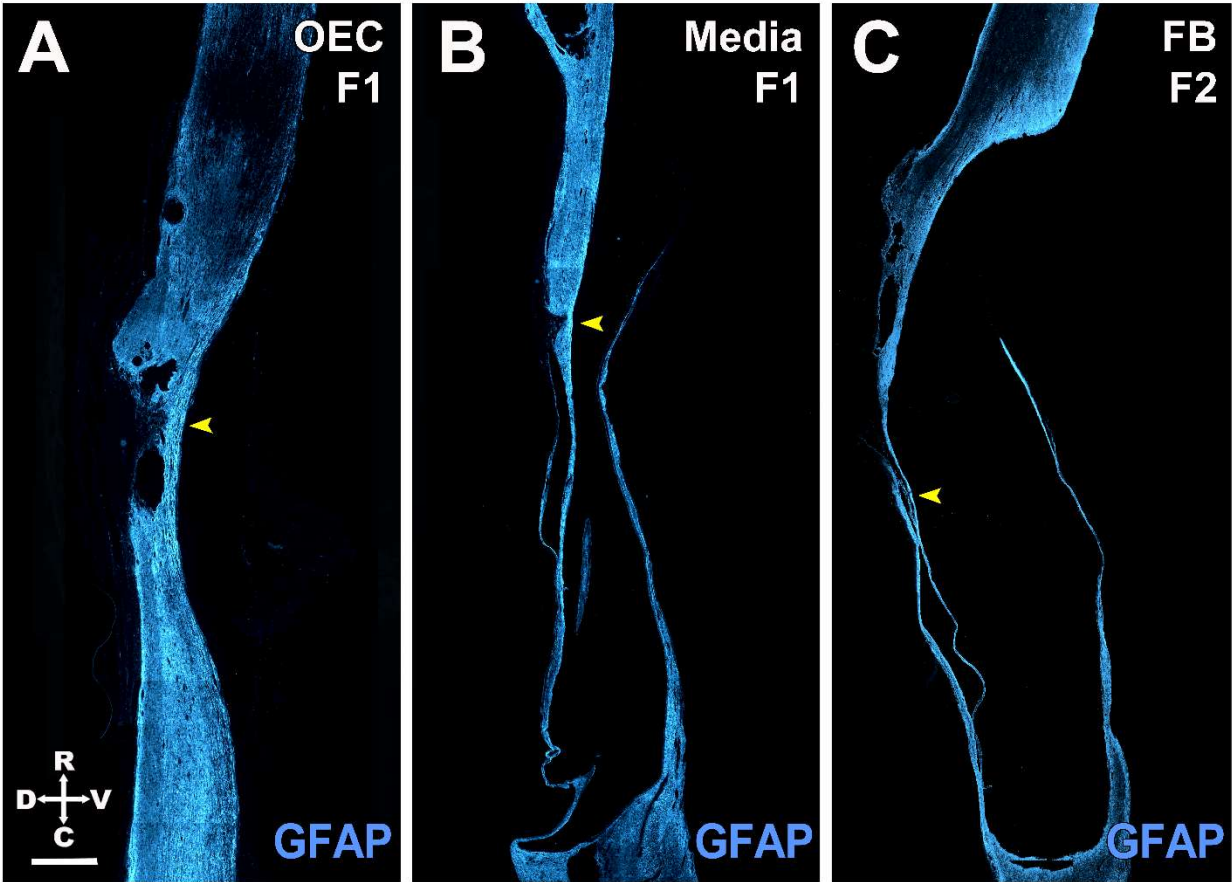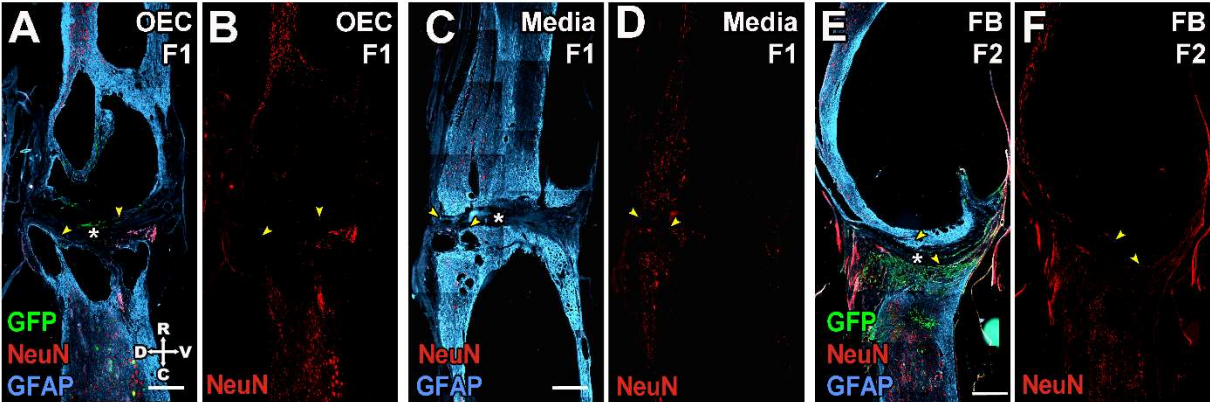
Figure 9:

Figure 9 Legend: Areas of GFAP-positive tissue continuity indicate incomplete injuries in spinal cords from both cohorts.

A-C: Spinal cord sections from 3 different rats show continuity of the astrocytic scar border (GFAP, light blue) across the ventral spinal cord (yellow arrowheads). In cohort F1, many rats had evidence of incomplete injuries with the largest incomplete injury in OEC-treated rats shown in A (OECs were removed digitally). Most commonly, incompletely injured rats had evidence of small ventral connections (B). One incompletely transected rat in cohort F2 had a thin, continuous section of GFAP (C). Large cysts that open into the caudal stump are seen in B and C. Scale bars: A-C = 1000 µm.

Figure 10:

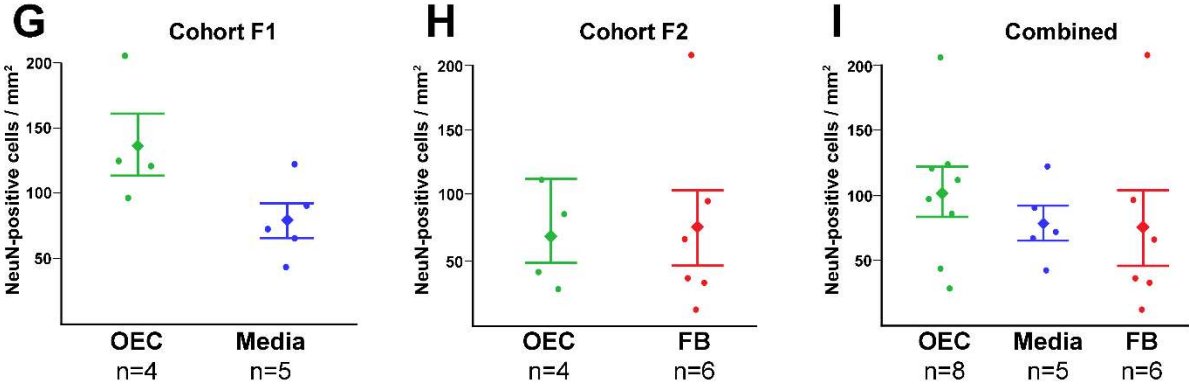Density of NeuN within 2 mm of the lesion epicenter

Figure 10 Legend: **The density of NeuN-positive neurons near the injury site did not differ between transplant groups.**

A-F: Representative images of OEC- (A, B), media- (C, D), and FB-treated (E, F) rats. The GFAP-labeled scar border (blue) is removed in B, D, and F to better visualize the NeuN-positive cell density (red, cells/mm^2). To determine neuronal survival near the injury site, NeuN-positive cells were counted within the spared tissue traced 1 mm rostral and caudal to the injury epicenter (asterisks). Transplanted cells and some PRV-positive neurons are labeled with GFP (green). Yellow arrowheads mark NeuN-positive cells closest to the rostral and caudal scar borders. (Background labeling of the pia and lateral scar tissue is evident.) **G-I:** The number of NeuN-positive cells were normalized to the tissue area. NeuN cell density did not differ between OEC- and media-treated controls (G, F1 cohort), nor between OEC- and FB-treated rats (H, F2 cohort). When the two OEC cohorts were combined, OEC-treated rats did not differ from either media- or FB- treated controls (I). Scale bars: A-F = 500µm.
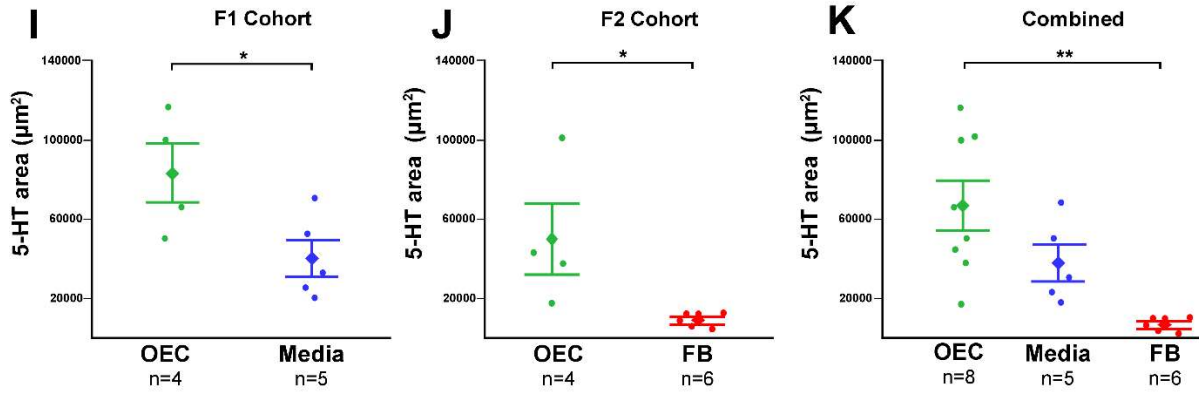
Figure 11:
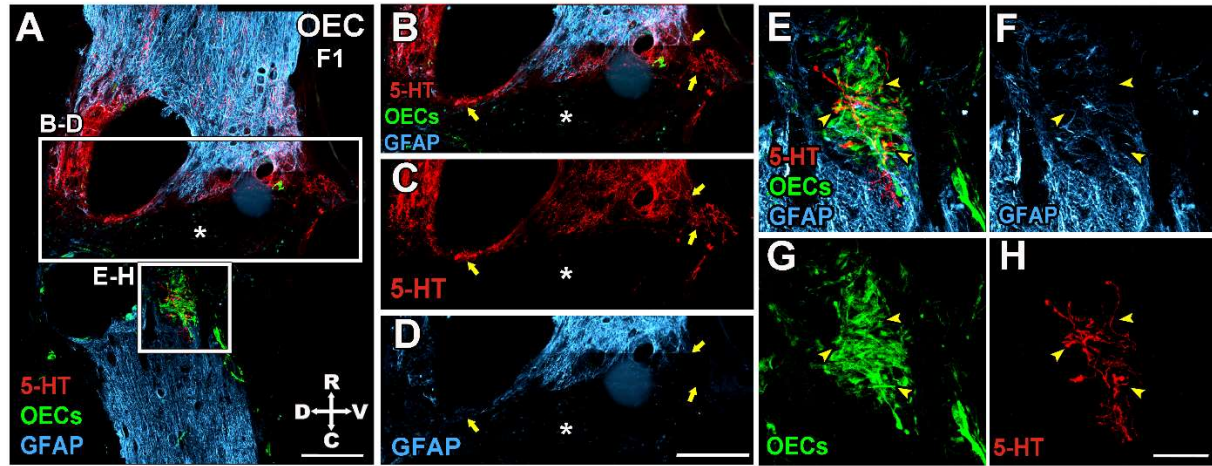
Figure 11 Legend: Serotonergic axon outgrowth into the lesion core was greater in OEC-transplanted rats than controls.

A-D: The injury site of an OEC-treated rat was immunolabeled for serotonergic motor axons (5-HT, red), OECs (green), and the glial scar border (GFAP, light blue). The rectangular box in A is enlarged in B-D. Arrows mark bundles of 5-HT-positive axons in the injury core. The GFAP-negative lesion core is indicated by asterisks. **E-H**: Enlargement of the square box in A shows numerous OECs (green) associated with 5-HT-positive axons on the caudal border of the injury. Arrowheads indicate areas of OEC, and 5-HT axon overlap in the GFAP-negative lesion core. **I-K:** The normalized area of 5-HT-positive axons in the lesion core was greater in OEC- than media-treated rats (I) in the F1 cohort and greater than FB-treated rats (J) in the F2 cohort. When OEC-treated rats from both cohorts were combined, the 5-HT area did not differ from media-treated rats but had more 5-HT-labeled axons than FB-treated rats (K). Scale bars: A-D = 500 µm, E-H = 100 µm. (* $p < 0.05$, ** $p < 0.01$).
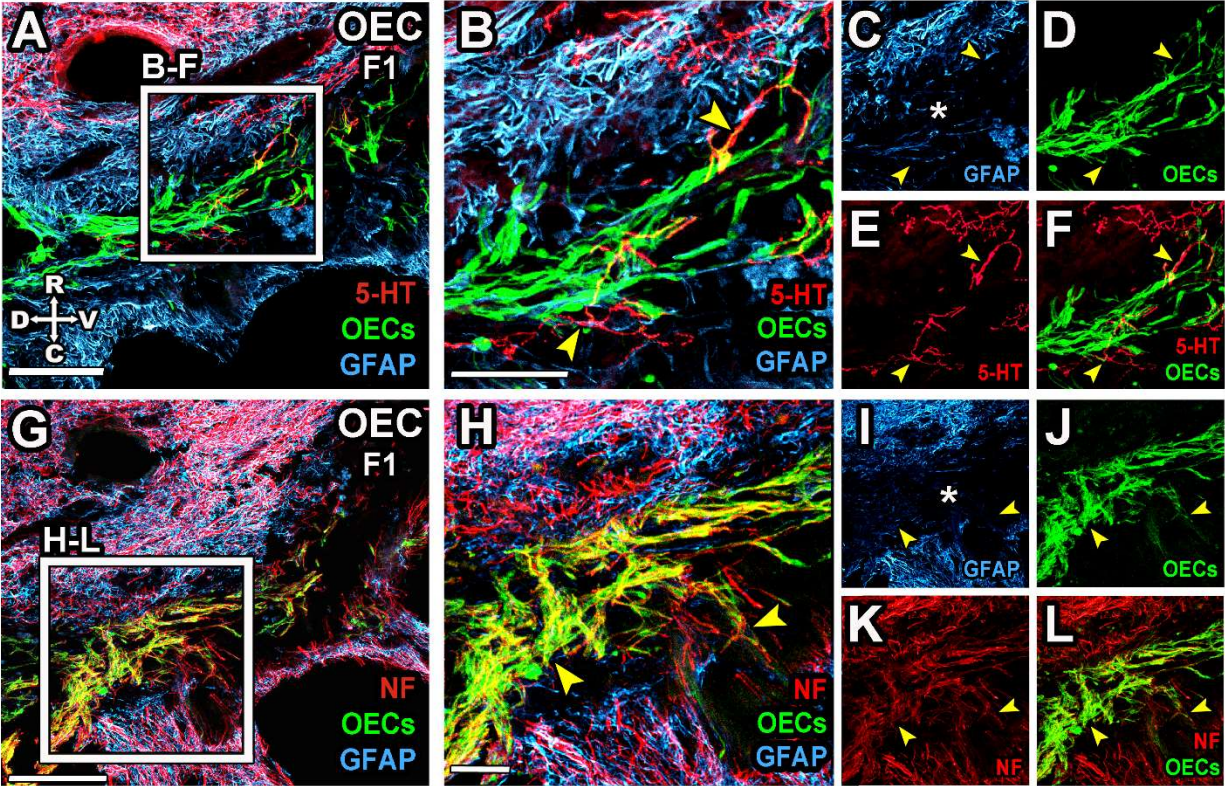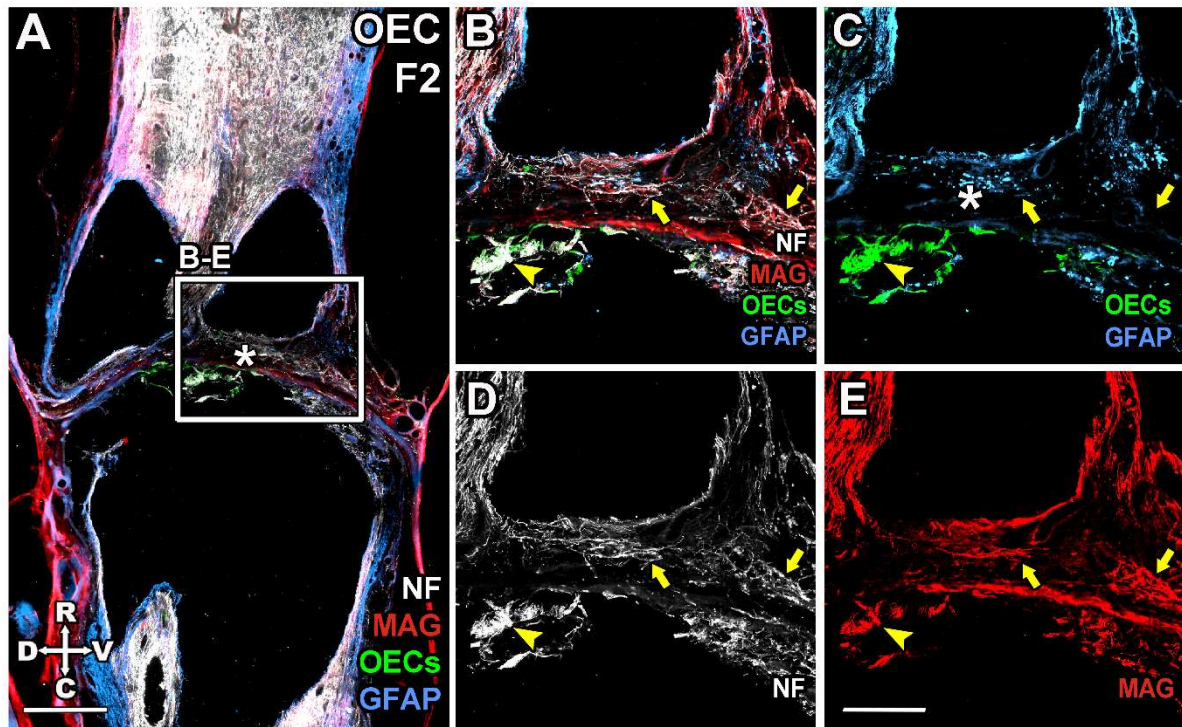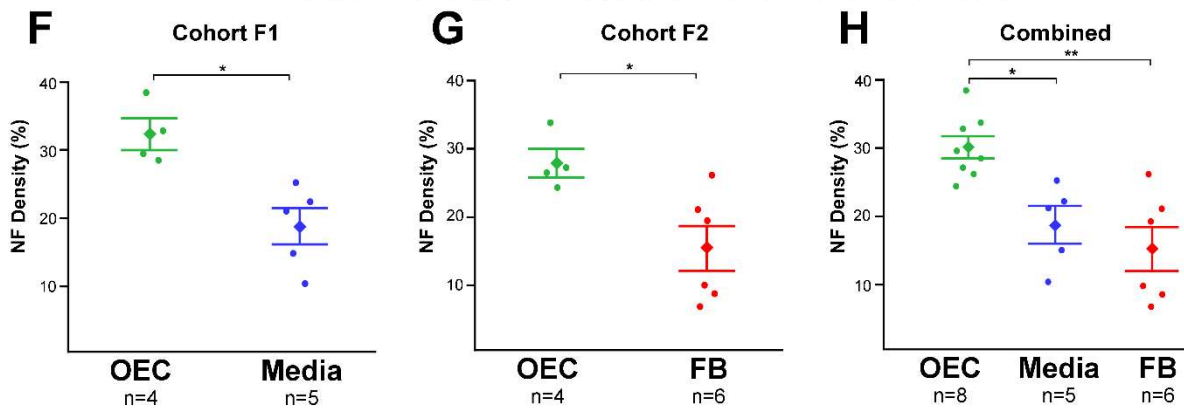
Figure 12:

Figure 12 Legend: Serotonergic and neurofilament-positive axons crossed the lesion core on OEC bridges in an OEC-treated rat.

A: The injury site of an OEC-treated rat was immunolabeled for serotonergic 5-HT-positive axons (red), OECs (green), and the glial scar border (GFAP, light blue). **B-F:** Enlargement of the box in A shows 5-HT axons (yellow arrowheads) crossing the GFAP-negative lesion core (asterisk) on GFP-OEC bridges (green). **G:** Injury site section 100 µm lateral to the section shown in A-F was labeled for neurofilament (NF)-positive axons (red), OECs (green), and the glial scar (light blue). **H-L:** Enlargement of the box in G shows NF-positive axons that filled the GFAP-negative lesion core (asterisk) in association with OEC bridges. Arrowheads mark examples of axon bundles crossing the caudal scar border. Scale bars: A, G = 500 µm, B-C, H-L = 100 µm.
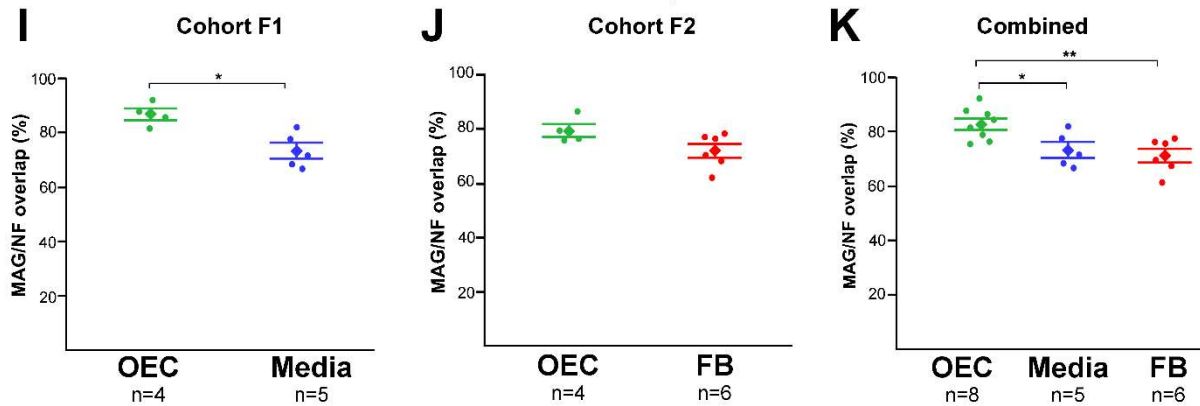
Figure 13:

Figure 13 Legend: **More axonal and myelin markers were present in the lesion core of OEC-treated rats than controls.**

A-E: The injury site of an OEC-treated rat labeled for neurofilament-positive axons (NF, white), myelin (MAG, red), OECs (GFP, green), and the glial scar border (GFAP, light blue). An enlargement of the injury site in A is shown in B-E. Arrows indicate NF/MAG-positive axons in the GFAP-negative lesion core (asterisks) and the arrowhead marks axons associated with OECs. **F-H:** NF-positive axons were found in a larger percentage of the lesion core area (average percent density of NF) in OEC- than in media-injected rats (H, F1 cohort) and in OEC- than in FB-treated rats (G, F2 cohort). When the OEC-treated rats from both cohorts were combined, they also had a greater average density of NF-positive axons than either media or FB controls (H). **I-K:** Of the total NF axons in the lesion core, a higher percentage overlapped with the myelin marker, MAG, in OEC-compared to media-treated rats (I, F1 cohort) but not in OEC- compared to FB-treated rats (J, F2 cohort). When data from the two cohorts were combined, OEC-treated rats had a greater NF/MAG overlap than media and FB controls (K). Scale bars: A = 500 μm, B-E = 250 μm. (* $p < 0.05$, ** $p < 0.01$).
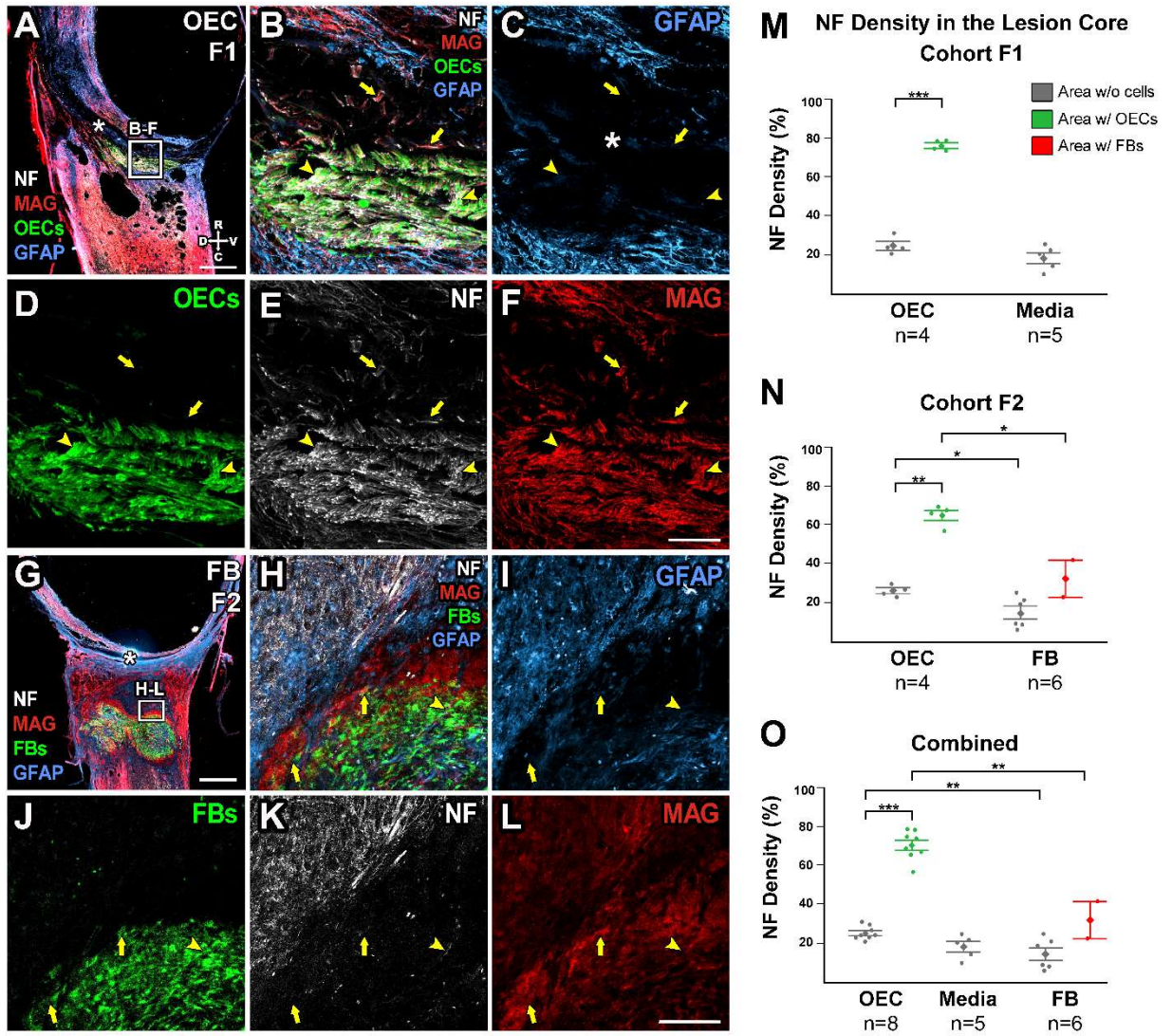
Figure 14:

Figure 14 Legend: **Neurofilament density in the lesion core varied depending on the presence of transplanted cells.**

A-F: The injury site of an OEC-treated rat was immunolabeled for neurofilament-positive axons (NF, white), myelin (MAG, red), OECs (GFP, green) and the glial scar border (GFAP, light blue). GFAP-negative lesion core is marked by an asterisk. Enlargement of the boxed area of the lesion core in A is shown in B-F. Arrowheads indicate NF/MAG-positive axons in areas containing OECs whereas arrows indicate NF/MAG-positive axons in areas of the lesion core without OECs. **G-L:** An image of a spinal section from an FB-treated rat from cohort F2 labeled for NF, MAG, OECs, and GFAP. Although we did not find FBs in the lesion core (asterisk), enlargement of the box in G illustrates surviving FBs that formed large clumps within the caudal stump and have a low density of NF-labeled axons (K, white). Arrows show MAG-positive, NF-negative areas within the transplanted FBs, and arrowheads mark regions of MAG/NF overlap. **M:** NF-positive axons in the F1 cohort were denser in areas with OECs (green dots) than the remainder of the lesion core (grey dots). Areas without OECs had a similar NF density as media-treated rats (grey dots, OEC vs. Media). **N:** Data from the F2 cohort shows a higher density of NF with OECs than without (green vs. grey dots). Areas with FBs in the lesion core did not differ from areas without cells (red vs. grey dots). Compared to areas with OECs, the NF density was lower in areas with FBs (green vs. red). **O:** When the OEC-treated rats from cohorts were combined, the same differences were apparent. Scale bars: A, G = 500 μm, B-F, H-L = 100 μm. (* $p < 0.05$, ** $p < 0.01$, *** $p < 0.001$)
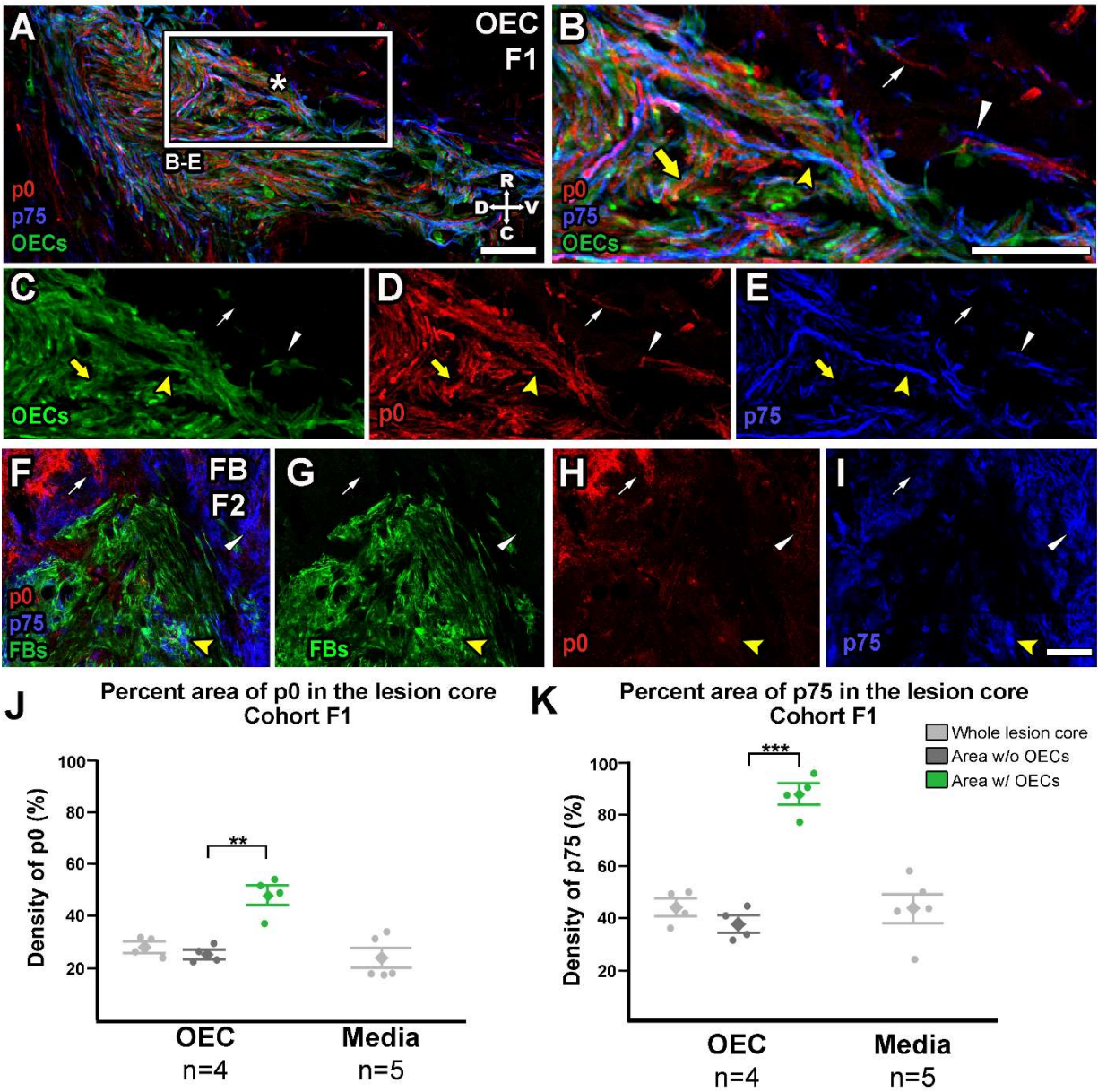
Figure 15:

Figure 15 Legend: **Schwann cell and OEC markers present in the lesion core did not differ between groups but were more highly expressed in areas with OECs than those without.**

A-E: A region of the lesion core in an OEC-treated rat. The box in A is enlarged in B-E. Myelinating and non-myelinating Schwann cells (SCs) in the lesion core (asterisk) were identified using antibodies against p0 (red, small white arrow) and p75 (dark blue, thin white arrowhead), respectively. Some OECs (green) either closely associated with or expressed p0 (yellow arrow) and p75 (yellow arrowhead). **F-I:** A clump of surviving transplanted FBs (green) is associated with low levels of immunoreactivity for p0 and p75 (yellow arrowhead). The areas surrounding the FBs contain high levels of both SC markers (p0, small white arrow, and p75, thin white arrowhead). **J:** Graphical representation of the density of p0-immunoreactivity in the lesion core. The overall density of p0 expression did not differ between OEC- and media-treated rats in cohort 1 (light grey dots). Areas with OECs had a higher density of p0 than those without (green vs dark grey dots). **K:** Density of p75-expression in the caudal stump of rats in cohort F1 did not differ between OEC- and media-treated rats (light grey). Immunoreactivity of p75 was more highly concentrated in areas with OECs than those without (green vs. dark grey). Scale bars: A-I = 100 µm. (** $p < 0.01$, *** $p < 0.001$)

Figure 16:
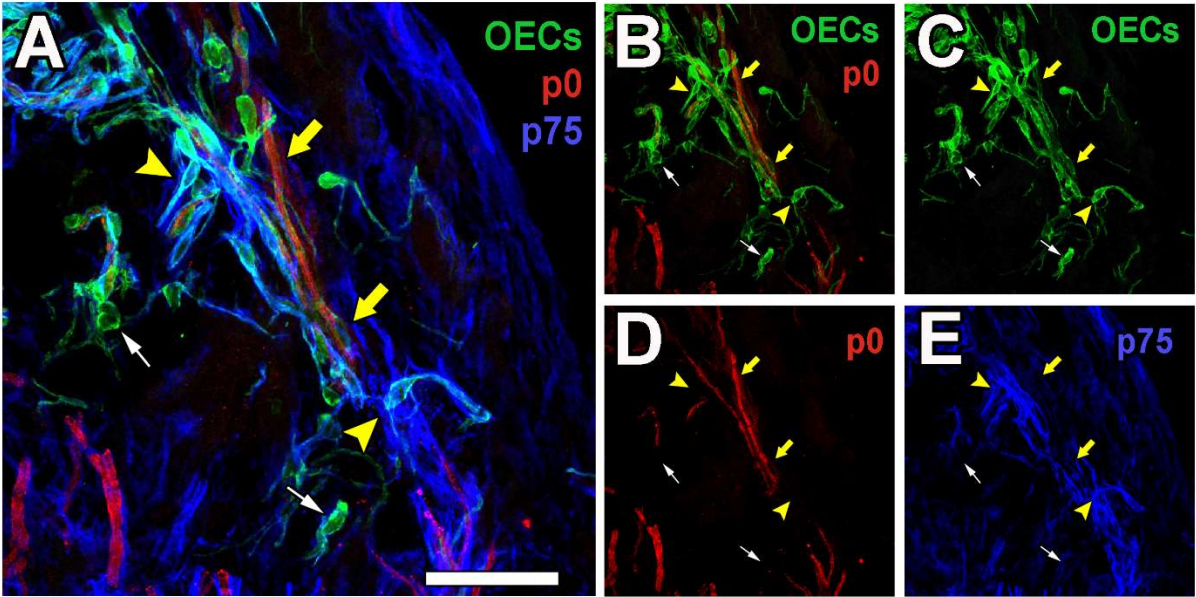
Figure 16 Legend: **Transplanted OECs varied in their expression of different markers and intermingled with Schwann cells in and around the injury core.**

A-E: Some OECs (green) in the injury core colocalized with p0- (green and red, yellow arrows), whereas other OECs appeared as p75-positive (green and blue, yellow arrowheads). GFP-positive, and p0- and p75-negative OECs (small white arrows) were also observed. OECs were also found intertwined with each other and with both myelinating (p0, red) and non-myelinating (p75, blue) Schwann cells. Scale bars: A-E = 50 μm.
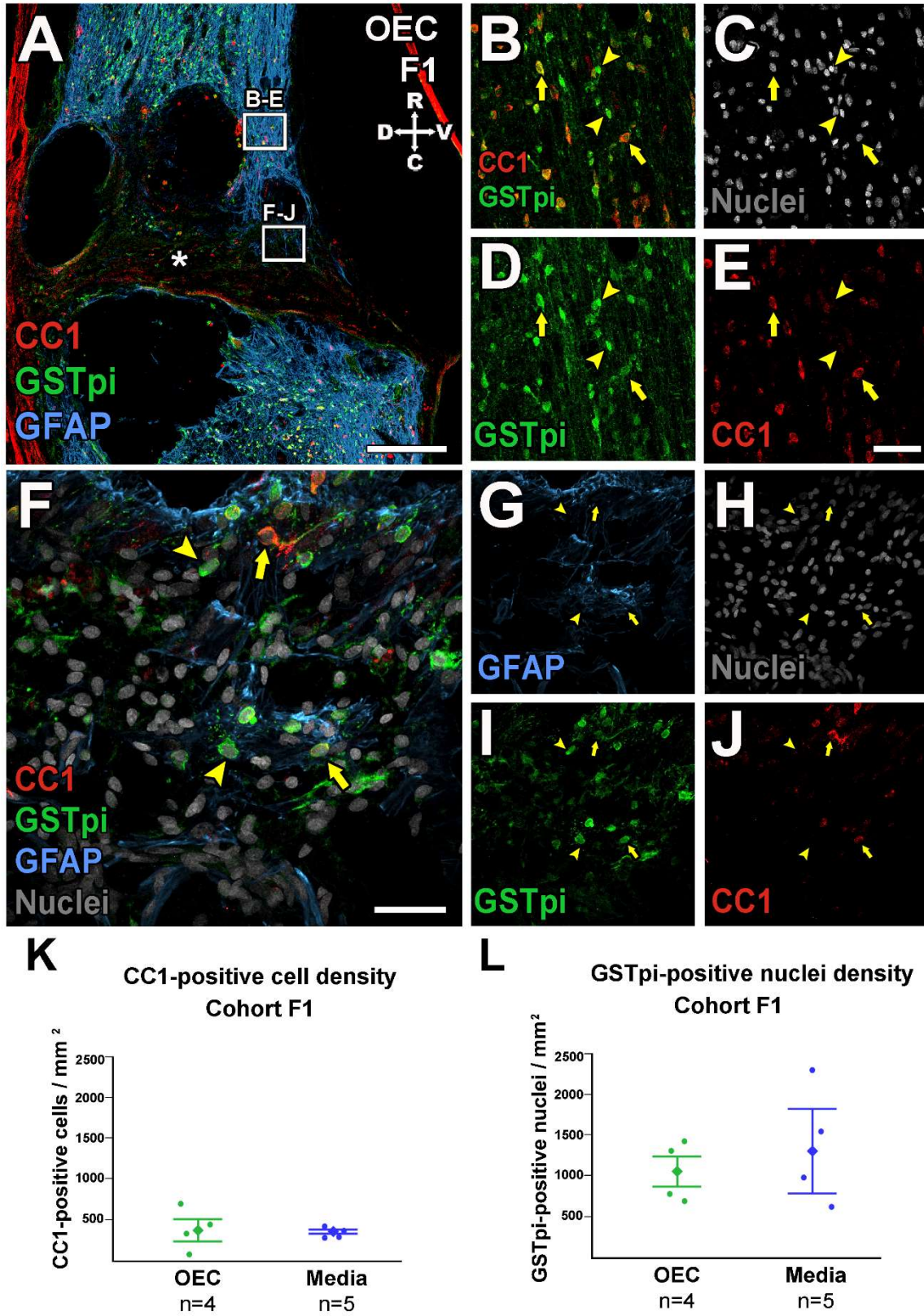
Figure 17:

Figure 17 Legend: **The density of oligodendrocytes and OPCs at the scar border did not differ between OEC- and media-treated rats.**

A: Low magnification of an injury site labeled for CC1-positive oligodendrocytes (red), GSTpi-positive oligodendrocyte progenitor cells (OPCs, green), and the glial scar border (GFAP, light blue). The boxes from the rostral stump and scar border in A are enlarged in B-E and F-J. Asterisk indicates the lesion core. **B-E:** Cytoplasmic CC1 is a marker for oligodendrocytes and nuclear GSTpi marks OPCs. Multiple CC1-positive oligodendrocytes (red, yellow arrows) and nuclear GSTpi-positive OPCs (green and grey overlap, yellow arrowheads) are illustrated from the rostral spinal stump. Hoechst-labeled nuclei are grey. **F-J:** Oligodendrocytes (yellow arrows) and OPCs (yellow arrowheads) were found in the lesion core with areas of low GFAP-immunoreactivity (light blue). **K, L:** Quantification of the number of CC1-positive cells (K) and cells with CC1 nuclear GSTpi (L) was normalized to the GFAP-positive tissue area within 500 μm of the lesion core. The density of either CC1- or GSTpi-positive cells did not differ between OEC- and media-treated rats in cohort F1. Scale bars: A = 500 μm, B-J = 50 μm.
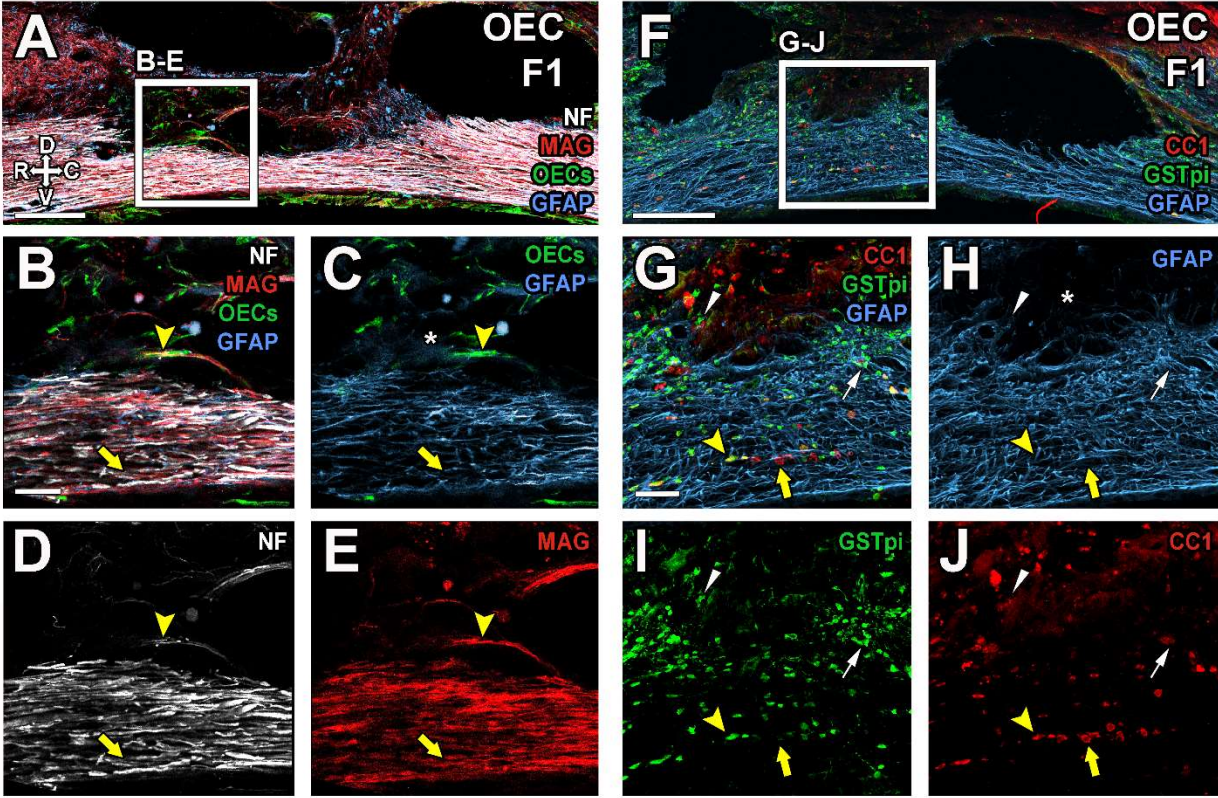
Figure 18:

Figure 18 Legend: Axons were likely myelinated by oligodendrocytes present in the spared ventral white matter of an OEC-treated rat with an incomplete lesion.

Dorsal is toward the top and rostral to the left in this image. **A:** Spared NF-positive axons (white) were closely associated with MAG (red) in the intact ventral white matter (GFAP, light blue) in this incomplete injury of an OEC-treated rat. OECs are shown in green. The box in A is enlarged in B-E. **B-E:** Most axons in the intact ventral white matter were straight, well organized, and typically associated with MAG (yellow arrow). Some MAG-positive axons also associated with OECs (yellow arrowhead) in the GFAP-negative lesion core (asterisk). **F:** In a section 125 μm lateral to A, CC1-positive oligodendrocytes (red), GSTpi-positive OPCs (green), and the glial scar border (GFAP, light blue) also were present in the spared ventral white matter. The box in F is enlarged in G-J. **G-J:** A large area of intact spinal tissue contained many mature (red, yellow arrow) and immature (red and green overlap, yellow arrowhead) oligodendrocytes in organized rows. GSTpi-positive OPCs were more concentrated around the dorsal lesion border (green, small white arrow), and in the lesion core (thin white arrowhead, asterisk). Scale bars: A = 200 μm, C-E, G-J = 50 μm, F = 250 μm.

Fig 19:
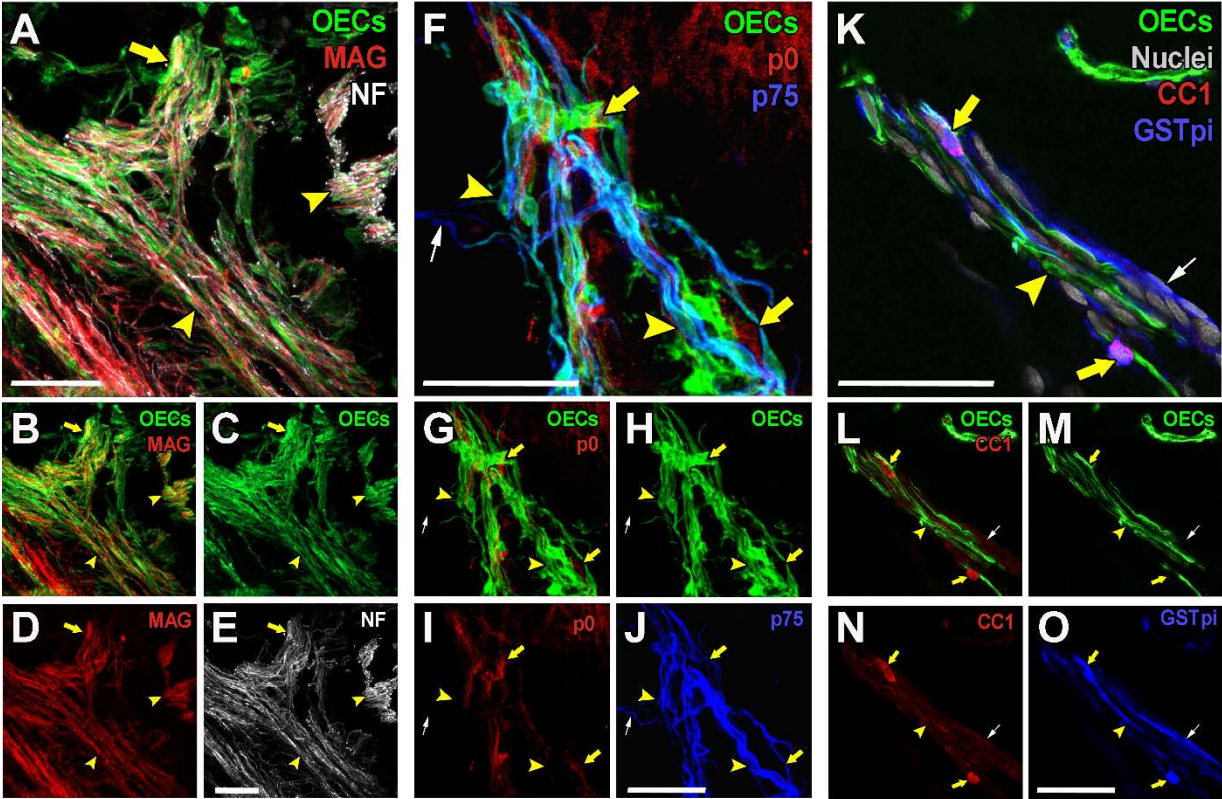
Figure 19 Legend: **OECs were closely associated with myelinating cells in the lesion core.**

A-E: OECs (green) in the injury site associated with NF-positive axons (white) and MAG (red). Yellow arrowheads indicate OECs that did not appear to express MAG intermingled with MAG-positive axons, and the yellow arrow indicates an area of close OEC and MAG overlap. **F-J:** Myelinating SCs (p0, red, yellow arrows) and p0-negative OECs (green) were found intertwined in the lesion core. Most OECs were p75-positive (blue, yellow arrowhead) and interacted with a few GFP-negative p75-positive non-myelinating SCs (blue, small white arrow). **K-O:** CC1- and GST-pi-positive oligodendrocytes (red and blue, yellow arrows) are shown associated with OECs (green, yellow arrowhead) in the lesion core. CC1-negative, GST-pi-positive OPCs were also present (blue, small white arrow). Hoechst-labeled nuclei are shown in grey (K). Scale bars: A-E = 100µm, F-J, K-O = 50µm.

CHAPTER 4. DISCUSSION

In this study we found that OEC treatment combined with EES and climb training had a slight effect on functional recovery but a substantial impact on the architecture of the injury site. While the spinal rats in both cohorts improved on the BBB locomotor test over time, there were very few consistent changes seen in their climbing performance. This study marks the first time we found that GFP-positive OECs and FBs survived in or near the injury site for 5-6 months post-transplantation. Although OEC treatment did not affect tissue sparing or neuron survival near the injury site, we did detect strong positive effects on axonal outgrowth and the association of axons and myelin in the lesion core compared to media- or FB-treated controls. Not only was the overall amount of NF- and 5-HT-positive axons in the lesion core greater in OEC- versus control-treated rats, but we also found evidence that surviving OECs strongly stimulated axonal outgrowth by directly associating with axons in the lesion core. OEC treatment also affected myelin and myelinating cells by increasing NF-positive axon association with MAG and interacting with SCs and oligodendrocytes in the lesion core. While OECs did not affect overall SC infiltration into the injury site or oligodendrocyte and OPC density at the scar border, the OECs exhibited distinct interactions with both the SCs and oligodendrocytes within the lesion core. We also observed differences in p0 and p75 expression in OECs, a finding that suggests there may be several OEC subtypes at the injury site.

Functional improvements occurred in open exploratory behavior, but analyses of motivated behavior during climbing tests were inconsistent

The BBB is widely used to measure gains in motor function in moderate, rather than severe, models of rat SCI (Basso et al., 1995; Barros Filho & Sleiman Molina, 2008). Here we saw modest improvements on the BBB compared to scores at month 1 in all groups of rats. As all of our spinal rats began the EES and climb training treatments after the first BBB test (1-month post-injury), it suggests that the EES contributed to the functional recovery measured by the BBB test. We did not, however, have controls without long-term EES and therefore cannot definitively conclude that EES plus climb training alone contributed to this change. As the BBB is not a task-based test, we also used the grid climbing task to ask if there were treatment effects on a motivated locomotor task.

Previous studies used grid climbing as a test of motor performance after injury and found that the number of grid pushoffs improved with OEC treatment (Ramon-Cueto et al., 2000; Ziegler et al., 2011). In the current study we found only a few examples of grid pushoffs for each trial and we thus developed a BBB-style evaluation of grid climbing (the cBBB) to obtain more information about changes in their motor function from the climbing data. Despite revisions to improve observer reliability, we did not find many differences between the groups of spinal rats in our study. The lack of consistent trends in these results for both the number of pushoffs and cBBB scores suggest either that OEC and EES treatment did not have a strong effect on climbing abilities or that the evaluative measures need further development and validation. The small size of our animal groups that completed the study and the variability in spinal cord transections, both likely contributed to these inconclusive findings.

Additionally, we analyzed the climbing tests using EMG recordings from hindlimb muscles. Ziegler et al. (2011) used similar embedded EMG wires to assess recovery during treadmill stepping. In the current study, however, the EMG recordings obtained were difficult to compare between transplant groups, timepoints, and stimulation conditions. This is likely due to several factors: 1) most rats (~80%) had evidence of at least one broken EMG wire determined by the lack of EMG signal despite movement on the video or vice versa, 2) the number of steps and pushoffs were low and inconsistent for each condition and therefore the number of EMG recordings analyzed per rat varied, 3) the timing of the breach periods that were analyzed were variable and some included bouts of inactivity, and 4) the approaches to climbing varied greatly for each rat. For example, many rats leaned to one side and dragged their bodies while climbing, which created noise in the recordings. Thus, we were unable to accurately assess changes in EMG patterns across groups.

Grid climb training may not be an optimal locomotor task for EES therapies in rodent models of SCI

EES has potent effects on motor recovery, especially when paired with specific locomotor tasks such as treadmill stepping (Gerasimenko et al., 2007; Ichiyama et al., 2008; Ichiyama et al., 2005). In the current study and in Thornton et al. (2018) we not only combined EES with a cell transplant therapy for the first time, but we also paired EES with a different motor task, i.e., climb training, rather than treadmill stepping. Neither study showed evidence of functional recovery of OEC- versus FB-treated rats.

Here we found that because all groups received EES and improved on the BBB over time, there may have been a stimulation effect. Unlike in other studies from the Edgerton lab, however, in which direct EES administration was able to stimulate stepping in fully transected rats (Ichiyama et al., 2008; Courtine et al., 2009; Gad et al., 2013), EES failed to have a clear, direct effect on behavioral results when combined with climb training. There may, therefore, be important therapeutic aspects of the treadmill task that are not replicated during climbing. Treadmill stepping requires on-going activation of repetitive movements that rely heavily on proprioceptive feedback, whereas grid climbing occurs in short bursts and requires complex movements and coordination. Climb training with EES also resulted in periods when the rat received stimulation while inactive or climbing incorrectly, thereby potentially reinforcing negative behavior. While grid climbing may be an attractive alternative to test cortical circuit recruitment, based on our findings, it may not be the most appropriate training regimen to pair with EES.

Changes in transplantation and injury methodology increased transplanted cell survival but had other unintended effects

There are few studies in the OEC field that have examined OEC transplant survival after injury and the latest time-point that transplanted OECs were observed was 4 months post-injury (Barbour et al., 2013; Lu et al., 2006; Roet et al., 2012). In our previous long-term studies (Kubasak et al., 2010; Takeoka et al., 2012; Ziegler et al., 2011), we could not explicitly determine OEC survival as there are no unique markers for OECs to distinguish them from other glial cells. In a recent short-term study we were able to track transplanted

cell survival by using GFP-expressing OECs and FBs and found that the cells died between 1-2 months post-transplantation, unless the rats were treated with cyclosporine A (Khankan et al., 2016). In the current study we made a number of changes to improve transplant survival. After conducting multiple pilot studies, we chose the inbred Fischer 344 rat model to reduce non-autologous transplant rejection, a microaspiration injury technique to reduce immune cell infiltration and tissue damage, and a delayed transplant paradigm to avoid the acute immune response that occurs after injury. Together, these changes had a marked effect on cell survival as OECs were identified in all OEC-treated rats at 5- and 6-months post-transplant. Unfortunately, some of these changes also had unintended effects on the study.

Unlike in our other previous work in outbred rats, some of our Fischer 344 rats died spontaneously during the study. After searching the literature, several publications reported that Fischer 344 rats frequently developed spontaneous leukemias that led to sudden death (Moloney et al., 1970; Thomas et al., 2007). We also found several incomplete injuries in the F1 cohort due to the microaspiration method that led to highly variable motor function. Due to the unexpected spontaneous deaths and variability of injuries, our sample sizes are small and do not include the controls we initially proposed. These small sample sizes limit significant results from behavioral analyses, but we detected a number of differences between transplant groups in anatomical analyses of the injury site.

OECs and FBs that survived over 5 months post-injury showed potent effects on axonal outgrowth and regeneration

Many studies report that OECs promote axonal outgrowth *in vitro* and *in vivo* and ensheathe and protect axons in the injury site at early time-points post-transplantation (Barbour et al., 2013; Khankan et al., 2016; Khankan et al., 2015; Roet & Verhaagen, 2014; Runyan & Phelps, 2009). Indeed, we found this was also true in the current study, however, the extent of NF-positive axon density in areas with OECs in the lesion core was much greater than previously reported. In addition, our finding that axons extend across the hostile lesion core on OEC bridges provides strong evidence that the OECs directly stimulated axon regeneration, rather than axonal sprouting (Steward et al., 2003). 5-HT-positive axons that crossed into the caudal glial scar border did not project far into the caudal stump. This result is consistent with an interpretation that the axons were severed during the initial injury and later regenerated across the lesion core associated with OECs. These findings suggest that OECs retain their growth-promoting abilities for at least 6 months post-transplantation and therefore are likely to provide continued benefits to axon regeneration over time.

Conversely, transplanted FBs appeared to have the opposite effect on axonal outgrowth; axons occasionally associated with a few FBs found in the lesion core, but larger areas with FBs in the spinal stumps characteristically had a stark absence of axonal markers such as NF and 5-HT. The lack of axon integration into grafts of FBs may be due to the axon growth-inhibitory molecules expressed by FBs such as chondroitin sulfate proteoglycans. Surprisingly, areas with surviving FBs had high levels of MAG immunoreactivity despite the lack of axons. These data suggest that dermal FBs may

promote the accumulation of inhibitory myelin debris, as opposed to OECs which can phagocytose and thus clear myelin fragments (Khankan et al., 2016; Lankford et al., 2008). These findings perhaps are not surprising given the dermal origin of the transplanted FBs that normally would not associate with the central nervous system. FBs from different origins, such as meningeal FBs, could have a different effect on axon growth and myelin protein accumulation (Toft et al., 2013).

OECs that survived over 5 months in the spinal cord revealed distinct interactions with myelinating cells and their progenitors

In addition to their effects on axonal outgrowth, OECs are used in transplantation therapies because of their beneficial effects on other cells around the injury site. OECs integrate well with astrocytes and therefore make the glial scar permissive for axon growth, signal to infiltrating macrophages to increase clearance of inhibitory debris, and even surround and protect neuronal cell bodies in the lesion core (Chuah, et al., 2011; Khankan et al., 2016, 2015). Here we also showed that the transplanted OECs integrated well with astrocytes and formed bridges across the lesion core to provide preferential sites for axons to project into the caudal stump.

Our study also focused on examining the poorly understood interactions of OECs with myelinating cells and their progenitors. We found that axons in the lesion core of OEC-treated rats more frequently associated with MAG than the axons in the media or FB controls. Although the association of axons with MAG may be indicative of axon myelination, MAG is known to be inhibitory to axon growth (McKerracher et al., 1994).

116

Despite their effects on increasing myelin in the injury core, we found that it did not appear to inhibit OEC-stimulated axonal outgrowth.

We then asked if the source of MAG was due to increased presence of either SCs or oligodendrocytes or if it was expressed by the OECs themselves. Based on our findings, the presence of OECs did not affect SC infiltration into the lesion core overall, but we frequently found that OECs closely intermingled with both myelinating and non-myelinating SCs in the lesion core and in the spinal stumps. This finding suggested that there may be a higher density of SCs in areas where OECs are present. Because SCs have similar morphologies, express similar markers, and associate closely with OECs, however, it was difficult to distinguish the two types of SCs from the OECs at low magnification in large areas of the lesion site. Despite higher levels of SC markers (p0 and p75) we were unable to definitively determine that SC infiltration into areas with OECs was greater than in other areas of the lesion core. High magnification confocal images revealed the intertwining relationships between the OECs and SCs, particularly in areas with high axon density, suggesting that the OECs and SCs may have synergistic effects on axon growth and myelination.

We also examined OEC interactions with oligodendrocytes and OPCs. Little is known about the effects of OECs on OPC proliferation and differentiation and the few studies that were conducted focused mainly on *in vitro* experiments (Carvalho et al., 2014; Lamond & Barnett, 2013; Sorensen et al., 2008). Results from this study, however, found that OECs may directly influence survival of oligodendrocytes and OPCs in the toxic lesion core. We found examples of OPCs and even some immature oligodendrocytes in the GFAP-negative lesion core, but almost exclusively in areas where OECs were

present. This finding suggests that OECs may interact with oligodendrocytes that contribute to axon myelination in the injury core itself. The presence of immature oligodendrocytes also suggests that the OECs may directly support newly differentiated oligodendrocytes in the injury core and promote the differentiation of oligodendrocytes in the spinal stumps and potentially contribute to remyelination. Further study on OEC and oligodendrocyte interactions is needed to determine if there are effects in areas other than the scar border, such as areas in the spinal stumps that contain OECs.

Differences in morphology and gene expression suggest that multiple subtypes of transplanted OECs are present at the injury site

The long-term transplant survival achieved in this study also provided the opportunity to better observe variations in OECs at the injury site. Interestingly, OECs cultured from the olfactory bulb upregulate their expression of p75 *in vitro* even though OECs in the olfactory bulb rarely express p75 in adults. In addition, cultured OECs also vary in morphology, ranging from flat, fibroblast-like cells to thin, spindle-shaped cells (Ramón-Cueto & Nieto-Sampedro, 1992; Khankan et al., 2015). Other studies of OECs describe "astrocyte-like" OECs that express GFAP and "myelinating, SC-like" OECs that express p0 (Ebel et al., 2013; Sasaki et al., 2006; Yao et al., 2018). In the current study we specifically examined immunolabeling of p75 and p0 in the GFP-positive transplanted OECs and found evidence of three subtypes based on their levels of protein expression: 1) p75-positive, 2) p0-positive, and 3) p75- and p0-negative. These OEC subtypes may or may not each carry out different functions, such as promoting axon outgrowth,

myelinating axons, and phagocytosing debris (Sasaki et al., 2006; Lankford et al., 2008; Khankan et al., 2016).

Beyond protein expression, OECs also exhibited different morphologies as they associated with each other. We found OECs in both the lesion core and spinal stumps in disorganized clusters (Fig. 14A-F and Fig. 15A-E), organized mesh-like patterns (Fig. 11E-H), chain-like structures (Fig. 12), and twisting and intertwining, rope-like formations (Fig. 16 and Fig. 19). These varying OEC interactions could also be related to different functions, such as providing substrates for axonal outgrowth, integrating into the glial scar, phagocytosing debris, or myelinating axons. Further comparisons of OECs in the lesion core and OECs in the spinal stumps may further reveal differences that are related to their proximity to the injury site and their interactions with surrounding cells.

CHAPTER 5. CONCLUSIONS

This thesis reports a complex long-term study combining treatments for severe rodent spinal cord injury (SCI) that used two different therapeutic mechanisms: olfactory ensheathing cell (OEC) transplantation that targeted the injury site, and electrical epidural stimulation (EES) and climb training that targeted spinal circuit reorganization. We found that the EES treatment likely had modest effects on the recovery of motor function whereas the OEC treatment was able to affect several factors in the lesion core that are beneficial for SCI recovery, particularly in areas where OECs survived. The discovery and analysis of the transplanted OECs in the lesion core provided particularly interesting insights into the long-term effects of OECs in the injury site; surviving OECs had robust effects on axonal outgrowth and increased axon association with myelin in the lesion core. We also discovered unique interactions between OECs and myelinating cells such as Schwann cells (SCs) and oligodendrocytes in the lesion core and detected several different types of OECs at the injury site. These findings have revealed further insights into the mechanisms behind OEC transplantation after SCI.

In addition to many studies in the field, the findings in this thesis expand and build specifically on data found in five previous studies from our labs and thus contribute to the larger picture of the efficacy of OEC transplantation therapies (Kubasak et al., 2008; Takeoka et al., 2011; Ziegler et al., 2011; Khankan et al., 2015; Thornton et al., 2018). Here, we will compare some of the previous findings with the recent contributions of the current study to provide a better understanding of the effects of OEC transplantation. As outlined in Table 3, each of these studies has somewhat different methodology that built

on the previous study. Therefore, due to the different experimental factors and sample sizes, our results have varied. For example, effects on functional recovery in this study did not replicate findings from Takeoka et al. (2011) or Ziegler et al. (2011). There are several common threads, however. In all these studies we found substantial and positive effects of OECs on axon regeneration and connectivity at the injury site.

In this thesis we detected improvements in functional recovery on the BBB test (Basso et al., 1995) after beginning EES and climb training treatment. While we found that there were moderate improvements in functional recovery over time, these changes did not appear to be affected by OEC treatment. This is contrary to evidence found in some previous long-term studies conducted in our labs (Kubasak et al., 2008, Takeoka et al., 2011, and Ziegler et al., 2011). While working on the current project we finished a manuscript on a long-term pilot study that also evaluated OEC-transplantation combined with EES and climb training in completely transected rats. Unlike the previous long-term studies, Thornton et al. (2018) found no differences in functional recovery over time. There were several important differences between the first three studies and the two most recent ones: 1) sample sizes were between 9-10 vs. 4-6 rats/group, 2) controls included transplant and no-training controls vs. only transplant controls, and 3) OEC treatment was paired with treadmill stepping vs. EES and climb training (Table 3). In the current study the sample sizes and controls were originally intended to match those in previous studies, however due to the poor health of the Fischer 344 rat strain, we were unable to complete the experiment as planned. Most likely, the inbred Fischer 344 rats were not appropriate for long-term complete transection studies. It is important to note that all the studies in our lab were conducted in a complete spinal cord transection model that typically has

limited possibilities for functional recovery. Therefore, in future studies, OEC effects in more moderate injury models such as a double hemisection or contusion may provide a more appropriate and interesting comparison.

Thornton et al. (2018) also evaluated OEC-transplantation combined with EES and climb training in completely transected rats. The injury and transplantation methods were identical to those in our only short-term study in which we found that the transplanted cells survived less than 2 months post-injury (Khankan et al., 2016). Similar to Thornton et al. (2018), the current study also used the same transsynaptic retrograde tracer, pseudorabies virus (PRV) and careful analysis of axon and astrocyte bridging at the injury site to assess connectivity with hindlimb motor circuits. Despite the lack of OEC survival in Thornton et al. (2018), compelling evidence of regenerated axonal connectivity above the injury site was detected in one OEC-treated rat. In addition to this rat, Thornton et al also found that one control FB-treated rat had substantially more PRV-positive cells rostral to the injury site than any other spinal rat. After careful examination of the injury sites, however, differences were discovered that indicated tissue sparing, rather than axon regeneration had occurred in the FB-, but not the OEC-treated rat. Specifically, we discovered an area of ventral spinal cord that was intact and contained axons that appeared straight and organized in the FB-treated rat. Conversely, the OEC-treated rat had axons that bridged the two halves of the spinal cord in a twisting and tortuous path on thin areas of tissue. The observation of disorganized axon growth fulfilled one of the several criteria of regenerated axons described in Steward et al. (2003) and we thus concluded that the connectivity was due to axon regeneration. The FB-treated rat,

however, failed to meet these requirements and our conclusion was that axon sparing had occurred due to an incomplete injury.

The establishment of methods used to distinguish regenerated versus spared axons in Thornton et al. (2018) proved invaluable in distinguishing the incompletely injured rats in this thesis. Here, we discovered several incompletely transected rats using similar methods that helped to determine the extent of axonal outgrowth. Unlike areas with evidence of incomplete injuries, in areas where axons associated with OEC bridges in the lesion core, axons did not appear straight or continuous. As in the previous study, we also further delineated axon connectivity by analyzing PRV-positive cells rostral to the lesion core. These data, however, are part of a thesis by a current master's student in the lab and thus do not appear in this dissertation.

One of the strengths of this thesis compared to the five previous studies was the long-term survival of the transplanted OECs. Because OECs do not have unique markers that can distinguish them from SCs and other cells at the injury site, we were previously unable to detect the transplanted cells before using GFP-labeled OECs. In the short-term study reported in Khankan et al. (2016) we transplanted GFP-labeled OECs and examined their direct effects on the injury site over time. We found that the OECs directly interacted with neuron cell bodies, neurofilament-positive and serotonergic axons, chondroitin sulfate proteoglycans, and myelin debris in the lesion core. We also found that some, but not all, of the beneficial effects of OECs at the injury site disappeared at later time points after the OECs had died. In Thornton et al. (2018) we did not find any surviving cells at 7-months post-injury, however there were some modest effects on axonal outgrowth and regeneration at the injury site which may have occurred while the

123

OECs were still alive. This suggests that OECs may have early effects on the injury site that are maintained over time. We believe, however, that improved OEC survival would be required to optimize the benefits of OEC transplantation.

Of the five previous studies that looked at changes at the injury site, all found that OEC treatment had some positive effect on axonal outgrowth, particularly of the 5-HT-positive serotonergic axons. This was also true in the current study, however the effects of OECs on axonal outgrowth were far more striking than seen previously. While we found both 5-HT- and neurofilament (NF)-positive axons that extended into the lesion core with OECs in Khankan et al. (2016), in the current study we observed 5-HT- and NF-positive axons that crossed the entire lesion core on OEC bridges. We also found that areas with OECs had a substantially greater density of axons than other areas in the lesion core, a finding that we had not observed previously. This suggests that OECs maintain their ability to promote axon regeneration even months after transplantation and that long-term OEC survival can have a dramatic impact on axonal outgrowth.

Beyond the direct interactions between OECs and axons, this dissertation also investigated the interactions between OECs and other cells in the lesion core. For the first time in our lab, we report the effects of OEC transplantation on myelin and myelin-producing cells. Much of our earlier work was focused on OEC effects on tissue sparing and axonal outgrowth, however axon myelination is an important therapeutic target that we had previously not assessed. Thus, in the current study we discovered that OEC-transplantation enhanced the association between axons and myelin in the lesion core. Additionally, Khankan et al. (2016) showed that OEC treatment decreased the presence of myelin debris and that OECs did phagocytize myelin fragments. In the current study,

we observed myelinating and non-myelinating SCs and oligodendrocytes in the glial scar borders and lesion core and found that they were able to integrate with surviving OECs. Possibly, the interactions between OECs and myelinating SCs could have increased axon-myelin association in the lesion core. Further, interactions with the non-myelinating SCs, which are also known to have benefits on axonal outgrowth, may have contributed to the substantial axon growth we detected in areas with OECs. Another surprising finding was the presence of oligodendrocytes associated with OECs in the lesion core. Similar to the neuron cell bodies found in the lesion core with OECs in Khankan et al. (2016), oligodendrocytes would not normally be found in the hostile lesion core environment. These results suggest that further studies on the OEC effects on myelin would be productive.

Although OECs do not myelinate axons in their native environment, several studies reported that OECs can myelinate axons when transplanted into the spinal cord (Sasaki et al., 2006, 2011; Lankford et al., 2008). We have not, however, had the opportunity to observe OECs that may have differentiated into a myelin-producing phenotype. In this study, not only did we find evidence of OECs that produced peripheral, SC-like myelin, but we also found evidence of two other subtypes of OECs based on their expression patterns. Despite the difference in expression of specific OEC markers, we were unable to further delineate the functions of these different subtypes. This discovery of different subtypes of OECs is an area of interest that we plan to pursue. In particular, we plan to further distinguish other markers or OEC subtypes and to study potential differences in function to determine if there are subtypes that may be more beneficial for SCI transplantation therapies than others.

In summary, our findings suggest that long-term survival of transplanted OECs may provide multiple benefits to changes at the lesion site after severe SCI. The effects of OEC treatment on axon growth and myelination seen in this study provide promising evidence for the use of OEC transplantation therapies. Clearly, further optimization is needed to maximize the therapeutic benefits of OEC transplantation combined with EES and climb training, and this study will provide a foundation for future study of multi-faceted combinatorial treatments for SCI.

Table 3:

	Kubasak et al. (2008)	Takeoka et al. (2011)	Ziegler et al. (2011)	Khankan et al. (2016)	Thornton et al. (2018)	Dixie et al. (current)
Rat strain	Wistar-Hannover	Wistar-Hannover	Wistar-Hannover	Sprague-Dawley	Sprague-Dawley	Fischer 344
Group sizes	9-10	9-11	10-11	4-6	5-6	4-6
Injury type	1) Microscissor transection	1) Microscissor transection	1) Microscissor transection	1) Microscissor transection	1) Microscissor transection	1) Microaspiration 2) Microscissor transection
OEC transplant	1) Acute	1) Acute	1) Acute	1) Acute 2) Acute plus cyclosporine A	1) Acute	1) Delayed & used Fibrin matrix & Calpain Inhibitor
Paired treatment	Treadmill step training	Treadmill step training	Treadmill step training	(None)	EES & climb training (all)	EES & climb training (all)
Experimental groups	1) OEC only 2) OEC & Stepping 3) Media Only 4) Media & Stepping	1) OEC only 2) OEC & Stepping 3) Media Only 4) Media & Stepping	1) OEC only 2) OEC & Stepping 3) Media Only 4) Media & Stepping	1) OECs 2) FBs (Each group at 1, 2, 4, and 8 wks)	1) OECs & EES 2) FBs & EES (Each received climb training)	1) OECs & EES 2) Media & EES 3) FBs & EES (Each received climb training)
Study Length (Post-Injury)	7 months	7 months	7 months	1-8 weeks	7 months	5.5-6.5 months
Behavioral analyses	1) Stepping (+)	1) Stepping (+) 2) MEPs (+/-)	1) Stepping (+) 2) MEPs (+) 3) Climbing pushoff & EMGs (+)	(None)	1) Pushoffs (0) 2) EMGs (0)	1) Pushoffs (0) 2) EMGs (0) 3) cBBB (0) 4) BBB (+ EES)
Surviving OECs	Unknown	Maybe (p75-positive)	Unknown	Yes until 4 to 8 weeks	No	Yes, in all OEC treated rats
Spared tissue	(+)	(+)	Unknown	(0)	(0)	(0)
Neurons	(+)	(+)	Unknown	(+)	(0)	(0)
Axon outgrowth	1) Noradrenergic fibers (+)	1) 5-HT (+)	Unknown	1) 5-HT (+) 2) NF (+)	1) 5-HT (+) 2) NF (+)	1) 5-HT (+) 2) NF (++)
Evidence of circuit connectivity	No	Yes – Re-transection & MEPs	Yes – MEPs	No	Yes – PRV & Axon bridges	Yes – Axon bridges & PRV*
OEC interactions in injury site	Unknown	Uncertain	Unknown	Yes – 5-HT & NF	(No cell survival)	Yes – 5-HT, NF, myelin, oligos, Schwann cells
Myelin	Unknown	Unknown	Unknown	Decreased myelin debris	Unknown	1) Increased myelin 2) OECs interact with myelinating cells

Table 3 Legend: Comparison between the current study and previous complete spinal cord injury studies in our lab.

Summary comparison of six OEC studies conducted in our lab: Kubasak et al. (2008), Takeoka et al. (2011), Ziegler et al. (2011), Khankan et al. (2016), Thornton et al. (2018), and the current study. Abbreviations: serotonergic axons (5-HT), electrical epidural stimulation (EES), electromyography (EMGs), fibroblasts (FBs), motor-evoked potentials (MEPs), neurofilament-positive axons (NF), olfactory ensheathing cells (OECs), pseudo-rabies virus (PRV). Findings are summarized as having positive OEC effects (+), negative effects (-), and no significant effects (0). (*PRV data on this study not reported in this thesis).

APPENDIX ITEM 1. CLIMBING ASSESSMENT GUIDE

The Climbing Assessment is split into 5 categories:

	Right Subscore:				Left Subscore				Body:	Total Score:
	1	2	3	4	1	2	3	4		

1) Limb Movement				2) Paw Placement				3) Weight Bearing				4) Steps			5) Body		
Hip	Knee	Ankle	Sweep	Dorsal	Back	Mid-Front	Freq	Back	Mid-Front	Curled	Freq	Pushoffs	Misses	Completions	Trunk	Tail	Abdomen
R L	R L	R L	R L	R L	R L	R L	R L	R L	R L	R L	R L	R L	R L	R L	R L	R L	R L
Ø Ø	Ø Ø	Ø Ø	Y Y	Y Y	Y Y	Y Y	O O	Y Y	Y Y	Y Y	O O	O O	O O	O O	Leaning	Leaning	Drag
S S	S S	S S	N N	N N	N N	N N	F F	N N	N N	N N	F F	F F	F F	F F	Wobbly	Wobbly	Parallel
E E	E E	E E					C C				C C		C C	C C	Stable	Stable	High

1) Limb Movement

- Limb movement measures are similar to those in Basso et al. (1995).
- To assess limb movement, look for range of motion (RoM) of 3 hindlimb joints:
    - **Hip**: The change in angle from the body and the femur (between 1 + 2).
    - **Knee:** The change in angle from the femur and the tibia (between 2 + 3).
    - **Ankle:** The change in angle from the tibia and the foot (between 3 + 4).
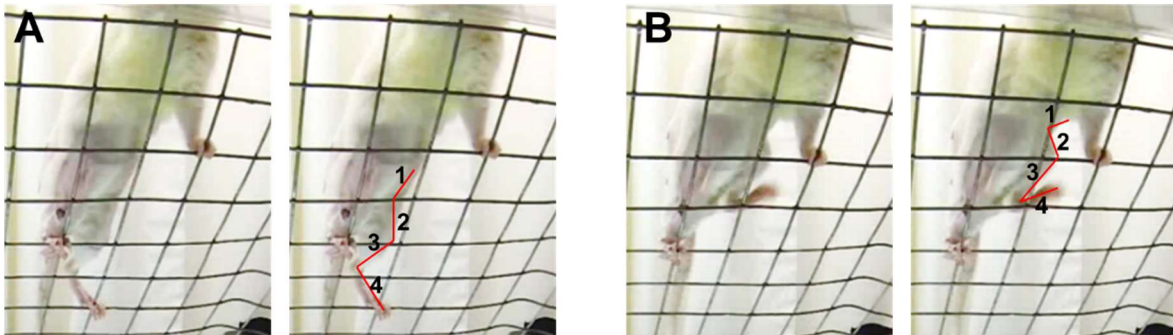
- Determining joint movement:
    - Depending on the angle of the rat, hindlimb joint extension and flexion can be difficult to determine. Some examples are given below:
    - Ankle movement is the easiest to see, especially from a side view, but if you are having trouble, look for subtle changes in distance from the grid. Is the foot moving further or closer to the grid while the tibia does not move?
    - Knees are more challenging but look for subtle changes in the tibia and ankle position as good indicators, both towards and from the grid and vertically. Is the body remaining in the same location while the foot, but not the ankle, is moving up and down?
    - Hips are the most challenging. These require some practice to assess movement. Look for patterns similar to those in the ankle and knee

129

assessments but focus more on the knee, femur, and leg as a whole. Is the knee changing positions?

- Extent of range of motion:
  - Full RoM for each joint is depicted above .
    - More challenging while climbing
  - Score of **0** indicates no movement of the joint was detected.
  - Score of **S** indicates slight movement of the joint .
    - <50% RoM, changes in joint angles are small.
  - Score of **E** indicated extensive movement of the joint.
    - >50% to full RoM, changes in joint angles are large.
  - If you see it once, you circle that score (ex., You saw extension of the knee one time but slight the others, you would still circle "E").
  - Score each leg individually.

- Sweeps:
  - A **sweep** is defined as coordinated movement of all 3 joints (such as a frog kick).
  - Score as a yes or no.

2) Paw Placement

- Paw placement is considered a somewhat "active" movement of the foot onto a bar:
  - **Dorsal**: The placement of the dorsal surface of the foot on the bar.
  - **Back:** The placement of the plantar surface of the heel on the bar.
  - **Mid-Front:** The placement of the middle, front, or toes of the plantar surface of the foot on the bar.

- Determining paw placement:
  - Active placement is difficult to determine- some form of limb movement should occur beforehand.
  - Random placement would include:
    - Limb dragging on grid and passively touching a grid bar.
    - Rat falls or slips backward, and foot happens to fall on a bar (no limb movement associated with the placement).
    - Rat is placed by the experimenter onto the grid intentionally.
  - Higher score takes precedent over a lower score.
  - Score as a yes or no for each foot

- Determining frequency:

- Score of **O** indicates <u>o</u>ccasional placement of the foot at the location of the highest score to the left (more than once, **between 2-5** occurrences).
- Score of **F** indicates <u>f</u>requent placement of the foot (**between 6-9** occurrences).
- Score of **C** indicates <u>c</u>onsistent placement of the foot (**10 or more** occurrences).

3) Weight Bearing

- Weight bearing occurs when a rat is using a hindleg to support some of its weight:
  - **Back:** The placement of the heel of the bottom plantar of the foot on the bar, with ankle and knee in a "loaded" position (see below).
  - **Mid-Front:** The placement of the middle, front, or 1-2 toes of the bottom surface of the foot on the bar, with ankle and knee in a "loaded" position.
  - **Curled:** The wrapping or grasping of 2 or more toes around the bar, with ankle and knee in a "loaded" position (see image below).

- Determining weight bearing:
  - Weight bearing may require additional confirmation, as it is often challenging determine. It can be subjective to decide if the legs are in a "loaded position".
  - Weight bearing begins with some form of paw placement, so as previously noted, watch out for random placement:
    - Limb dragging on grid and passively touching a grid bar.
    - Rat falls or slips backward, and foot happens to fall on a bar (no limb movement associated with the placement).
    - Rat is placed by the experimenter onto the grid intentionally.

  - To determine "loading of muscles" (see image):
    - Observe bend in joints as the rat rests her weight on the bar. During that time, look for slight movements that might indicate there is weight supported by that foot.
    - Determine where the animal is resting her weight. Is she leaning to one side and simply resting her other foot on the grid?
    - Determine if the rat is supporting her weight mainly with the forelimbs.

- Weight bearing may need further confirmation with the EMG pattern of the rat. Please record the frame number of each incidence you observe so confirmation can be obtained.
- As above, a higher score takes precedent over a lower score.
- Score as a <u>yes</u> or <u>no</u> for each foot.

- Determining frequency:
  - Score of **O** indicates <u>o</u>ccasional weight bearing (more than once, **between 2-5** occurrences).
  - Score of **F** indicates <u>f</u>requent weight bearing (**between 6-9** occurrences).
  - Score of **C** indicates <u>c</u>onsistent weight bearing (**10 or more** occurrences).
  - The exact number and corresponding video frames of weight-bearing incidents should also be recorded at the bottom of the scoring sheet for future reference.

4) Steps

- "Steps" are considered as a fluid movement of the foot from one bar to the next.
  - **Pushoff**: The rat begins with the foot placed on a bar and either moves the leg off the bar in a fluid manner or pushes leg off the bar but does not try to extend the rest of the leg to complete the stepping movement.
  - **Miss:** The rat begins with the foot placed on a bar and either moves the leg off the bar in a fluid manner or pushes leg off of the bar and attempts to move it higher up the grid but is <u>unsuccessful</u> and misses the next bar.
  - **Completion:** Same as above, however the attempt is <u>successful</u> and the rat is able to move her leg from one bar to another higher up the grid.

- Determining a step:
  - Like weight bearing, steps are vulnerable to subjectivity and it is difficult to decide what a fluid movement may be.
  - Stepping begins with some form of paw placement, usually with weight bearing (but not always).
  - To determine if a "step" has occurred:
    - Observe if the step begins with some form of paw placement, or weight bearing.

- Observe the joint movements. Are all three joints moving? Is there a coordinated movement?
- Determining fluid movement requires distinguishing fluid vs spastic movements. Look at the real time video, is the movement very fast? Does the rat have a big response to the movement (jumping back)? Or does it seem controlled?
- Images above show the stages of a pre-injury step completion, beginning with placement, stretch, flexion, extension, shift in weight, and final foot placement on the grid. Not every step looks the same, however. (Consult pre-injury videos for more examples.)
- Look closely at the change in position of the ankle relative to the bars.

- Steps almost always need further confirmation with the EMG pattern of the rat. Please record the frame number of each incidence you observe so confirmation can be obtained.
- A step may also be considered as a "pushoff" if you observe clear evidence of the rat pushing her hindlimb off of the grid instead of simply lifting it. Make a note at the corresponding frames on the scoring sheet.
- You may also write "potential step" if you are not sure and consult others.

- Determining frequency:
  - Score of **O** indicates occasional steps at least once, **between 1-5** occurrences) *Note this is different than above.
  - Score of **F** indicates frequent steps (**between 6-9** occurrences).
  - Score of **C** indicates consistent steps (**10 or more** occurrences).
  - The number of steps should also be recorded at the bottom of the scoring sheet as pushoff and steps can be reported as individual measures.

5) Body Control

- Body control is determined through three different measures:
  - **Trunk Stability:** The relative control and position of the body trunk (hindlimbs and abdomen) while the rat is climbing.
  - **Tail Stability:** The relative control and position of the tail while the rat is climbing.
  - **Abdomen Location:** The location of the abdomen in relation to the grid while the rat is climbing.

- Determining body control:
  - For trunk stability, focus on the position of the lower body in relation to the upper body and in relation to a vertical bar on the grid.

- Is the body moving from side to side a lot, is the rat leaning on one side, or is it staying mostly centered relative to her arms and head?
  - For the tail, it is similar to trunk stability, except you should focus on the tail movement in relation to the body.
    - Is the tail trailing behind, leaning to one side, flailing about, or staying centered and controlled?
  - Abdomen location refers to the way an animal moves up the grid. Pre-injured rights assume a "high" posture as in they are supporting their weight with their limbs and therefore the abdomen is supported further from the surface of the grid. Injured animals more often drag their bellies or have them only slightly off of the grid surface.
    - How close is the trunk to the grid while the rat is moving? Is it dragging, fairly close but not quite dragging, or is it pushed further away?
  - Only consider body posture <u>while the rat is moving</u> (note that they may lean as they rest but perform better as they climb).

- How to score body control:
  - **<u>Leaning</u>:** The rat has one side closer to the grid than the others the majority of the time while climbing (circle which side on the scoring sheet).
  - **<u>Wobbly</u>:** The relative position of the body or tail is often moving from side to side while climbing.
  - **<u>Stable</u>:** The rat has good control of her body and is centered most of the time.

  - **<u>Drag</u>:** The abdomen is touching the grid as the rat moves.
  - **<u>Parallel</u>:** The rat is not dragging her abdomen but is pushed slightly away from the grid. The body does not touch the grid as she moves.
  - **<u>High</u>:** The rat is most often supporting weight on her limbs and is pushed further back from the grid as she climbs.

General advice: Go slowly- move through points of interest by moving forward and reverse frame by frame, but also play in real time to distinguish spasticity from control. You can generally fast forward through areas where the rat is not moving at all.

Reference:

Basso, D. M., Beattie, M. S., & Bresnahan, J. C. (1995). A sensitive and reliable locomotor rating scale for open field testing in rats. J. Neurotrauma 12, 1–21.

REFERENCES

Akiyama, Y., Lankford, K., Radtke, C., Greer, C. A., Jeffery, D., & Kocsis, J. D. (2004). Remyelination of spinal cord axons by olfactory ensheathing cells and Schwann cells derived from a transgenic rat expressing alkaline phosphatase marker gene. *Neuron Glia Biol.* **1**, 47–55.

Al-majed, A. A., Brushart, T. M., & Gordon, T. (2000). Electrical stimulation accelerates and increases expression of BDNF and trkB mRNA in regenerating rat femoral motoneurons. *Eur. J Neuro.* **12**, 4381–4390.

Al-majed, A. A., Neumann, C. M., Brushart, T. M., & Gordon, T. (2000). Brief electrical stimulation promotes the speed and accuracy of motor axonal regeneration. *J Neurosci.* **20**, 2602–2608.

Alam, M., Garcia-Alias, G., Jin, B., Keyes, J., Zhong, H., Roy, R. R., Gerasimenko, Y., Lu, D. C., & Edgerton, V. R. (2017). Electrical neuromodulation of the cervical spinal cord facilitates forelimb skilled function recovery in spinal cord injured rats. *Exp. Neurol.* **291**, 141–150.

Almad, A., Sahinkaya, F. R., & McTigue, D. M. (2011). Oligodendrocyte fate after spinal cord injury. *Neurotherapeutics* **8**, 262–73.

Alto, L. T., Havton, L. A., Conner, J. M., Hollis, E. R., Blesch, A., & Tuszynski, M. H. (2009). Chemotropic guidance facilitates axonal regeneration and synapse formation after spinal cord injury. *Nat. Neurosci.* **12**, 1106–1113.

Alvarez, J. I., Katayama, T., & Prat, A. (2013). Glial influence on the blood brain barrier.

Glia **61**, 1939–58.

Anderson, M. A., Burda, J. E., Ren, Y., Ao, Y., O'Shea, T. M., Kawaguchi, R., Coppola, G., Khakh, B. S., Deming, T. J., & Sofroniew, M. V. (2016). Astrocyte scar formation aids central nervous system axon regeneration. *Nature* **532**, 195–200.

Andrews, M. R., & Stelzner, D. J. (2007). Evaluation of olfactory ensheathing and Schwann cells after implantation into a dorsal injury of adult rat spinal cord. *J Neurotrauma* **24**, 1773–1792.

Assinck, P., Duncan, G. J., Plemel, J. R., Lee, M. J., Stratton, J. A., Manesh, S. B., Liu, J., Ramer, L. M., Kang, S. H., Bergles, D. E., Biernaskie, J., & Tetzlaff, W. (2017). Myelinogenic plasticity of oligodendrocyte precursor cells following spinal cord contusion injury. *J Neurosci.* **37**, 8635–8654.

Au, E., Richter, M. W., Vincent, A. J., Tetzlaff, W., Aebersold, R., Sage, E. H., & Roskams, A. J. (2007). SPARC from olfactory ensheathing cells stimulates Schwann cells to promote neurite outgrowth and enhances spinal cord repair. *J Neurosci.* **27**, 7208–7221.

Au, E., & Roskams, A. J. (2003). Olfactory ensheathing cells of the lamina propria in vivo and in vitro. *Glia* **41**, 224–236.

Babiarz, J., Kane-Goldsmith, N., Basak, S., Liu, K., Young, W., & Grumet, M. (2011). Juvenile and adult olfactory ensheathing cells bundle and myelinate dorsal root ganglion axons in culture. *Exp. Neurol.* **229**, 72–9.

Barakat, D. J., Gaglani, S. M., Neravetla, S. R., Sanchez, A. R., Andrade, C. M.,

Pressman, Y., Puzis, R., Garg, M. S., Bunge, M. B., & Pearse, D. D. (2005). Survival, integration, and axon growth support of glia transplanted into the chronically contused spinal cord. *Cell Transplant.* **14**, 225–240.

Barbour, H. R., Plant, C. D., Harvey, A. R., & Plant, G. W. (2013a). Tissue sparing , behavioral recovery , supraspinal axonal sparing / regeneration following sub-acute glial transplantation in a model of spinal cord contusion. *BMC Neurosci.* **14**, 1–22.

Barbour, H. R., Plant, C. D., Harvey, A. R., & Plant, G. W. (2013b). Tissue sparing, behavioral recovery, supraspinal axonal sparing/regeneration following sub-acute glial transplantation in a model of spinal cord contusion. *BMC Neurosci.* **14**, 1.

Bareyre, F. M., Kerschensteiner, M., Raineteau, O., Mettenleiter, T. C., Weinmann, O., & Schwab, M. E. (2004). The injured spinal cord spontaneously forms a new intraspinal circuit in adult rats. *Nat. Neurosci.* **7**, 269–277.

Barnabé-Heider, F., Göritz, C., Sabelström, H., Takebayashi, H., Pfrieger, F. W., Meletis, K., & Frisén, J. (2010). Origin of new glial cells in intact and injured adult spinal cord. *Cell Stem Cell* **7**, 470–82.

Barriere, G., Leblond, H., Provencher, J., & Rossignol, S. (2008). Prominent role of the spinal central pattern generator in the recovery of locomotion after partial spinal cord. *J. Neurosci.* **28**, 3976–3987.

Barton, M. J., St John, J., Clarke, M., Wright, A., & Ekberg, J. (2017). The glia response after peripheral nerve injury: A comparison between Schwann cells and olfactory ensheathing cells and their uses for neural regenerative therapies. *Int. J. Mol. Sci.*

18, 1–19.

Basso, D. M., Beattie, M. S., & Bresnahan, J. C. (1995). A sensitive and reliable locomotor rating scale for open field testing in rats. *J. Neurotrauma* **12**, 1–21.

Baumann, N., & Pham-dinh, D. (2019). Biology of oligodendrocyte and myelin in the mammalian central nervous system. *Physiol. Rev.* **81**, 871–927.

Bethea, J. R., & Dietrich, W. D. (2002). Targeting the host inflammatory response in traumatic spinal cord injury. *Curr. Opin. Neurol.* **15**, 355–360.

Bhat, R. V., Axt, K. J., Fosnaugh, J. S., Smith, K. J., Johnson, K. A., Hill, D. E., Kinzler, K. W., & Baraban, J. M. (1996). Expression of the APC tumor suppressor protein in oligodendroglia. *Glia* **17**, 169–174.

Black, J. A., Felts, P., Smith, K. J., Kocsis, J. D., & Waxman, S. G. (1991). Distribution of sodium channels in chronically demyelinated spinal cord axons: immuno-ultrastructural localization and electrophysiological observations. *Brain Res.* **544**, 59–70.

Blakemore, W. F. (1974). Pattern of remyelination in the CNS. *Nature* **249**, 577–578.

Bradbury, E. J., Popat, R. J., Bennett, G. S., Patel, P. N., McMahon, S. B., Moon, L. D. F., Fawcett, J. W., & King, V. R. (2002). Chondroitinase ABC promotes functional recovery after spinal cord injury. *Nature* **416**, 636–640.

Burchiel, K. J., & Hsu, F. P. K. (2001). Pain and Spasticity After Spinal Cord Injury Mechanisms and Treatment. *Spine (Phila. Pa. 1976).* **26**, 146–160.

Burda, J. E., & Sofroniew, M. V. (2014). Reactive gliosis and the multicellular response

to CNS damage and disease. *Neuron* **81**, 229–48.

Burns, A. S., Marino, R. J., Kalsi-ryan, S., Middleton, J. W., Tetreault, L. A., Dettori, J. R., Mihalovich, K. E., & Fehlings, M. G. (2017). Type and timing of rehabilitation following acute and subacute spinal cord injury : a systematic review. *Glob. Spine J.* **7(3S)**, 175S-194S.

Cao, Q., He, Q., Wang, Y., Cheng, X., Howard, R. M., Zhang, Y., DeVries, W. H., Shields, C. B., Magnuson, D. S. K., Xu, X.-M., Kim, D. H., & Whittemore, S. R. (2010). Transplantation of ciliary neurotrophic factor-expressing adult oligodendrocyte precursor cells promotes remyelination and functional recovery after spinal cord injury. *J. Neurosci.* **30**, 2989–3001.

Cao, Q., Xu, X.-M., Devries, W. H., Enzmann, G. U., Ping, P., Tsoulfas, P., Wood, P. M., Bunge, M. B., & Whittemore, S. R. (2005). Functional recovery in traumatic spinal cord injury after transplantation of multineurotrophin-expressing glial-restricted precursor cells. *J. Neurosci.* **25**, 6947–57.

Card, P. J., & Enquist, L. W. (1999). Transneuronal circuit analysis with pseudorabies viruses. *Curr. Protoc. Neurosci.* **1**, 1–28.

Carvalho, L. A., Vitorino, L. C., Guimarães, R. P. M. M., Allodi, S., de Melo Reis, R. A., & Cavalcante, L. A. (2014). Selective stimulatory action of olfactory ensheathing glia-conditioned medium on oligodendroglial differentiation, with additional reference to signaling mechanisms. *Biochem. Biophys. Res. Commun.* **449**, 338–343.

Carwardine, D., Prager, J., Neeves, J., Muir, E. M., Uney, J., Granger, N., & Wong, L. (2017). Transplantation of canine olfactory ensheathing cells producing chondroitinase ABC promotes chondroitin sulphate proteoglycan digestion and axonal sprouting following spinal cord injury. *PLoS One* **12**, 1–19.

Casarosa, S., Bozzi, Y., & Conti, L. (2014). Neural stem cells: ready for therapeutic applications? *Mol. Cell. Ther.* **2**, 31.

Caudle, K. L., Atkinson, D. A., Brown, E. H., Donaldson, K., Seibt, E., Chea, T., Smith, E., Chung, K., Shum-siu, A., Cron, C. C., & Magnuson, D. S. K. (2015). Hindlimb stretching alters locomotor function after spinal cord injury in the adult rat. *Neurorehabil. Neural Repair* **29**, 268–277.

Centenaro, L. A., da Cunha Jaeger, M., Ilha, J., de Souza, M. A., Balbinot, L. F., do Nascimento, P. S., Marcuzzo, S., & Achaval, M. (2013). Implications of olfactory lamina propria transplantation on hyperreflexia and myelinated fiber regeneration in rats with complete spinal cord transection. *Neurochem. Res.* **38**, 371–81.

Centenaro, L. A., Jaeger, M. da C., Ilha, J., de Souza, M. A., Kalil-Gaspar, P. I., Cunha, N. B., Marcuzzo, S., & Achaval, M. (2011). Olfactory and respiratory lamina propria transplantation after spinal cord transection in rats: Effects on functional recovery and axonal regeneration. *Brain Res.* **1426**, 54–72.

Cha, J., Heng, C., Reinkensmeyer, D. J., Roy, R. R., Edgerton, V. R., & De Leon, R. D. (2007). Locomotor ability in spinal rats is dependent on the amount of activity imposed on the hindlimbs during treadmill training. *J. Neurotrauma* **24**, 1000–1012.

Chen, C.-H., Sung, C.-S., Huang, S.-Y., Feng, C.-W., & Hung, H.-C. (2016). The role of the PI3K / Akt / mTOR pathway in glial scar formation following spinal cord injury. *Exp. Neurol.* **278**, 27–41.

Chen, K., Liu, J., Assinck, P., Bhatnagar, T., Streijger, F., Zhu, Q., Dvorak, M. F., Kwon, B. K., Tetzlaff, W., & Oxland, T. R. (2015). Differential histopathological and behavioral outcomes eight weeks after rat spinal cord injury by contusion, dislocation, and distraction mechanisms. *J. Neurotrauma* **33**, 1667–1684.

Chuah, M. I., Hale, D. M., & West, A. K. (2011). Interaction of olfactory ensheathing cells with other cell types in vitro and after transplantation: glial scars and inflammation. *Exp. Neurol.* **229**, 46–53.

Cote, M.-P., & Gossard, J.-P. (2004). Step training-dependent plasticity in spinal cutaneous pathways. *J. Neurosci.* **24**, 11317–11327.

Courtine, G., Gerasimenko, Y., Van Den Brand, R., Yew, A., Musienko, P., Zhong, H., Song, B., Ao, Y., Ichiyama, R. M., Lavrov, I., Roy, R. R., Sofroniew, M. V., Edgerton, V. R., Brand, R. Van Den, Yew, A., Zhong, H., Song, B., Ao, Y., Ichiyama, R. M., Lavrov, I., Roy, R. R., Sofroniew, M. V., & Edgerton, V. R. (2009). Transformation of nonfunctional spinal circuits into functional states after the loss of brain input. *Nat. Neurosci.* **12**, 1333–1342.

Courtine, G., Song, B., Roy, R. R., Zhong, H., Herrmann, J. E., Ao, Y., Qi, J., Edgerton, V. R., & Sofroniew, M. V. (2008). Recovery of supraspinal control of stepping via indirect propriospinal relay connections after spinal cord injury. *Nat. Med.* **14**, 69–74.

Crowe, M., Bresnahan, J. C., Shuman, S., Masters, J. N., & Beattie, M. S. (1997). Apoptosis and delayed degeneration after spinal cord injury in rats and monkeys. *Nat. Med.* **3**, 73–76.

D'Urso, D., Ehrhardt, P., & Müller, H. W. (2018). Peripheral myelin protein 22 and protein zero: a novel association in peripheral nervous system myelin. *J. Neurosci.* **19**, 3396–3403.

Daniels, D., Miselis, R., & Flanagan-Cato, L. (2001). Transneuronal tracing from sympathectomized lumbar epaxial muscle in female rats. *J Neurobiol.* **48**, 278–290.

De Leon, R. D., See, P. A., & Chow, C. H. T. (2011). Differential effects of low versus high amounts of weight supported treadmill training in spinally transected rats. *J. Neurotrauma* **28**, 1021–1033.

Deng, L. X., Walker, C., & Xu, X. M. (2015). Schwann cell transplantation and descending propriospinal regeneration after spinal cord injury. *Brain Res.* **1619**, 104–114.

Deuchars, S. A., & Lall, V. K. (2015). Sympathetic preganglionic neurons: Properties and inputs. *Compr. Physiol.* **5**, 829–869.

Dityatev, A., Seidenbecher, C. I., & Schachner, M. (2010). Compartmentalization from the outside : the extracellular matrix and functional microdomains in the brain. *Trends Neurosci.* **33**, 503–512.

Dlouhy, B. J., Awe, O., Rao, R. C., Kirby, P. A., & Hitchon, P. W. (2014). Autograft-derived spinal cord mass following olfactory mucosal cell transplantation in a spinal

cord injury patient. *J. Neurosurg. Spine* **21**, 618–622.

Dou, C.-L., & Levine, J. M. (1994). Inhibition of neurite growth by the NG2 chondroitin proteoglycan. *J. Neuro* **14**, 7616–7628.

Du, K., Zheng, X. S., Zhang, Q., Li, S., Gao, X., Wang, J., Jiang, L., & Liu, K. (2015). PTEN deletion promotes regrowth of corticospinal tract axons 1 year after spinal cord injury. *J. Neurosci.* **35**, 9754–9763.

Ebel, C., Brandes, G., Radtke, C., Rohn, K., & Wewetzer, K. (2013). Clonal in vitro analysis of neurotrophin receptor p75-immunofluorescent cells reveals phenotypic plasticity of primary rat olfactory ensheathing cells. *Neurochem. Res.* **38**, 1078–87.

Edgerton, V. R., Sayenko, D. G., Atkinson, D. A., Floyd, T. C., Gorodnichev, R. M., Moshonkina, T. R., Harkema, S. J., Edgerton, V. R., & Gerasimenko, Y. P. (2015). Effects of paired transcutaneous electrical stimulation delivered at single and dual sites over lumbosacral spinal cord. *Neurosci. Lett.* **609**, 229–234.

Ekberg, J., & St John, J. (2015). Olfactory ensheathing cells for spinal cord repair: crucial differences between subpopulations of the glia. *Neural Regen. Res.* **10**, 1395.

Eloy Pessoa de Barros Filho, T., & Eira Iague Sleiman Molina, A. (2008). Analysis of the sensitivity and reproducibility of the Basso, Beattie, Bresnahan (BBB) scale in Wistar rats. *Clinics* **63**, 103–108.

Erceg, S., Ronaghi, M., Oria, M., Roselló, M. G., Aragó, M. A. P., Lopez, M. G., Radojevic, I., Moreno-Manzano, V., Rodríguez-Jiménez, F.-J., Bhattacharya, S. S.,

Cordoba, J., & Stojkovic, M. (2010). Transplanted oligodendrocytes and motoneuron progenitors generated from human embryonic stem cells promote locomotor recovery after spinal cord transection. *Stem Cells* **28**, 1541–9.

Faulkner, J. R., Herrmann, J. E., Woo, M. J., Tansey, K. E., Doan, N. B., & Sofroniew, M. V. (2004). Reactive astrocytes protect tissue and preserve function after spinal cord injury. *J. Neurosci.* **24**, 2143–55.

Fields, R. D. (2015). A new mechanism of nervous system plasticity : activity-dependent myelination. *Nat. Rev. Neurosci.* **16**, 756–767.

Filli, L., & Schwab, M. E. (2015). Structural and functional reorganization of propriospinal connections promotes functional recovery after spinal cord injury. *Neural Regen. Res.* **10**, 509–513.

Flynn, J. R., Graham, B. A., Galea, M. P., & Callister, R. J. (2011). The role of propriospinal interneurons in recovery from spinal cord injury. *Neuropharmacology* **60**, 809–822.

Fontana, X., Hristova, M., Costa, C. Da, Patodia, S., Thei, L., Makwana, M., Spencer-dene, B., Latouche, M., Mirsky, R., Jessen, K. R., Klein, R., Raivich, G., & Behrens, A. (2012). c-Jun in Schwann cells promotes axonal regeneration and motoneuron survival via paracrine signaling. *J. Cell Biol.* **198**, 127–141.

Forni, P. E., Taylor-Burds, C., Melvin, V. S., Williams, T., & Wray, S. (2011). Neural crest and ectodermal cells intermix in the nasal placode to give rise to GnRH-1 neurons, sensory neurons, and olfactory ensheathing cells. *J. Neurosci.*

Fouad, K., & Tetzlaff, W. (2012). Rehabilitative training and plasticity following spinal cord injury. *Exp. Neurol.* **235**, 91–99.

Fournier, A. E., Gould, G. C., Liu, B. P., & Strittmatter, S. M. (2002). Truncated soluble Nogo receptor binds Nogo-66 and blocks inhibition of axon growth by myelin. *J. Neurosci.* **22**, 8876–8883.

Franklin, R. J.M., Gilson, J. M., Franceschini, I. A., & Barnett, S. C. (1996). Schwann cell-like myelination following transplantation of an olfactory bulb-ensheathing cell line into areas of demyelination in the adult CNS. *Glia* **17**, 217–224.

Franklin, Robin J.M. (2003). Remyelination by transplanted olfactory ensheathing cells. *Anat. Rec. - Part B New Anat.* **271**, 71–76.

Franssen, E. H. P., De Bree, F. M., Essing, A. H. W., Ramon-Cueto, A., & Verhaagen, J. (2008). Comparative gene expression profiling of olfactory ensheathing glia and Schwann cells indicates distinct tissue repair characteristics of olfactory ensheathing glia. *Glia* **56**, 1285–98.

Frostick, S. P., Yin, Q. I., & Kemp, G. J. (1998). Schwann cells, neurotrophic factors, and peripheral nerve regeneartion. *Microsurgery* **5**, 397–405.

Gad, P., Choe, J., Nandra, M. S., Zhong, H., Roy, R. R., Tai, Y., & Edgerton, V. R. (2013). Development of a multi-electrode array for spinal cord epidural stimulation to facilitate stepping and standing after a complete spinal cord injury in adult rats. *J NeuroEng. Rehab.* **10**, 1–17.

Gardinier, M. V., Amiguet, P., Linington, C., & Matthieu, J. -M. (1992).

Myelin/oligodendrocyte glycoprotein is a unique member of the immunoglobulin superfamily. *J. Neurosci. Res.* **33**, 177–187.

Gaudet, A. D., Popovich, P. G., & Ramer, M. S. (2011). Wallerian degeneration: gaining perspective on inflammatory events after peripheral nerve injury. *J. Neuroinflammation* **8**, 110.

Geoffroy, G., & Hilton, B. J. (2016). Evidence for an age-dependent decline in axon regeneration in the adult mammalian central report evidence for an age-dependent decline in axon regeneration in the adult mammalian central nervous system. *Cell Rep.* **15**, 238–246.

Gerasimenko, Y. P., Ichiyama, R. M., Lavrov, I. A., Courtine, G., Cai, L., Zhong, H., Roy, R. R., & Edgerton, V. R. (2007). Epidural spinal cord stimulation plus quipazine administration enable stepping in complete spinal adult rats. *J. Neurophysiol.* **98**, 2525–2536.

Ghosh, M., & Pearse, D. D. (2015). The role of the serotonergic system in locomotor recovery after spinal cord injury. *Front. Neural Circuits* **8**, 1–14.

Goldman, S., & Osorio, J. (2014). So many progenitors, so little myelin. *Nat. Neurosci.* **17**, 483–5.

Gomez-Sanchez, J. A., Pilch, K. S., van der Lans, M., Fazal, S. V., Benito, C., Wagstaff, L. J., Mirsky, R., & Jessen, K. R. (2017). After nerve injury, lineage tracing shows that myelin and remak Schwann cells elongate extensively and branch to form repair Schwann cells, which shorten radically on remyelination. *J. Neurosci.* **37**,

9086–9099.

Goncalves, M. B., Malmqvist, T., Clarke, E., Hubens, C. J., Grist, J., Hobbs, C., Trigo, X., Risling, X. M., Angeria, M., Damberg, P., Carlstedt, T. P., & Corcoran, J. P. T. (2015). Neuronal RAR-Beta signaling modulates PTEN activity directly in neurons and via exosome transfer in astrocytes to prevent glial scar formation and induce spinal cord regeneration. *J. Neurosci.* **35**, 15731–15745.

Griffin, J. W., & Thompson, W. J. (2008). Biology and pathology of nonmyelinating Schwann cells. *Glia* **1531**, 1518–1531.

Grumbles, R. M., Thomas, C. M., Wood, P. M., & Thomas, C. K. (2013). Acute stimulation of transplanted neurons improves motoneuron survival, axon growth, and muscle reinnervation. *J. Neurotrauma* **1069**, 1062–1069.

Guérout, N., Derambure, C., Drouot, L., Bon-Mardion, N., Duclos, C., Boyer, O., & Marie, J.-P. (2010). Comparative gene expression profiling of olfactory ensheathing cells from olfactory bulb and olfactory mucosa. *Glia* **58**, 1570–80.

Guerrero, A. R., Uchida, K., Nakajima, H., Watanabe, S., Nakamura, M., Okada, S., Johnson, W. E. B., & Baba, H. (2014). Blockade of interleukin-6 effects on cytokine profiles and macrophage activation after spinal cord injury in mice. *J. Neuroinflammation* **9**, 203–212.

Guertin, A. D., Zhang, D. P., Mak, K. S., Alberta, J. A., & Kim, H. A. (2005). Microanatomy of axon / glial signaling during Wallerian degeneration. *J. Neurosci.* **25**, 3478–3487.

Guest, J. D., Hiester, E. D., & Bunge, R. P. (2005). Demyelination and Schwann cell responses adjacent to injury epicenter cavities following chronic human spinal cord injury. *Exp. Neurol.* **192**, 384–393.

Hackett, A. R., & Lee, J. K. (2016). Understanding the NG2 glial scar after spinal cord injury. *Front. Neurol.* **7**, 1–10.

Han, Q., Cao, C., Ding, Y., So, K., Wu, W., Qu, Y., & Zhou, L. (2015). Plasticity of motor network and function in the absence of corticospinal projection. *Exp. Neurol.* **267**, 194–208.

Harel, N. Y., & Strittmatter, S. M. (2006). Can regenerating axons recapitulate developmental guidance during recovery from spinal cord injury ? *Nat. Neurosci.* **7**, 603–616.

Harrop, J. S., Hashimoto, R., Norvell, D., Raich, A., Aarabi, B., Grossman, R. G., Guest, J. D., Tator, C. H., Chapman, J., & Fehlings, M. G. (2012). Evaluation of clinical experience using cell-based therapies in patients with spinal cord injury: a systematic review. *J. Neurosurg. Spine* **17**, 230–46.

Hesp, Z. C., Goldstein, E. Z., Miranda, C. J., Kaspar, X. B. K., & Mctigue, D. M. (2015). Chronic oligodendrogenesis and remyelination after spinal cord injury in mice and rats. *J Neurosci.* **35**, 1274–1290.

Higginson, J. R., & Barnett, S. C. (2011). The culture of olfactory ensheathing cells (OECs)-a distinct glial cell type. *Exp. Neurol.* **229**, 2–9.

Hill, C. E., Moon, L. D. F., Wood, P. M., & Bunge, M. B. (2006). Labeled Schwann cell

transplantation: Cell loss, host Schwann cell replacement, and strategies to enhance survival. *Glia* **53**, 338–343.

Honmou, O., Felts, P. A., & Waxman, G. (1996). Restoration of normal conduction properties in demyelinated spinal cord axons in the adult rat by transplantation of exogenous Schwann cells. *J Neurosci.* **16**, 3199–3208.

Hu, J., Zeng, L., Huang, J., Wang, G., & Lu, H. (2015). miR-126 promotes angiogenesis and attenuates inflammation after contusion spinal cord injury in rats. *Brain Res.* **1608**, 191–202.

Ichiyama, R. M., Gerasimenko, Y. P., Yang, G. J., Van Den Brand, R., Lavrov, I. A., Zhong, H., Roy, R. R., & Edgerton, V. R. (2008). Step training reinforces specific spinal locomotor circuitry in adult spinal rats. *J. Neurosci.* **28**, 7370–7375.

Ichiyama, R. M., Gerasimenko, Y. P., Zhong, H., Roy, R. R., & Edgerton, V. R. (2005). Hindlimb stepping movements in complete spinal rats induced by epidural spinal cord stimulation. *Neurosci. Lett.* **383**, 339–344.

Iyer, S., Maybhate, A., Presacco, A., & All, A. H. (2010). Multi-limb acquisition of motor evoked potentials and its application in spinal cord injury. *J. Neurosci. Methods* **193**, 210–216.

Jain, A., Kim, Y.-T., McKeon, R. J., & Bellamkonda, R. V. (2006). In situ gelling hydrogels for conformal repair of spinal cord defects, and local delivery of BDNF after spinal cord injury. *Biomaterials* **27**, 497–504.

Jang, S. Y., Shin, Y. K., Park, S. Y., Park, J. Y., Lee, H. J., Yoo, Y. H., Kim, J. K., &

Park, H. T. (2016). Autophagic myelin destruction by Schwann cells during Wallerian degeneration and segmental demyelination. *Glia* **64**, 730–742.

Jasmin, L., Janni, G., Moallem, T. M., Lappi, D. A., & Ohara, P. T. (2000). Schwann cells are removed from the spinal cord after effecting recovery from paraplegia. *J Neurosci.* **20**, 9215–9223.

Jasmin, L., & OHara, P. T. (2002). Remyelination within the CNS: do Schwann cells pave the way for oligodendrocytes ? *Neurosci.* **8**, 198–203.

Jessen, K. R., & Mirsky, R. (2005). The origin and development of glial cells in peripheral nerves. *Nat. Rev. Neurosci.* **6**, 671–82.

Jones, L. L., Yamaguchi, Y., Stallcup, W. B., & Tuszynski, M. H. (2002). NG2 Is a major chondroitin sulfate proteoglycan produced after spinal cord injury and is expressed by macrophages and oligodendrocyte progenitors. *J. Neurosci.* **22**, 2792–2803.

Joosten, E. a J. (2012). Biodegradable biomatrices and bridging the injured spinal cord: the corticospinal tract as a proof of principle. *Cell Tissue Res.* **349**, 375–95.

Karnovsky, M. (1965). A formaldehyde glutaraldehyde fixative of high osmolality for use in electron microscopy. *J. Cell Biol.* **27**, 1964–1965.

Keirstead, H. S., Nistor, G., Bernal, G., Totoiu, M., Cloutier, F., Sharp, K., & Steward, O. (2005). Human embryonic stem cell-derived oligodendrocyte progenitor cell transplants remyelinate and restore locomotion after spinal cord injury. *J. Neurosci.* **25**, 4694–705.

Kerman, I. A., Enquist, L. W., Watson, S. J., & Yates, B. J. (2003). Brainstem substrates

of sympatho-motor circuitry identified using trans-synaptic tracing with pseudorabies virus recombinants. *J. Neurosci.* **23**, 4657–4666.

Kerschensteiner, M., Schwab, M. E., Lichtman, J. W., & Misgeld, T. (2005). In vivo imaging of axonal degeneration and regeneration in the injured spinal cord. *Nat. Med.* **11**, 572–577.

Keung, A. J., Asuri, P., Kumar, S., & Schaffer, D. V. (2012). Soft microenvironments promote the early neurogenic differentiation but not self-renewal of human pluripotent stem cells. *Integr. Biol.* **4**, 1049–1058.

Keyvan-Fouladi, N., Raisman, G., & Li, Y. (2003). Functional Repair of the Corticospinal Tract by Delayed Transplantation of Olfactory Ensheathing Cells in Adult Rats. *J. Neurosci.* **23**, 9428–9434.

Khankan, R. R., Griffis, K. G., Haggerty-Skeans, J. R., Zhong, H., Roy, R. R., Edgerton, V. R., & Phelps, P. E. (2016). Olfactory ensheathing cell transplantation after a complete spinal cord transection mediates neuroprotective and immunomodulatory mechanisms to facilitate regeneration. *J Neurosci.* **36**, 6269–6286.

Khankan, R. R., Wanner, I. B., & Phelps, P. E. (2015). Olfactory ensheathing cell – neurite alignment enhances neurite outgrowth in scar-like cultures. *Exp. Neurol.* **269**, 93–101.

King, V. R., Alovskaya, A., Wei, D. Y. T., Brown, R. a, & Priestley, J. V. (2010). The use of injectable forms of fibrin and fibronectin to support axonal ingrowth after spinal cord injury. *Biomaterials* **31**, 4447–56.

Klapka, N., Hermanns, S., Straten, G., Masanneck, C., Duis, S., Hamers, F. P. T., Zuschratter, W., Mu, H. W., & Mu, D. (2005). Suppression of fibrous scarring in spinal cord injury of rat promotes long-distance regeneration of corticospinal tract axons , rescue of primary motoneurons in somatosensory cortex and significant functional recovery. *Eur. J. Neurosci.* **22**, 3047–3058.

Kocsis, J. D., Lankford, K. L., Sasaki, M., & Radtke, C. (2009). Unique in vivo properties of olfactory ensheathing cells that may contribute to neural repair and protection following spinal cord injury. *Neurosci. Lett.* **456**, 137–42.

Kubasak, M D, Hedlund, E., Roy, R. R., Carpenter, E. M., Edgerton, V. R., & Phelps, P. E. (2005). L1 CAM expression is increased surrounding the lesion site in rats with complete spinal cord transection as neonates. *Exp. Neurol.* **194**, 363–75.

Kubasak, Marc D, Jindrich, D. L., Zhong, H., Takeoka, A., Kimberly, C., Muñoz-Quiles, C., Roy, R. R., Edgerton, V. R., & Phelps, P. E. (2008). OEG implantation and step training enhance hindlimb-stepping ability in adult spinal transected rats. *Brain* **131**, 264–276.

Kucher, K., Johns, D., Maier, D., Abel, R., Badke, A., Baron, H., Thietje, R., Casha, S., Meindl, R., Gomez-mancilla, B., & Pfister, C. (2018). First-in-man intrathecal application of nneurite growth-promoting anti-Nogo-A antibodies in acute spinal cord injury. *Neurorehabil. Neural Repair* **32**, 578–589.

Kumamaru, H., Lu, P., Rosenzweig, E. S., & Tuszynski, M. H. (2018). Activation of intrinsic growth state enhances host axonal regeneration into neural progenitor cell grafts. *Stem Cell Reports* **11**, 861–868.

Lakatos, A., Barnett, S. C., & Franklin, R. J. . (2003). Olfactory ensheathing cells induce less host astrocyte response and chondroitin sulphate proteoglycan expression than schwann cells following transplantation into adult CNS white matter. *Exp. Neurol.* **184**, 237–246.

Lakatos, A., Franklin, R. J., & Barnett, S. C. (2000). Olfactory ensheathing cells and Schwann cells differ in their in vitro interactions with astrocytes. *Glia* **32**, 214–25.

Lamond, R., & Barnett, S. C. (2013). Schwann cells but not olfactory ensheathing cells inhibit CNS myelination via the secretion of connective tissue growth factor. *J. Neurosci.* **33**, 18686–97.

Lankford, K. L., Sasaki, M., Radtke, C., & Kocsis, J. D. (2008). Olfactory ensheathing cells exhibit unique migratory, phagocytic, and myelinating properties in the X-irradiated spinal cord not shared by Schwann cells. *Glia* **56**, 1664–78.

Lavrov, I., Courtine, G., Dy, C. J., Van Den Brand, R., Fong, A. J., Gerasimenko, Y., Zhong, H., Roy, R. R., & Edgerton, V. R. (2008). Facilitation of stepping with epidural stimulation in spinal rats: role of sensory input. *J. Neurosci.* **28**, 7774–7780.

Lavrov, I., Dy, C. J., Fong, A. J., Gerasimenko, Y., Courtine, G., Zhong, H., Roy, R. R., & Edgerton, V. R. (2008). Epidural stimulation induced modulation of spinal locomotor networks in adult spinal rats. *J. Neurosci.* **28**, 6022–6029.

Lavrov, I., Gerasimenko, Y. P., Ichiyama, R. M., Courtine, G., Zhong, H., Roy, R. R., & Edgerton, V. R. (2006). Plasticity of spinal cord reflexes after a complete

transection in adult rats: relationship to stepping ability. *J. Neurophysiol.* **96**, 1699–1710.

Liu, G., Detloff, M. R., Miller, K. N., Santi, L., & Houlé, J. D. (2012). Exercise modulates microRNAs that affect the PTEN / mTOR pathway in rats after spinal cord injury. *Exp. Neurol.* **233**, 447–456.

Liu, K., Lu, Y., Lee, J. K., Samara, R., Willenberg, R., Sears-Kraxberger, I., Tedeschi, A., Park, K. K., Jin, D., Cai, B., Xu, B., Connolly, L., Steward, O., Zheng, B., & He, Z. (2010). PTEN deletion enhances the regenerative ability of adult corticospinal neurons. *Nat. Neurosci.*

Liu, X., Xu, X. M., Hu, R., Du, C., Zhang, S. X., McDonald, J. W., Dong, H. X., Wu, Y. J., Fan, G. S., Jacquin, M. F., Hsu, C. Y., & Choi, D. W. (1997). Neuronal and glial apoptosis after traumatic spinal cord injury. *J. Neurosci.* **17**, 5395–406.

Lopez, P. H. H., Ahmad, A. S., Mehta, N. R., Toner, M., Elizabeth, A., Zhang, J., Doré, S., & Schnaar, R. L. (2012). Myelin-associated glycoprotein protects neurons from excitotoxicity. *J. Neurochem.* **116**, 900–908.

Lu, P., Jones, L. L., & Tuszynski, M. H. (2007). Axon regeneration through scars and into sites of chronic spinal cord injury. *Exp. Neurol.* **203**, 8–21.

Lu, P., Wang, Y., Graham, L., McHale, K., Gao, M., Wu, D., Brock, J., Blesch, A., Rosenzweig, E. S., Havton, L. a, Zheng, B., Conner, J. M., Marsala, M., & Tuszynski, M. H. (2012). Long-distance growth and connectivity of neural stem cells after severe spinal cord injury. *Cell* **150**, 1264–73.

Lu, P., Woodruff, G., Wang, Y., Graham, L., Hunt, M., Wu, D., Boehle, E., Ahmad, R., Poplawski, G., Brock, J., Goldstein, L. S. B., & Tuszynski, M. H. (2014). Long-distance axonal growth from human induced pluripotent stem cells after spinal cord injury. *Neuron* **2**, 1–8.

Lu, P., Yang, H., Culbertson, M., Graham, L., Roskams, A. J., & Tuszynski, M. H. (2006). Olfactory ensheathing cells do not exhibit unique migratory or axonal growth-promoting properties after spinal cord injury. *J. Neurosci.* **26**, 11120–11130.

Ludwin, S. K., & Maitland, M. (1984). Long-term remyelination fails to reconstitute normal thickness of central myelin sheaths. *J. Neurol. Sci.* **64**, 193–198.

Ma, S. F., Chen, Y. J., Zhang, J. X., Shen, L., Wang, R., Zhou, J. S., Hu, J. G., & Lü, H. Z. (2015). Adoptive transfer of M2 macrophages promotes locomotor recovery in adult rats after spinal cord injury. *Brain. Behav. Immun.* **45**, 157–170.

Mahad, D. H., Trapp, B. D., & Lassmann, H. (2015). Pathological mechanisms in progressive multiple sclerosis. *Lancet Neurol.* **14**, 183–193.

Maikos, J. T., & Shreiber, D. I. (2007). Immediate damage to the blood-spinal cord barrier due to mechanical trauma. *J. Neurotrauma* **24**, 492–507.

Mckeon, R. J., Jurynec, M. J., & Buck, C. R. (1999). The chondroitin sulfate proteoglycans neurocan and phosphacan are expressed by reactive astrocytes in the chronic CNS glial scar. *J. Neurosci.* **19**, 10778–10788.

McKerracher, L., David, S., Jackson, D. L., Kottis, V., Dunn, R. J., & Braun, P. E. (1994). Identification of myelin-associated glycoprotein as a major myelin-derived

inhibitor of neurite growth. *Neuron* **13**, 805–811.

McTigue, D. M., Wei, P., & Stokes, B. T. (2001). Proliferation of NG2-positive cells and altered oligodendrocyte numbers in the contused rat spinal cord. *J. Neurosci.* **21**, 3392–400.

Medalha, C. C., Jin, Y., Yamagami, T., Haas, C., & Fischer, I. (2014). Transplanting neural progenitors into a complete transection model of spinal cord injury. *J. Neurosci. Res.* **92**, 607–618.

Mekhail, M., Almazan, G., & Tabrizian, M. (2012). Oligodendrocyte-protection and remyelination post-spinal cord injuries: a review. *Prog. Neurobiol.* **96**, 322–39.

Mennerick, S., & Zorumski, C. F. (2000). Neural activity and survival in the developing nervous system. *Mol. Neurobiol.* **22**, 41–54.

Merkler, D., Metz, G. A. S., Raineteau, O., Dietz, V., Schwab, M. E., & Fouad, K. (2001). Locomotor recovery in spinal cord-injured rats treated with an antibody neutralizing the myelin-associated neurite growth inhibitor Nogo-A. *J. Neurosci.* **21**, 3665–3673.

Metz, G. A., & Whishaw, I. Q. (2009). The ladder rung walking task: a scoring system and its practical application. *J. Vis. Exp.* 1204.

Meves, J. M., Geoffroy, C. G., Kim, N. D., Kim, J. J., & Zheng, B. (2018). Oligodendrocytic but not neuronal Nogo restricts corticospinal axon sprouting after CNS injury. *Exp. Neurol.*

Mi, S., Miller, R. H., Lee, X., Scott, M. L., Shulag-Morskaya, S., Shao, Z., Chang, J.,

Thill, G., Levesque, M., Zhang, M., Hession, C., Sah, D., Trapp, B., He, Z., Jung, V., McCoy, J. M., & Pepinsky, R. B. (2005). LINGO-1 negatively regulates myelination by oligodendrocytes. *Nat. Neurosci.* **8**, 745–751.

Milde, S., Adalbert, R., Elaman, M. H., & Coleman, M. P. (2015). Neurobiology of aging axonal transport declines with age in two distinct phases separated by a period of relative stability. *Neurobiol. Aging* **36**, 971–981.

Moloney, W. C., Boschetti, E., & King, V. P. (1970). Spontaneous Leukemia in Fischer Rats1. *Cancer Res.* **30**, 41–43.

Mousavi, M., Hedayatpour, A., Mortezaee, K., Mohamadi, Y., & Abolhassani, F. (2019). Schwann cell transplantation exerts neuroprotective roles in rat model of spinal cord injury by combating inflammasome activation and improving motor recovery and remyelination. *Metab. Brain Dis.*

Muniswami, D. M., & Tharion, G. (2018). Functional recovery following the transplantation of olfactory ensheathing cells in rat spinal cord injury model. *Asian Spine J.* **12**, 998–1009.

Myers, S. A., Bankston, A. N., Burke, D. A., Ohri, S. S., & Whittemore, S. R. (2016). Does the preclinical evidence for functional remyelination following myelinating cell engraftment into the injured spinal cord support progression to clinical trials? *Exp. Neurol.* **283**, 560–572.

Nagoshi, N., Shibata, S., Hamanoue, M., Mabuchi, Y., Matsuzaki, Y., Toyama, Y., Nakamura, M., & Okano, H. (2011). Schwann cell plasticity after spinal cord injury

shown by neural crest lineage tracing. *Glia* **59**, 771–784.

Nakhjavan-shahraki, B., Yousefifard, M., & Rahimi-movaghar, V. (2018).
Transplantation of olfactory ensheathing cells on functional recovery and
neuropathic pain after spinal cord injury; systematic review and meta-analysis. *Sci.
Rep.* **8**, 1–12.

National Spinal Cord Injury Statistical Center. (2019). National Spinal Cord Injury
Statistical Center, facts and figures at a glance.

Novikova, L. N., Lobov, S., Wiberg, M., & Novikov, L. N. (2011). Efficacy of olfactory
ensheathing cells to support regeneration after spinal cord injury is influenced by
method of culture preparation. *Exp. Neurol.* **229**, 132–42.

Okada, S., Nakamura, M., Katoh, H., Miyao, T., Shimazaki, T., Ishii, K., Yamane, J.,
Yoshimura, A., Iwamoto, Y., Toyama, Y., & Okano, H. (2006). Conditional ablation
of Stat3 or Socs3 discloses a dual role for reactive astrocytes after spinal cord
injury. *Nat. Med.* **12**, 829–834.

Omar, M., Hansmann, F., Kreutzer, R., Kreutzer, M., Brandes, G., & Wewetzer, K.
(2013). Cell type- and isotype-specific expression and regulation of β-tubulins in
primary olfactory ensheathing cells and Schwann cells in vitro. *Neurochem. Res.*
38, 981–8.

Onifer, S. M., Zhang, O., Whitnel-Smith, L. K., Raza, K., O'Dell, C. R., Lyttle, T. S.,
Rabchevsky, A. G., Kitzman, P. H., & Burke, D. A. (2011). Horizontal ladder task-
specific re-training in adult rats with contusive thoracic spinal cord injury. *Restor.*

Neurol. Neurosci. **29**, 275–286.

Ould-Yahoui, A., Sbai, O., Baranger, K., Bernard, A., Gueye, Y., Charrat, E., Clément, B., Gigmes, D., Dive, V., Girard, S. D., Féron, F., Khrestchatisky, M., & Rivera, S. (2012). Role of matrix metalloproteinases in migration and neurotrophic properties of nasal olfactory stem and ensheathing cells. *Cell Transplant.* **22**, 993–1010.

Pan, W., & Kastin, A. J. (1999). Penetration of neurotrophins and cytokines across the blood–brain / blood–spinal cord barrier. *Adv. Drug Deliv. Rev.* **36**, 291–298.

Panni, P., Ferguson, I. a, Beacham, I., Mackay-Sim, A., Ekberg, J. a K., & St John, J. a. (2013). Phagocytosis of bacteria by olfactory ensheathing cells and Schwann cells. *Neurosci. Lett.* **539**, 65–70.

Pearse, D. D., Sanchez, A. R., Pereira, F. C., Andrade, C. M., Puzis, R., Pressman, Y., Golden, K., Kitay, B. M., Blits, B. A. S., Wood, P. M., & Bunge, M. B. (2007). Transplantation of Schwann cells and / or olfactory ensheathing glia into the contused spinal cord: survival , migration, axon association, and functional recovery. *Glia* **1000**, 976–1000.

Pineau, I., Sun, L., Bastien, D., & Lacroix, S. (2010). Astrocytes initiate inflammation in the injured mouse spinal cord by promoting the entry of neutrophils and inflammatory monocytes in an IL-1 receptor / MyD88-dependent fashion. *Brain Behav. Immun.* **24**, 540–553.

Plant, G. W., Christensen, C. L., Oudega, M., & Bunge, M. B. (2003). Delayed Transplantation of Olfactory Ensheathing Glia Promotes Sparing / Regeneration of

Supraspinal Axons in the Contused Adult Rat Spinal Cord. *J. Neurotrauma* **20**.

Plant, G. W., Currier, P. F., Cuervo, E. P., Bates, M. L., Pressman, Y., Bunge, M. B., & Wood, P. M. (2018). Purified adult ensheathing glia fail to myelinate axons under culture conditions that enable Schwann cells to form myelin. *J. Neurosci.* **22**, 6083–6091.

Poliak, S., & Peles, E. (2003). The local differentiation of myelinated axons at nodes of ranvier. *Nat. Rev. Neurosci.* **4**, 968–980.

Povysheva, T. V, Mukhamedshina, Y. O., Rizvanov, A. A., & Chelyshev, Y. A. (2018). PTEN expression in astrocytic processes after spinal cord injury. *Mol. Cell. Neurosci.* **88**, 231–239.

Powers, B. E., Lasiene, J., Plemel, J. R., Shupe, L., Perlmutter, S. I., Tetzlaff, W., & Horner, P. J. (2012). Axonal thinning and extensive remyelination without chronic demyelination in spinal injured rats. *J. Neurosci.* **32**, 5120–5.

Powers, B. E., Sellers, D. L., Lovelett, E. A., Cheung, W., Aalami, S. P., Zapertov, N., Maris, D. O., & Horner, P. J. (2013). Remyelination reporter reveals prolonged refinement of spontaneously regenerated myelin. *Proc. Natl. Acad. Sci.* **110**, 4075–4080.

Prang, P., Mu, R., Eljaouhari, A., Heckmann, K., Kunz, W., Weber, T., Faber, C., Vroemen, M., Bogdahn, U., & Weidner, N. (2006). The promotion of oriented axonal regrowth in the injured spinal cord by alginate-based anisotropic capillary hydrogels. *Biomaterials* **27**, 3560–3569.

Ramón-Cueto, A., Isabel Cordero, M., Santos-Benito, F., & Avila, J. (2000). Functional recovery of paraplegic rats and motor axon regeneration in their spinal cords by olfactory ensheathing glia. *Neuron* **25**, 425–435.

Ramón-Cueto, A., & Nieto-Sampedro, M. (1992). Glial cells from adult rat olfactory bulb: Immunocytochemical properties of pure cultures of ensheathing cells. *Neuroscience* **47**, 213–220.

Ramón-Cueto, Almudena, & Avila, J. (1998). Olfactory ensheathing glia: Properties and function. *Brain Res. Bull.* **46**, 175–187.

Ramón-Cueto, Almudena, & Valverde, F. (1995). Olfactory bulb ensheathing glia: A unique cell type with axonal growth-promoting properties. *Glia* **14**, 163–173.

Raposo, C., & Schwartz, M. (2014). Glial scar and immune cell involvement in tissue remodeling and repair following acute CNS injuries. *Glia* 1–10.

Rodriguez, J. P., Coulter, M., Miotke, J., Meyer, R. L., Takemaru, K.-I., & Levine, J. M. (2014). Abrogation of B-Catenin signaling in oligodendrocyte precursor cells reduces glial scarring and promotes axon regeneration after CNS injury. *J. Neurosci.* **34**, 10285–10297.

Roet, K. C. D., Bossers, K., Franssen, E. H. P., Ruitenberg, M. J., & Verhaagen, J. (2011). A meta-analysis of microarray-based gene expression studies of olfactory bulb-derived olfactory ensheathing cells. *Exp. Neurol.* **229**, 10–45.

Roet, K. C. D., Eggers, R., & Verhaagen, J. (2012). Noninvasive bioluminescence imaging of olfactory ensheathing glia and schwann cells following transplantation

into the lesioned rat spinal cord. *Cell Transplant.* **21**, 1853–65.

Roet, K. C. D., & Verhaagen, J. (2014). Understanding the neural repair-promoting properties of olfactory ensheathing cells. *Exp. Neurol.* **261**, 594–609.

Rosner, J., Avalos, P., Acosta, F., Liu, J., & Drazin, D. (2012). The potential for cellular therapy combined with growth factors in spinal cord injury. *Stem Cells Int.* **2012**, 1–12.

Rotto-Percelay, D. M., Wheeler, J. G., Osorio, F. A., Platt, K. B., & Loewy, A. D. (1992). Transneuronal labeling of spinal interneurons and sympathetic preganglionic neurons after pseudorabies virus injections in the rat medial gastrocnemius muscle. *Brain Res.* **574**, 291–306.

Runyan, S. A., & Phelps, P. E. (2009). Mouse olfactory ensheathing glia enhance axon outgrowth on a myelin substrate in vitro. *Exp. Neurol.* **216**, 95–104.

Sanchez, J. A. G., Carty, L., Lejarreta, M. I., Irigoyen, M. P., Rey, M. V., Griffith, M., Hantke, J., Camara, N. M., Azkargorta, M., Aurrekoetxea, I., Juan, V. G. De, Jefferies, H. B. J., Aspichueta, P., Elortza, F., Aransay, A. M., Chantar, M. L. M., Baas, F., Mato, J. M., Mirsky, R., Woodhoo, A., & Jessen, K. R. (2015). Schwann cell autophagy, myelinophagy, initiates myelin clearance from injured nerves. *J. Cell Biol.* **210**.

Sangari, S., Lundell, H., Kirshblum, S., Perez, M. A., & Perez, M. A. (2019). Residual descending motor pathways influence spasticity after spinal cord injury. *Ann. Neurol.* **86**, 28–41.

Sasaki, M., Black, J. A., Lankford, K. L., Tokuno, H. A., Waxman, S. G., & Kocsis, J. D. (2006). Molecular reconstruction of nodes of ranvier after remyelination by transplanted olfactory ensheathing cells in the demyelinated spinal cord. *J. Neurosci.* **26**, 1803–1812.

Sasaki, M., Lankford, K. L., Radtke, C., Honmou, O., & Kocsis, J. D. (2011). Remyelination after olfactory ensheathing cell transplantation into diverse demyelinating environments. *Exp. Neurol.* **229**, 88–98.

Sasaki, M., Lankford, K. L., Zemedkun, M., & Kocsis, J. D. (2013). Identified olfactory ensheathing cells transplanted into the transected dorsal funiculus bridge the lesion and form myelin. *J Neurosci.* **185**, 974–981.

Segovia, K. N., Mcclure, M., Moravec, M., Luo, N. L., Wan, Y., Gong, X., Riddle, A., Craig, A., Struve, J., Sherman, L. S., & Back, S. A. (2008). Arrested oligodendrocyte lineage maturation in chronic perinatal white matter injury. *Ann. Neurol.* **63**, 520–530.

Sethi, R., Sethi, R., Redmond, A., & Lavik, E. (2014). Olfactory ensheathing cells promote differentiation of neural stem cells and robust neurite extension. *Stem Cell Rev.* **10**, 772–785.

Shah, P. K., Sureddi, S., Alam, M., Zhong, H., Roy, R. R., Edgerton, V. R., & Gerasimenko, Y. (2016). Unique spatiotemporal neuromodulation of the lumbosacral circuitry shapes locomotor success after spinal cord injury. *J. Neurotrauma* **1723**, 1709–1723.

Silva, N. A., Sousa, N., & Reis, R. L. (2014). From basics to clinical: A comprehensive review on spinal cord injury. *Prog. Neurobiol.* **114**, 25–57.

Soderblom, C., Luo, X., Blumenthal, E., Bray, E., Lyapichev, K., Ramos, J., Krishnan, V., Lai-hsu, C., Park, K. K., Tsoulfas, P., & Lee, J. K. (2013). Perivascular fibroblasts form the fibrotic scar after contusive spinal cord injury. *J. Neurosci.* **33**, 13882–13887.

Song, W., Volosin, M., Cragnolini, A. B., Hempstead, B. L., & Friedman, W. J. (2010). ProNGF induces PTEN via p75NTR to suppress Trk-mediated survival signaling in brain neurons. *J. Neurosci.* **30**, 15608–15.

Sorensen, A., Moffat, K., Thomson, C., & Barnett, S. C. (2008). Astrocytes, but not olfactory ensheathing cells or Schwann cells, promote myelination of CNS axons in vitro. *Glia* **56**, 750–63.

Stepanova, O. V, Voronova, A. D., Chadin, A. V, Valikhov, M. P., Abakumov, M. A., Reshetov, I. V, & Chekhonin, V. P. (2018). Isolation of rat olfactory ensheathing cells and their use in the therapy of posttraumatic cysts of the spinal cord. *Cell Technol. Biol.* 132–135.

Sternberger, N. H., Quarles, R. H., Itoyama, Y., & Webster, H. D. (1979). Myelin-associated glycoprotein demonstrated immunocytochemically in myelin and myelin-forming cells of developing rat. *Proc. Natl. Acad. Sci.* **76**, 1510–1514.

Steward, O., & Willenberg, R. (2017). Rodent spinal cord injury models for studies of axon regeneration. *Exp. Neurol.* **287**, 374–383.

Steward, O., Zheng, B., & Tessier-Lavigne, M. (2003). False resurrections: Distinguishing regenerated from spared axons in the injured central nervous system. *J. Comp. Neurol.* **8**, 1–8.

Stidworthy, M. F., Genoud, S., Suter, U., Mantei, N., & Franklin, R. J. M. (2003). Quantifying the early stages of remyelination following cuprizone-induced demyelination. *Brain Pathol.* **13**, 329–339.

Stoeckenius, W. (1959). An Electron Microscope Study of Myelin Figures. *J. Cell Biol.* **5**, 491–500.

Stoll, G., Griffin, J. w., Li, C. Y., & Trapp, B. D. (1989). Wallerian degeneration in the peripheral nervous system : participation of both Schwann cells and macrophages in myelin degradation. *J. Neurocytol.* **683**, 671–683.

Sun, L., Liu, S., Sun, Q., Li, Z., Xu, F., Hou, C., Harada, T., Chu, M., Xu, K., Feng, X., Duan, Y., Zhang, Y., & Wu, S. (2014). Inhibition of TROY Promotes OPC Differentiation and Increases Therapeutic Efficacy of OPC Graft for Spinal Cord Injury. *Stem Cells Dev.* **00**, 1–15.

Sun, Y., Xu, C.-C., Li, J., Guan, X.-Y., Gao, L., Ma, L.-X., Li, R.-X., Peng, Y.-W., & Zhu, G.-P. (2013). Transplantation of oligodendrocyte precursor cells improves locomotion deficits in rats with spinal cord irradiation injury. *PLoS One* **8**.

Tabakow, P., Raisman, G., Fortuna, W., Czyz, M., Huber, J., Li, D., Szewczyk, P., Okurowski, S., Miedzybrodzki, R., Czapiga, B., Salomon, B., Halon, A., Li, Y., Lipiec, J., Kulczyk, A., & Jarmundowicz, W. (2014). Functional Regeneration of

Supraspinal Connections in a Patient With Transected Spinal Cord Following Transplantation of Bulbar Olfactory Ensheathing Cells With Peripheral Nerve Bridging. *Cell Transplant.* **23**, 1631–1655.

Takashima, A. (1998). Establishment of Fibroblast Cultures. *Curr. Protoc. Cell Biol.* **00**, 2.1.1-2.1.12.

Takeoka, A., Jindrich, D. L., Muñoz-Quiles, C., Zhong, H., Van Den Brand, R., Edgerton, V. R., & Phelps, P. E. (2011). Axon regeneration can facilitate or suppress hindlimb function after olfactory ensheathing glia transplantation. *J. Neurosci.* **31**, 4298–4310.

Takeoka, A., Kubasak, M. D., Zhong, H., Roy, R. R., & Phelps, P. E. (2010). Serotonergic innervation of the caudal spinal stump in rats after complete spinal transection: Effect of olfactory ensheathing glia. *J. Comp. Neurosci.* **515**, 664–676.

Tamura, Y., Kataoka, Y., Cui, Y., Takamori, Y., Watanabe, Y., & Yamada, H. (2007). Intracellular translocation of glutathione S-transferase pi during oligodendrocyte differentiation in adult rat cerebral cortex in vivo. *Neuroscience* **148**, 535–540.

Tan, A. M., Zhang, W., & Levine, J. M. (2005). NG2: a component of the glial scar that inhibits axon growth. *J. Anat.* **207**, 717–25.

Taniike, M., Mohri, I., Eguchi, N., Beuckmann, C. T., Suzuki, K., & Urade, Y. (2002). Perineuronal oligodendrocytes protect against neuronal apoptosis through the production of lipocalin-type prostaglandin D synthase in a genetic demyelinating model. *J. Neurosci.* **22**, 4885–4896.

Techangamsuwan, S., Kreutzer, R., Kreutzer, M., Imbschweiler, I., Rohn, K., Wewetzer, K., & Baumgärtner, W. (2009). Transfection of adult canine Schwann cells and olfactory ensheathing cells at early and late passage with human TERT differentially affects growth factor responsiveness and in vitro growth. *J. Neurosci. Methods* **176**, 112–20.

Thomas, J., Haseman, J. K., Goodman, J. I., Ward, J. M., Jr, T. P. L., & Spencer, P. J. (2007). A review of large granular lymphocytic leukemia in Fischer 344 rats as an initial step toward evaluating the implication of the endpoint to human cancer risk assessment. *Toxicol. Sci.* **99**, 3–19.

Thomas, K. E., & Moon, L. D. F. (2011). Will stem cell therapies be safe and effective for treating spinal cord injuries? *Br. Med. Bull.* **98**, 127–42.

Thomas, P. K., & King, R. H. M. (1974). The degeneration of unmyelinated axons following nerve section: An ultrastructural study. *J. Neurocytol.* **3**, 497–512.

Thomas, S. A. M., Seidlits, K., Goodman, A. G., Kukushliev, T. V., Hassani, D. M., Cummings, B. J., Anderson, A. J., & Shea, L. (2014). Sonic hedgehog and neurotrophin-3 increase oligodendrocyte numbers and myelination after spinal cord injury. *Integr. Biol.* **00**.

Thompson, R. E., Pardieck, J., Smith, L., Kenny, P., Crawford, L., Shoichet, M., & Sakiyama-elbert, S. (2018). Effect of hyaluronic acid hydrogels containing astrocyte-derived extracellular matrix and / or V2a interneurons on histologic outcomes following spinal cord injury. *Biomaterials* **162**, 208–223.

Thompson, R. J., Roberts, B., Alexander, C. L., Williams, S. K., & Barnett, S. C. (2000). Comparison of neuregulin-1 expression in olfactory ensheathing cells, Schwann cells and astrocytes. *J. Neurosci. Res.* **61**, 172–85.

Thornton, M. A., Mehta, M. D., Morad, T. T., Ingraham, K. L., Khankan, R. R., Griffis, K. G., Yeung, A. K., Zhong, H., Roy, R. R., Edgerton, V. R., & Phelps, P. E. (2018). Evidence of axon connectivity across a spinal cord transection in rats treated with epidural stimulation and motor training combined with olfactory ensheathing cell transplantation. *Exp. Neurol.* **309**, 119–133.

Tillakaratne, N. J. K., Duru, P., Fujino, H., Zhong, H., Xiao, M. S., Edgerton, V. R., & Roy, R. R. (2014). Identification of interneurons activated at different inclines during treadmill locomotion in adult rats. *J. Neurosci. Res.* **92**, 1714–1722.

Toft, A., Tome, M., Barnett, S. C., & Riddell, J. S. (2013). A comparative study of glial and non-neural cell properties for transplant-mediated repair of the injured spinal cord. *Glia* **61**, 513–28.

Totoiu, M. O., & Keirstead, H. S. (2005). Spinal cord injury is accompanied by chronic progressive demyelination. *J. Comp. Neurol.* **486**, 373–83.

Tuszynski, M. H., & Steward, O. (2012). Primer concepts and methods for the study of axonal regeneration in the CNS. *Neuron* **74**, 777–791.

Ueno, M., Nakamura, Y., Li, J., Goulding, M., Baccei, M. L., Ueno, M., Nakamura, Y., Li, J., Gu, Z., Niehaus, J., Maezawa, M., & Crone, S. A. (2018). Corticospinal circuits from the sensory and motor cortices differentially regulate skilled movements

through distinct spinal interneurons. *CellReports* **23**, 1286-1300.e7.

Ulrich, R., Imbschweiler, I., Kalkuhl, A., Lehmbecker, A., Ziege, S., Kegler, K., Becker, K., Deschl, U., Wewetzer, K., & Baumgärtner, W. (2014). Transcriptional profiling predicts overwhelming homology of Schwann cells, olfactory ensheathing cells, and Schwann cell-like glia. *Glia* **62**, 1559–1581.

Vargas, M. E., & Barres, B. A. (2007). Why is Wallerian degeneration in the CNS so slow? *Annu. Rev. Neurosci.* **30**, 153–179.

Vavrek, R., Girgis, J., Tetzlaff, W., Hiebert, G. W., & Fouad, K. (2006). BDNF promotes connections of corticospinal neurons onto spared descending interneurons in spinal cord injured rats. *Brain* **129**, 1534–1545.

Vaynman, S., & Gomez-Pinilla, F. (2005). License to run: exercise impacts functional plasticity in the intact and injured central nervous system by using neurotrophins. *Neurorehabil. Neural Repair* **19**, 283–295.

Venkatesh, K., Ghosh, S. K., Mullick, M., Manivasagam, G., & Sen, D. (2019). Spinal cord injury: pathophysiology, treatment strategies, associated challenges, and future implications. *Cell Tissue Res.*

Walker, C. L., & Xu, X. (2014). PTEN inhibitor bisperoxovanadium protects oligodendrocytes and myelin and prevents neuronal atrophy in adult rats following cervical hemicontusive spinal cord injury. *Neurosci. Lett.* **573**, 64–68.

Wang, S., Bates, J., Li, X., Schanz, S., Chandler-Militello, D., Levine, C., Maherali, N., Studer, L., Hochedlinger, K., Windrem, M., & Goldman, S. a. (2013). Human iPSC-

derived oligodendrocyte progenitor cells can myelinate and rescue a mouse model of congenital hypomyelination. *Cell Stem Cell* **12**, 252–64.

Wang, T., Cong, R., Yang, H., Wu, M.-M., Luo, N., Kuang, F., & You, S.-W. (2011). Neutralization of BDNF attenuates the in vitro protective effects of olfactory ensheathing cell-conditioned medium on scratch-insulted retinal ganglion cells. *Cell. Mol. Neurobiol.* **31**, 357–64.

Wenger, N., Moraud, E. M., Gandar, J., Musienko, P., Capogrosso, M., Baud, L., Goff, C. G. Le, Barraud, Q., Pavlova, N., Dominici, N., Minev, I. R., Asboth, L., Hirsch, A., Duis, S., Kreider, J., Mortera, A., Haverbeck, O., Kraus, S., Schmitz, F., Digiovanna, J., Van Den Brand, R., Bloch, J., & Detemple, P. (2016). Spatiotemporal neuromodulation therapies engaging muscle synergies improve motor control after spinal cord injury. *Nat. Med.* **22**, 5–7.

West, A. E., & Greenberg, M. E. (2011). Neuronal activity – regulated gene transcription in synapse development and cognitive function. *Cold Spring Harb. Perspect. Biol.* 1–22.

Wewetzer, K., Verdú, E., Angelov, D. N., & Navarro, X. (2002). Olfactory ensheathing glia and Schwann cells: Two of a kind? *Cell Tissue Res.* **309**, 337–345.

Whetstone, W. D., Hsu, J. C., Eisenberg, M., Werb, Z., & Noble-haeusslein, L. J. (2003). Blood-spinal cord barrier after spinal cord injury: relation to revascularization and wound healing. *J. Neurosci. Res.* **239**, 227–239.

Wilkins, A., Majed, H., Layfield, R., Compston, A., & Chandran, S. (2003).

Oligodendrocytes promote neuronal survival and axonal length by distinct intracellular mechanisms: a novel role for oligodendrocyte-derived glial cell line-derived neurotrophic factor. *J. Neurosci.* **23**, 4967–74.

Windus, L. C. E., Chehrehasa, F., Lineburg, K. E., Claxton, C., Mackay-Sim, A., Key, B., & St John, J. a. (2011). Stimulation of olfactory ensheathing cell motility enhances olfactory axon growth. *Cell. Mol. Life Sci.* **68**, 3233–47.

Woodhoo, a, Sahni, V., Gilson, J., Setzu, A., Franklin, R. J. M., Blakemore, W. F., Mirsky, R., & Jessen, K. R. (2007). Schwann cell precursors: a favourable cell for myelin repair in the Central Nervous System. *Brain* **130**, 2175–85.

Xu, D., Wu, D., Qin, M., Nih, L. R., Liu, C., Cao, Z., Ren, J., Chen, X., Li, J., Harley, D., Xu, B., Hou, L., Chen, I. S. Y., Wen, J., Chen, W., Pourtaheri, S., & Lu, Y. (2019). Efficient delivery of nerve growth factors to the central nervous system for neuralregeneration. *Adv. Mater.* **1900727**, 1–8.

Yang, H., He, B.-R., & Hao, D.-J. (2014). Biological roles of olfactory ensheathing cells in facilitating neural regeneration: A systematic review. *Mol. Neurobiol.*

Yang, Z., Wu, Y., Zheng, L., Zhang, C., Yang, J., Shi, M., Feng, D., Wu, Z., & Wang, Y.-Z. (2013). Conditioned medium of Wnt/β-catenin signaling-activated olfactory ensheathing cells promotes synaptogenesis and neurite growth in vitro. *Cell. Mol. Neurobiol.* **33**, 983–90.

Yao, R., Murtaza, M., Velasquez, J. T., Todorovic, M., Rayfield, A., Ekberg, J., Barton, M., & John, J. S. (2018). Olfactory Ensheathing Cells for Spinal Cord Injury :

Sniffing Out the Issues. *Cell Transplant.* **27**, 879–889.

Zaviskova, K., Tukmachev, D., Dubisova, J., Vackova, I., Hejcl, A., Bystronova, J., Pravda, M., Scigalkova, I., Sulakova, R., Velebny, V., Wolfova, L., & Kubinova, S. (2018). Injectable hydroxyphenyl derivative of hyaluronic acid hydrogel modified with RGD as scaffold for spinal cord injury repair. *J. Biomed. Mater. Res.* **106a**, 1129–1140.

Zhang, J., Chen, H., Duan, Z., Chen, K., Liu, Z., Zhang, L., Yao, D., & Li, B. (2017). The effects of co-transplantation of olfactory ensheathing cells and Schwann cells on local inflammation environment in the contused spinal cord of rats. *Mol. Neurobiol.* **54**, 943–953.

Zhang, S., Huang, F., Gates, M., & Holmberg, E. G. (2011). Scar ablation combined with LP / OEC transplantation promotes anatomical recovery and P0-positive myelination in chronically contused spinal cord of rats. *Brain Res.* **1399**, 1–14.

Zhang, S., Huang, F., Gates, M., & Holmberg, E. G. (2013). Role of endogenous Schwann cells in tissue repair after spinal cord injury. *Neural Regen. Res.* **8**, 177–185.

Zhu, H., Xie, R., Liu, X., Shou, J., Gu, W., Gu, S., & Che, X. (2017). MicroRNA-494 improves functional recovery and inhibits apoptosis by modulating PTEN / AKT / mTOR pathway in rats after spinal cord injury. *Biomed. Pharmacother.* **92**, 879–887.

Ziegler, M. D., Hsu, D., Takeoka, A., Zhong, H., Ramón-Cueto, A., Phelps, P. E., Roy,

R. R., & Edgerton, V. R. (2011). Further evidence of olfactory ensheathing glia facilitating axonal regeneration after a complete spinal cord transection. *Exp. Neurol.* **229**, 109–19.